ABSTRACT

Title of Document:	Design and Synthesis of New Group (IV) Cyclopentadienyl Amidinate and Guanidinate Initiators for Controlling the Microstructure of Poly(α-olefins) During Living Coordinative Chain Transfer Polymerizations
	Cathryn Gail Blakley, Doctor of Philosophy, 2014
Directed By:	Professor Lawrence R. Sita Department of Chemistry & Biochemistry University of Maryland – College Park

C_1-symmetric, cationic group 4 metal (Zr and Hf) mono-methyl complexes, {(η5-C_5Me_5)M[N(^{t}Bu)C(Me)N(Et)](Me)}[B(C_6F_5)$_4$], are highly active initiators for the living and stereo-selective (isotactic) coordinative polymerization of propene and longer-chain α-olefins. Utilizing technology previously discovered but not yet fully utilized, it is possible to demonstrate the remarkable ability to stereo-engineer poly(α-olefins) with the use of a single initiator. A two-state living coordination polymerization process can be engaged by controlling the relative populations of the active and dormant species as a function of time to incorporate stereo-errors in a programmed fashion. Secondly, in the presence of excess equivalents of a main group metal alkyl such as diethylzinc (DEZ), rapid and reversible chain transfer between the active propagating species and the 'surrogate' main group metal alkyl, which occurs at a rate that is significantly greater than propagation, serves as a work-around solution to the 'one-chain-per-metal-site' limitation of a living polymerization. Successful adaptation of this reversible group transfer technology can include the rapid and reversible transfer of a polymeric group

between ‘tight’ and ‘loose’ propagating ion pairs that mediated by excess DEZ to precisely control co-monomer incorporation.

While this process of living coordinative chain transfer polymerization (LCCTP) can provide practical quantities of precision polyolefins, the exchange process results in loss of stereo-regularity in the final polymer microstructure. Strategies for achieving a high degree of stereo-regularity during LCCTP include the synthesis of new classes of configurationally stable and optically pure cyclopentadienyl, amidinate and guanidinate initiators that incorporate a distal, chiral substituent. A second strategy to create enantiomerically pure propagating species involves the adaptation of hydrozirconation to create a new class of terpene substituted cyclopentadienyl-amidinate complexes *via* insertion of an olefin into a Zr-H bond. The last attempt to impart stereocontrol under LCCTP conditions involves the addition of an enantiomerically substituent to the N-amidinate to ensure the same enantiofacial insertion.

Design and Synthesis of New Group (IV) Cyclopentadienyl Amidinate and Guanidinate Initiators for Controlling the Microstructure of Poly(!-olefins) During Living Coordinative Chain Transfer Polymerizations

By

Cathryn Gail Blakley

Dissertation submitted to the Faculty of the Graduate School of the
University of Maryland, College Park, in partial fulfillment
of the requirements for the degree of
Doctor of Philosophy
2014

Advisory Committee:

Professor Lawrence R. Sita - Advisor
Professor Jeffrey Davis
Professor Andrei Vedernikov
Professor Efrain Rodriguez
Professor Mohamad Al-Sheikhly

Per aspera ad astra.

Acknowledgements

First I'd like to thank Professor Lawrence R. Sita for his guidance during my research at the University of Maryland as my advisor. Without a doubt he has taught me a great deal about the kind of scientist I aspire to be.

I would also like to thank my committee members for their support and advice throughout these four years. Without Prof. Jeffrey Davis, Prof. Bryan Eichhorn, Prof. Andrei Verdernikov, Prof. Efrain Rodriguez and Prof. Mohamad Al-Sheikhly this research would not possible.

A special thanks to: Dr. Jonathan Reeds, Dr. Rennisha Wickham, Dr. Jia Wei, Dr. Brendan Yonke, Andrew Keane, Wesley Farrell, Kaitlyn Crawford, Tessy Thomas, Kerry DeMella, Kyle Reddick, and Kyle Augustine for making the last four years enjoyable. I certainly appreciate everyone's support and friendship.

NMR and singe crystal analysis would not have been possible without the help from Dr. Yiu-Fai Lam, Dr. Yinde Wang, and Dr. Peter Zavalij.

I would like to thank Keersten & Robert Davis, Andy & Shelley Schmidt, Tom Boone, Andrew & Jenny Misenheimer, Joseph & Ashley Sizemore, Brad & Hilary Schafer, and Phil Monkowski for their continued friendship and ever present humor.

Most importantly, I would like to thank my family for their unwavering encouragement and support, especially my mother Lynn Blakley and my grandfather Ray Hayes. Without any of them, none of this would have ever been possible.

Table of Contents

List of Abbreviations

acac	acetylaceton
AFM	atomic force microscopy
CCTcoP	coordinative chain transfer copolymerization
CCTP	coordinative chain transfer polymerization
CGC	constrained geometry catalyst
ChloDeT	chloride degenerative transfer
Cp	cyclopentadienyl (η^5-C_5H_5)
Cp*	pentamethylcyclopentadienyl (η^5-$C_{10}H_{15}$)
CSA	chain shuttling agent
CTA	chain transfer agent
DEZ	diethyl zinc
DSC	differential scanning calorimetry
Et_2O	diethyl ether
GPC	gel permeation chromatography
i-Bu	*iso*-butyl
kDa	kilo daltons
LCCTP	living coordinative chain transfer polymerization
MeDeT	methyl degenerative transfer
NMR	nuclear magnetic resonance
OBC	olefin block copolymer
PB	poly(1-butene)
PDI	polydispersity
PE	polyethylene
PH	poly(1-hexene)
PhCl	chlorobenzene
PP	polypropylene
SDTL	stereomodulated degenerative transfer living
t-Bu	*tert*-butyl
T_c	crystallization temperature
T_g	glass transition temperature
TGA	thermogravimetric analys
T_m	melting temperature
WAXD	wide angle diffraction

List of Tables

List of Figures

List of Schemes

List of Numbered Compounds

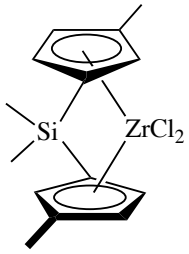

1

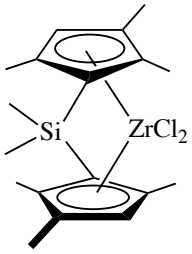

2

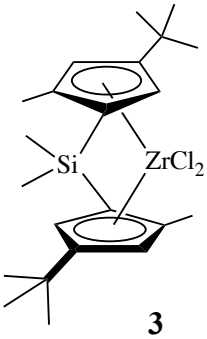

3

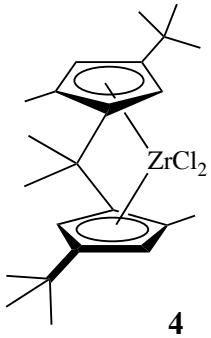

4

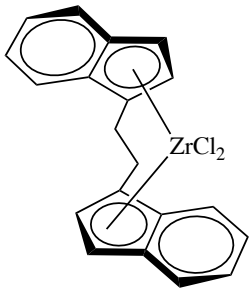

5

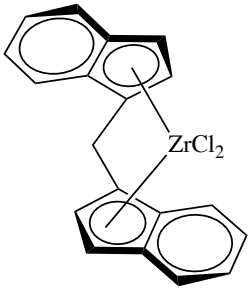

6

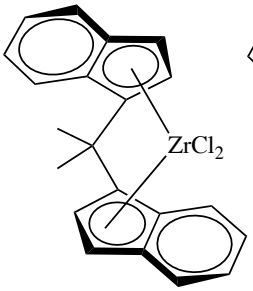

7

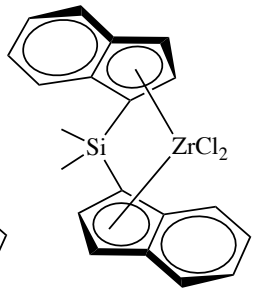

8

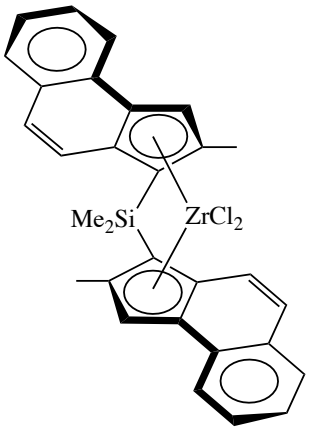

9

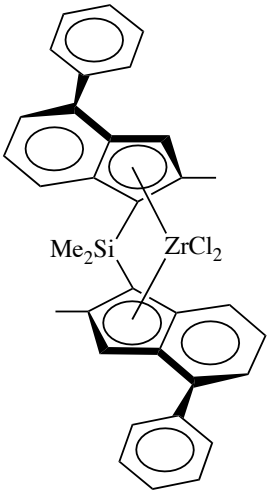

10

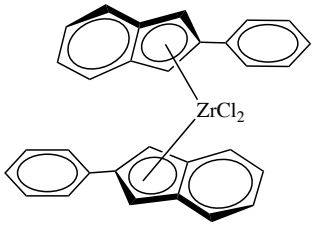

11

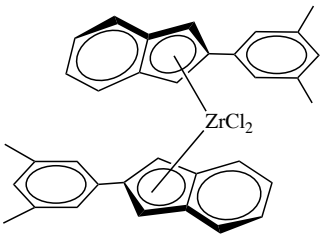

12

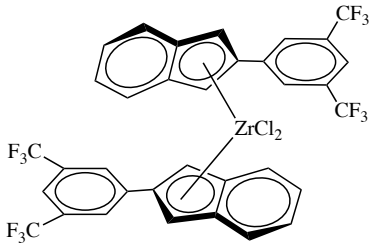

13

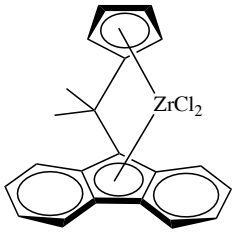

14

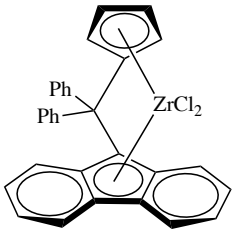

15

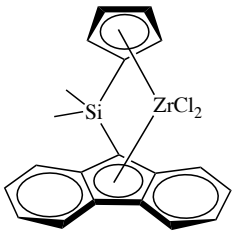

16

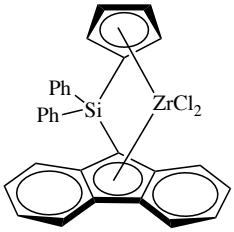

17

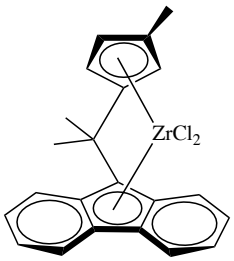

18

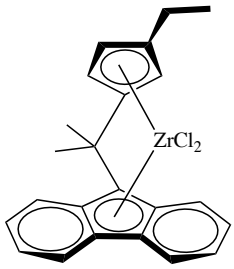

19

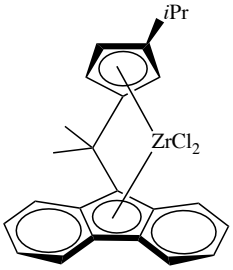

20

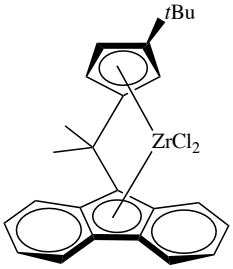

21

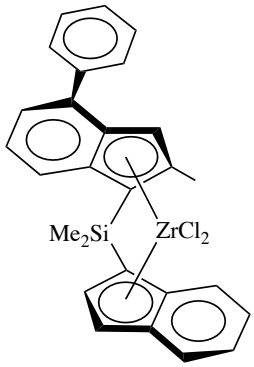

22

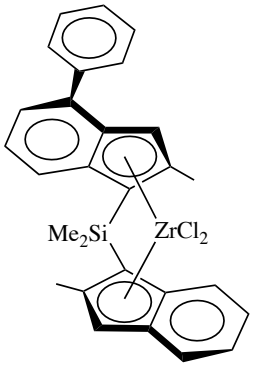

23

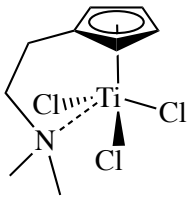

24

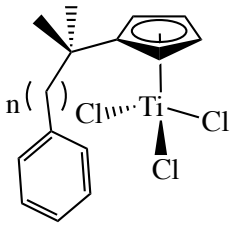

25a n = 0
25b n = 1

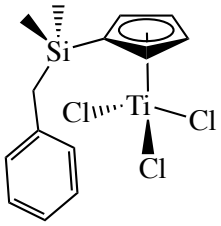

26

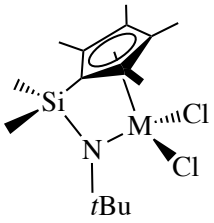

27a M = Ti
27b M = Zr

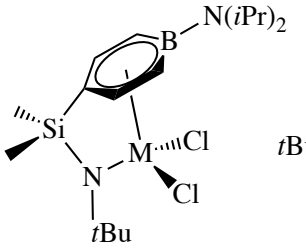

28a M = Ti
28b M = Zr

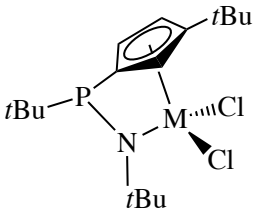

29a M = Ti
29b M = Zr

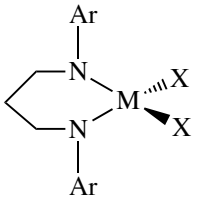

30a M = Ti, X = Me
30b M = Ti, X = Cl
30c M = Zr, X = CH_2Ph

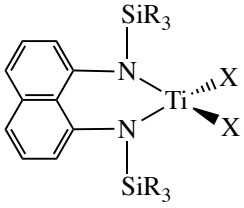

31

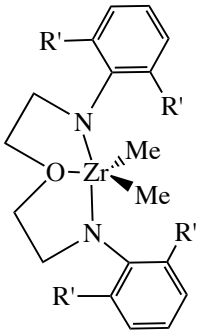

32

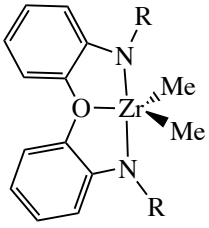

33

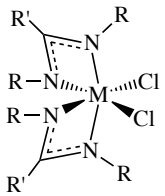

34

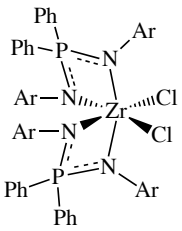

35

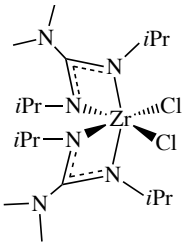

36

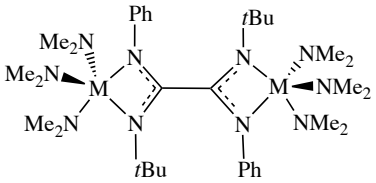

37

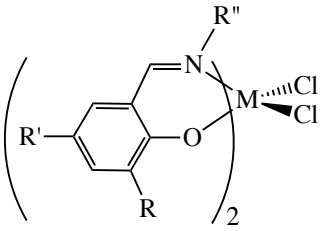

38

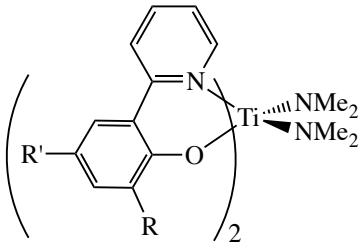

39

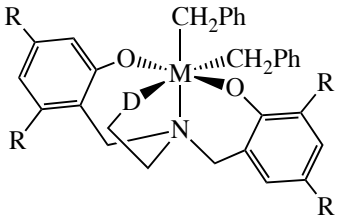

40a M = Ti, R = *t*Bu, D = OMe
40b M = Zr, R = *t*Bu, D = OMe
40c M = Zr, R = *t*Bu, D = NMe_2
40d M = Ti, R = *t*Bu, D = NMe_2

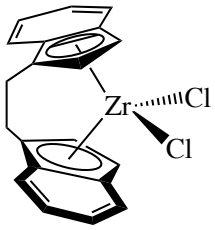

41

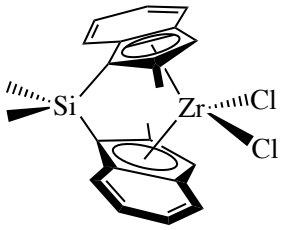

42

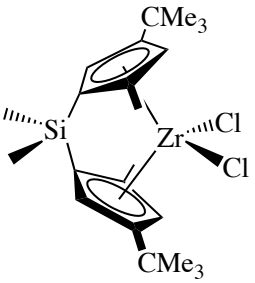

43

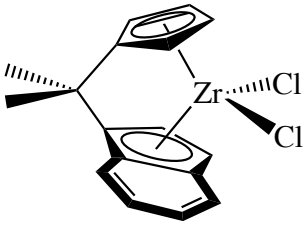

44

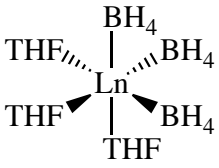

45a Ln = Nd
45b Ln = La
45c Ln = Sm

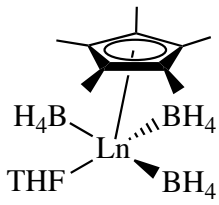

46a Ln = Nd
46b Ln = La

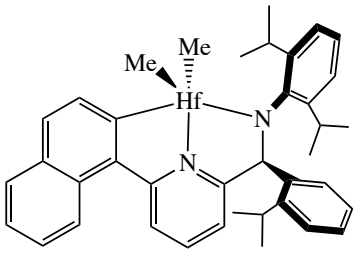

47

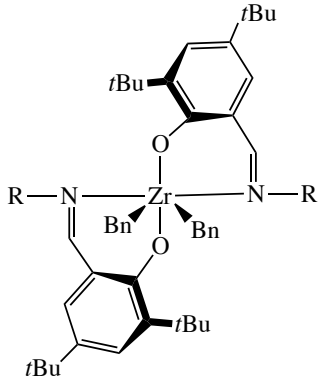

48

$[PhNHMe_2][B(C_6F_5)_4]$
49

$[Ph_3C][B(C_6F_5)_4]$
50

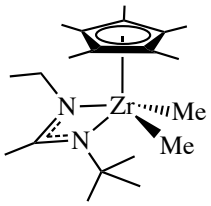

51

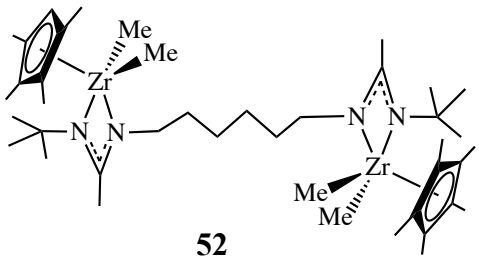

52

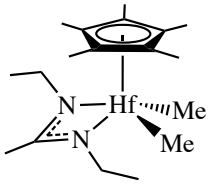

53

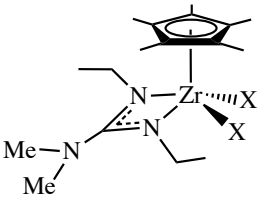

54 X = Cl
58 X = Me

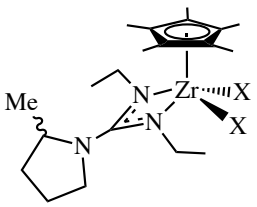

55 X = Cl
59 X = Me

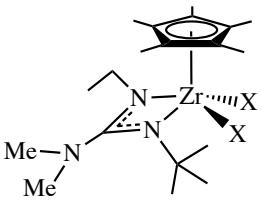

56 X = Cl
60 X = Me

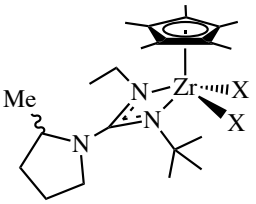

57 X = Cl
61 X = Me/Cl

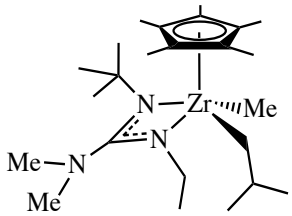

$B(C_6F_5)_4$

63

62

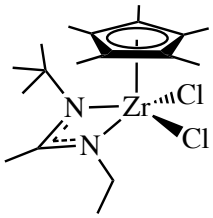

64

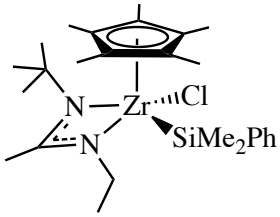

65

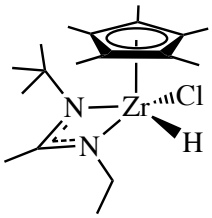

66

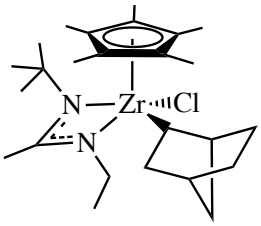

67

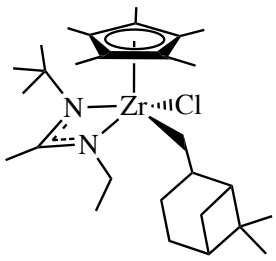

68

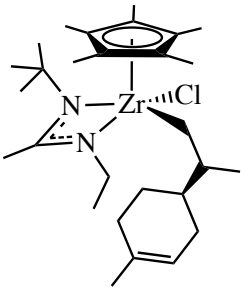

69

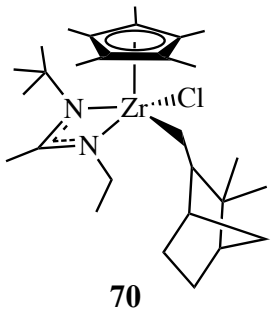

70

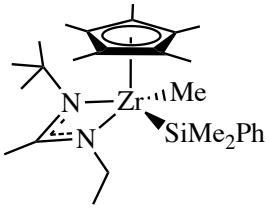

71

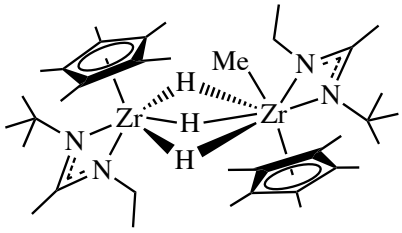

72

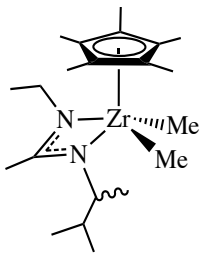
N
Zr
Me
Me
N

73

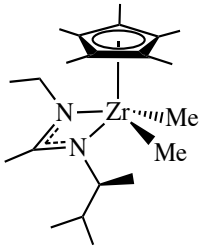
N
Zr
Me
Me
N

74

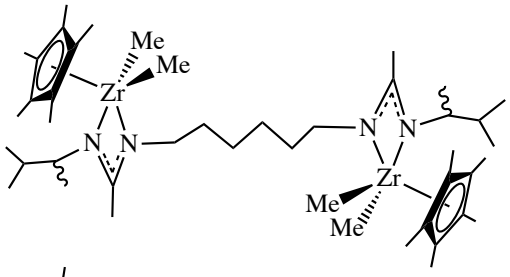
Me
Me
Zr
N
N
N
N
Zr
Me
Me

75

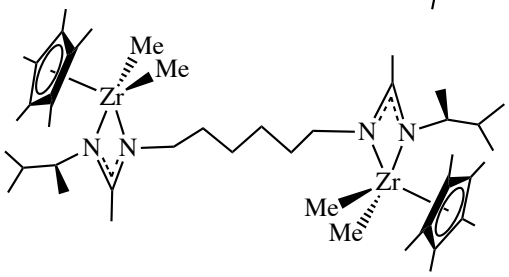
Me
Me
Zr
N
N
N
N
Zr
Me
Me

76

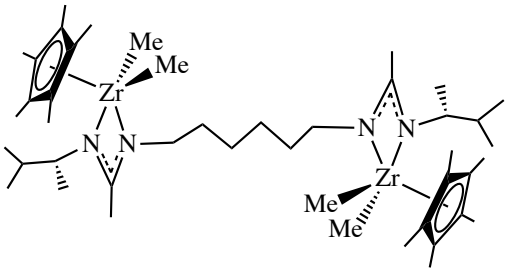
Me
Me
Zr
N
N
N
N
Zr
Me
Me

77

Chapter 1

Introduction

1.1 Ziegler-Natta Polymerizations

1.1.1 Discovery

The global demand for plastics derived from polyolefins is expected to reach 200 million tons produced annually by the year 2020 as a result of the commercialization of Ziegler and Natta's discovery of transition metal mediated polymerizations of ethylene and propene nearly six decades ago.[1-3] The development and production of plastic materials from polyolefins drives one of the largest chemical industries in the world. Versatility and robustness have allowed Ziegler-Natta polymerizations to take over the polyolefin industry, making it one of the most profitable achievements in organometallic chemistry. A Ziegler-Natta catalyst is typically composed of a group 4 transition metal component in combination with a main group metal alkyl component.

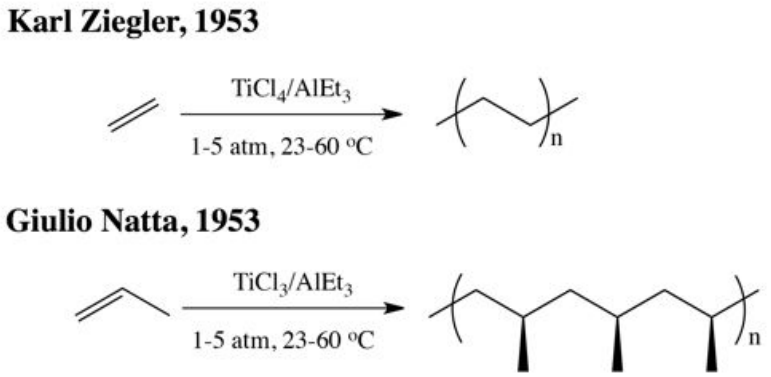

Figure 1. Ziegler and Natta's contribution to the 1963 Nobel Prize for Chemistry.

Karl Ziegler of Germany first reported the production of high-density polyethylene (HDPE) from a heterogeneous catalyst using $TiCl_4/AlEt_3$ at low pressures of ethylene in 1955.[2] From Ziegler's discovery, Giulio Natta of Italy subsequently developed a similar heterogeneous system using $TiCl_3/AlEt_3$ to prepare isotactic polypropylene and other stereoregular α-olefins.[1,4-7] This discovery would ultimately lead the two scientists to share a Nobel Prize for chemistry in 1963 (Figure 1).

Scheme 1. Activation and propagation steps for the Cossee-Arlman Mechanism (non-participating Cl's not shown).

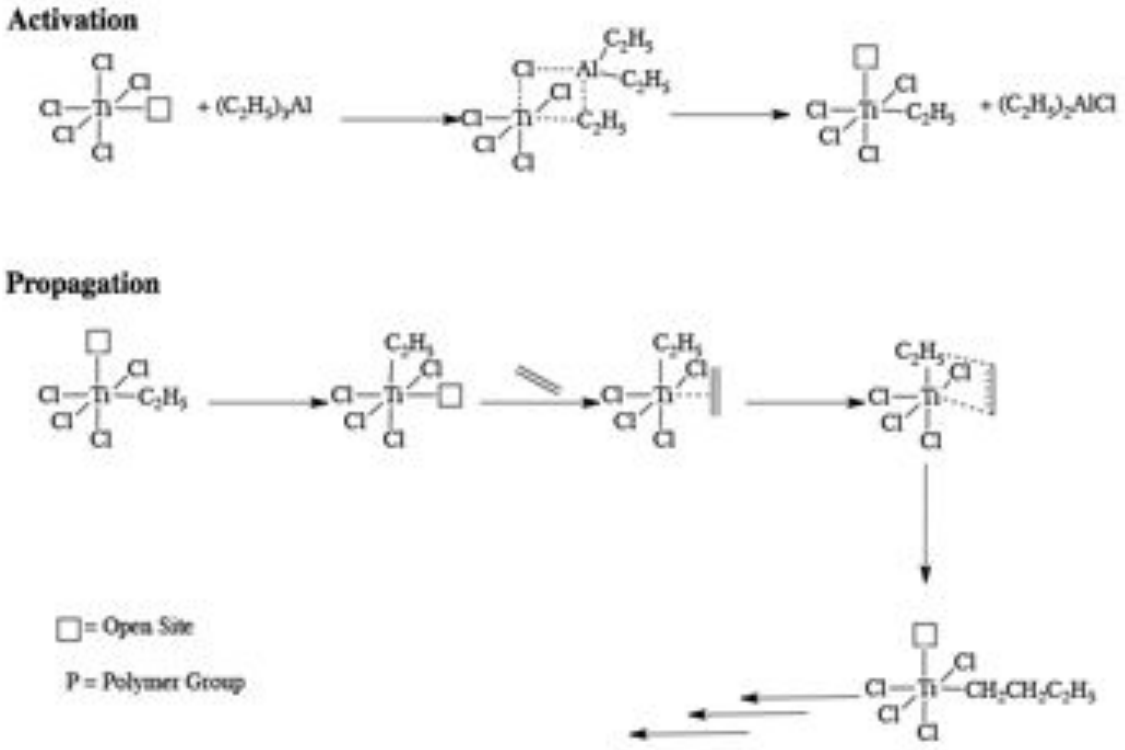

Despite nearly six decades after the initial discovery, the mechanism of action is not fully understood. Cossee and Arlman have proposed the most widely accepted

polymerization mechanism shown in Scheme 2.[8-12] Activation begins with chloride abstraction from the $TiCl_4$ crystal lattice with $AlEt_3$ to produce an active titanium alkyl species with an open coordination site. After the coordination site is opened up, the titanium center undergoes rearrangement so that the open site is axial to allow for facile olefin insertion. From there the ethylene unit inserts via a π-complex and creates the propagating species after going through a four-membered metallocycle transition state. After the coordination site is reopened, rearrangement occurs to enable the insertion of another ethylene unit and continue propagation. As shown in Scheme 2, termination of the growing polymer chain can either occur from β-elimination with a hydride transfer to (1) the titanium center, (2) the monomer, or (3) chain transfer to the aluminum alkyl species.

Scheme 2. Termination pathways for the Cossee-Arlman Mechanism.

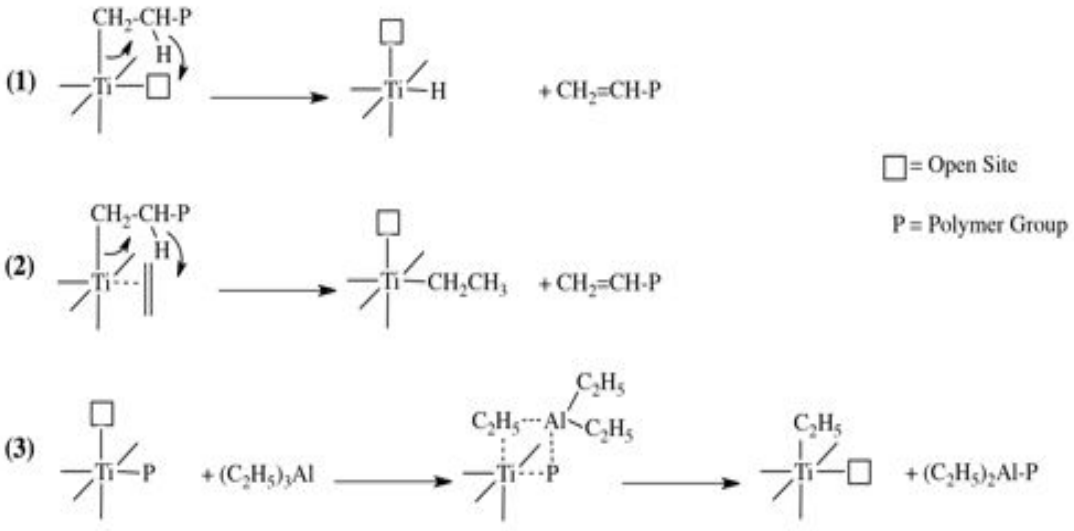

The mechanism of polymerization for propene and other higher α-olefins is the same; however, there is a pendant group on the backbone of the polymer chain whose

relative stereochemistry can vary from the last inserted monomer unit. The arrangements of these pendant groups, or tacticity, play an important role in determining the physical properties of the materials. For propene, when the relative stereochemistry of the pendant methyl groups is random, the material is considered atactic. Atactic polypropylene is an amorphous material displaying no crystallinity. Secondly, when the relative stereochemistries of the pendant groups have alternating configurations, the material is syndiotactic. These materials are typically 30% crystalline with a melting temperature around 130 ^{o}C.[13] Lastly, isotactic polypropylene makes up a majority of the commercially produced polypropylene materials, where the relative stereochemistry are all the same - the pendant methyl groups can all be found on the same side of polymer backbone. This produces a valuable thermoplastic material with a melting temperature from 160-165 ^{o}C and can be found in a large variety of household goods and automotive components.[13]

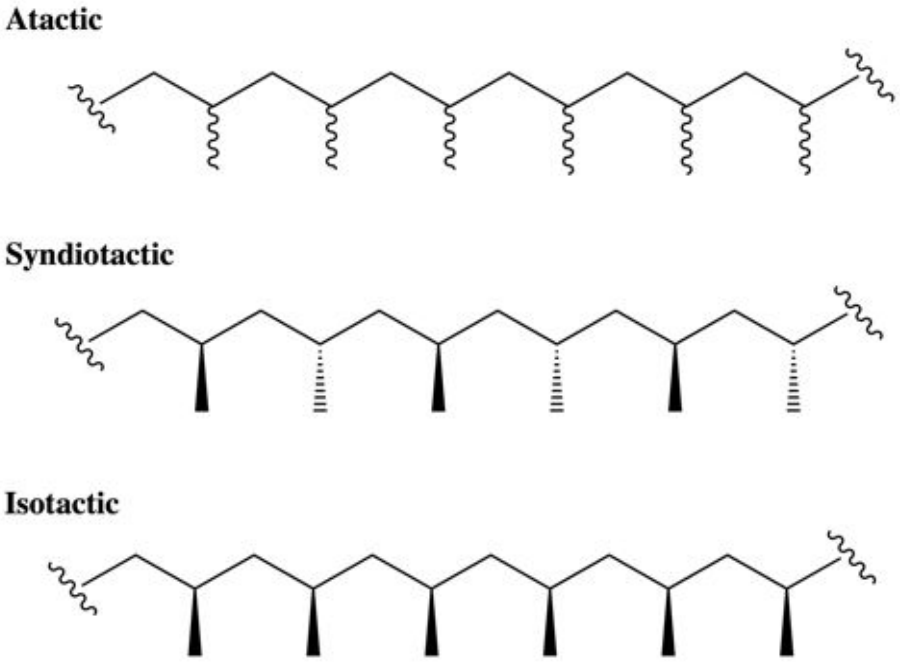

Figure 2. General polypropylene microstructures

1.2 The Metallocene Era

Ziegler-Natta catalyst systems are the largest producers of highly isotactic polypropylene, but the discovery of metallocene initiators opened up a wider range of microstructures to be commercially accessible. A metallocene is an organometallic complex composed of two cyclopentadienyl ligands.[14] With olefin polymerizations, these metallocene complexes are typically composed of group 4 metals with the general formula Cp_2MX_2, where Cp is the cyclopentadienyl system, M is Ti, Zr, or Hf, and X is either a halide or methyl group. The dichloride-substituted metallocenes are the most commonly used analogues. The homogeneity of the system allowed for more thorough investigations into their mechanisms of action.

Scheme 3. General activation of a metallocenes with a Lewis Acidic cocatalyst.

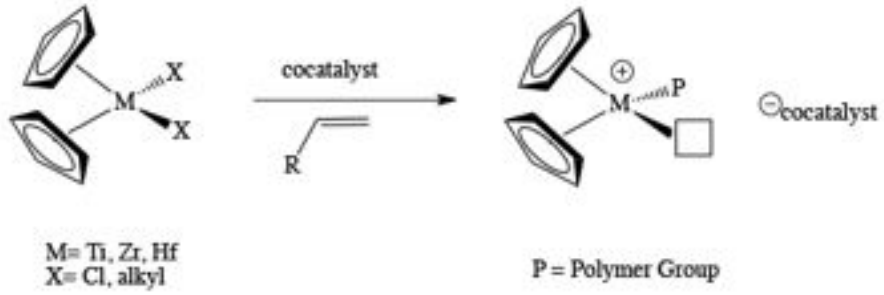

Before they can be used for polymerization, they are activated with the addition of a Lewis acidic cocatalyst to abstract a chloride to open up a coordination site for olefin insertion (Scheme 3). This creates a cationic, d^0/14-electron, metal center that is active towards polymerization. With regard to the dichloride metallocenes, methylaluminoxane (MAO) is the most common cocatalyst used; however, other aluminum alkyls and boron-centered species can be used as well.[15,16] Even with its popularity amongst the community, the exact structure of MAO is still unknown. It is generally thought to contain a mixture of Al(O)-Me oligomers as it is produced from the controlled hydrolysis of $AlMe_3$.[17] Ratios of 1000:1 or higher of [Al]:[M] are used due to the overall inefficiency of MAO as an activator. Despite its inefficiency for activation, MAO has been shown to greatly enhance the polymerization activity for metallocenes, produce ethylene/α-olefin copolymers, and have a greater control over the molecular weight of the resulting polymer.[18-20]

Scheme 4. General propagation of propene with metallocenes (L=cyclopentadienyl system).

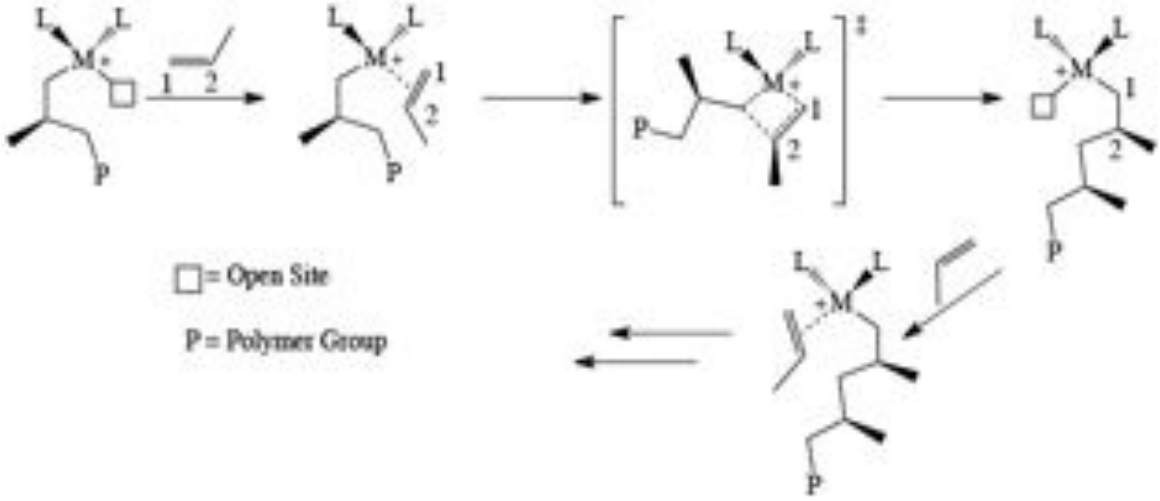

Propylene propagation occurs with the olefin coordinating to the metal center followed by 1,2-insertion into the polymer chain (Scheme 4). 2,1-insertion and 3,1-insertion can occur, but due to steric congestion from the ligand environment the 1,2-insertion is favored because it allows the less substituted carbon free to bond to the metal center.[21-23] After the insertion occurs, the monomer coordination site now bears the growing polymer chain, freeing up the site previously holding the polymer chain to insert the next monomer unit.

There are two types of enantiofacial selectivity associated with metallocenes: enantiomorphic site control and chain end control. Enantiomorphic site control occurs when the structure of the metallocene is responsible for the stereoselectivity. This can be a combination of the steric contributions from the ligand and metal center during propagation. Chain end control occurs when the last inserted monomer unit influences the selectivity of the next monomer unit. Isotactic polypropylene is produced when the

pendant methyl groups end up on the same side of the polymer chain after consecutive insertions of the same enantioface (*m* dyad). Syndiotactic material is produced when the pendant methyl groups alternate insertions into different enantiofaces (*r* dyad).

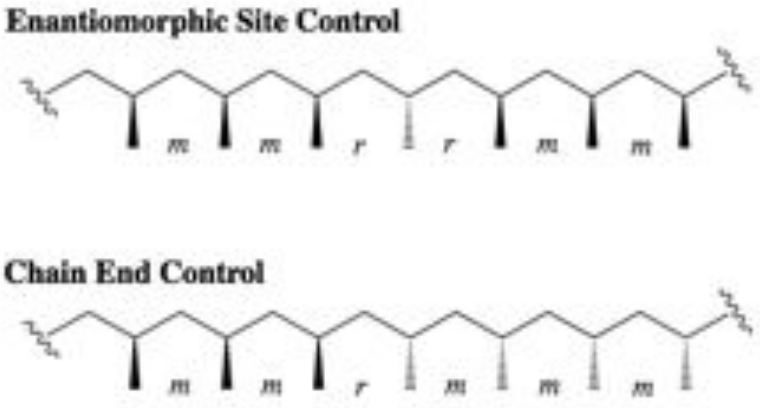

Figure 3. Enantioselectivity and resulting microstructure.

With enantiomorphic site control, the catalyst's ligand environment is able to 'correct' itself if a misinsertion occurs. After a misinsertion occurs, the incoming monomer will insert 'properly' as expected (creating another *r* dyad) as a result of the unchanging steric environment from the ligands attached to the metal center (Figure 3). As a result the pentad *mrrm* in combination with the *mmrr* pentad will be detectable in a 1:1 ratio by ^{13}C analysis.[24] If chain end control is at work, then it's expected that the stereoerror will continue throughout subsequent insertions until another stereoerror occurs. The signature pentads for this event is a ratio of 1:1 of the stereoerrors *mmrm* to *mmmr*.[24]

Scheme 5. Common termination pathways for metallocenes.

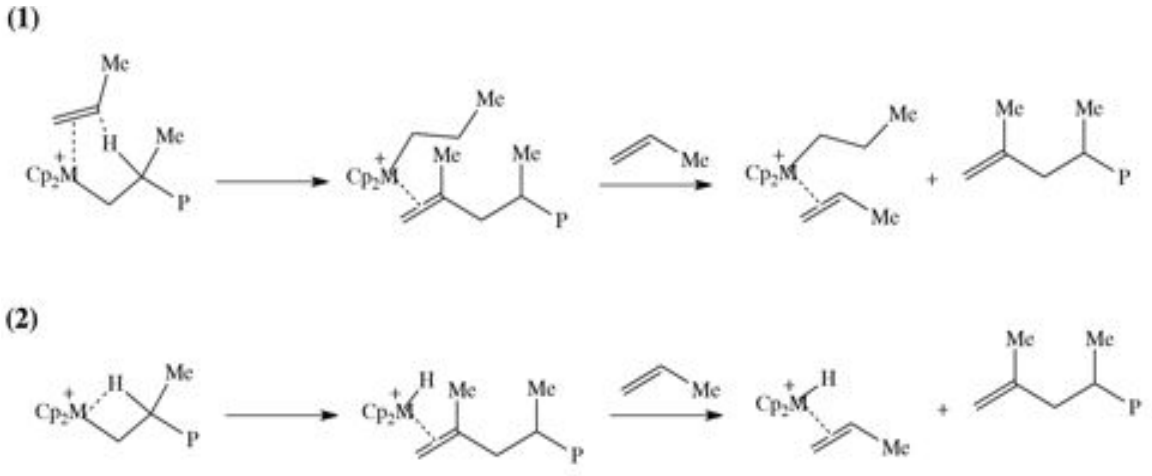

As shown in Scheme 5, the two most common methods of termination are β-hydride to the monomer (1) or β-hydride transfer to the metal center (2).[17] It is worth noting that both of these termination pathways produce identical end groups and are only discernable by kinetic studies. As seen with the heterogeneous Ziegler-Natta systems, the chains can be terminated via chain transfer to the aluminum alkyl species present.

The synthetic versatility of the metallocene gives it an edge over the heterogeneous Ziegler-Natta catalysts. It is easy to rationalize that several hundreds, if not thousands, of different metallocenes with group 4 metals have been synthesized and characterized since the complex started gaining popularity for olefin polymerization. In addition to adding substituents directly to the cyclopentadienyl systems, the cyclopentadienyl ligands can be connected to each other to make what's known as the '*ansa*-metallocene' to add more dimensionality for tuning. This synthetic flexibility makes the metallocene remarkably profitable in that polymers with specific properties can be achieved through adjustment of the ligand framework. Ewen and Kaminsky were

the first to thoroughly map out the symmetry effects the catalyst imparted on the polymer's microstructure (Figure 4).[25,26]

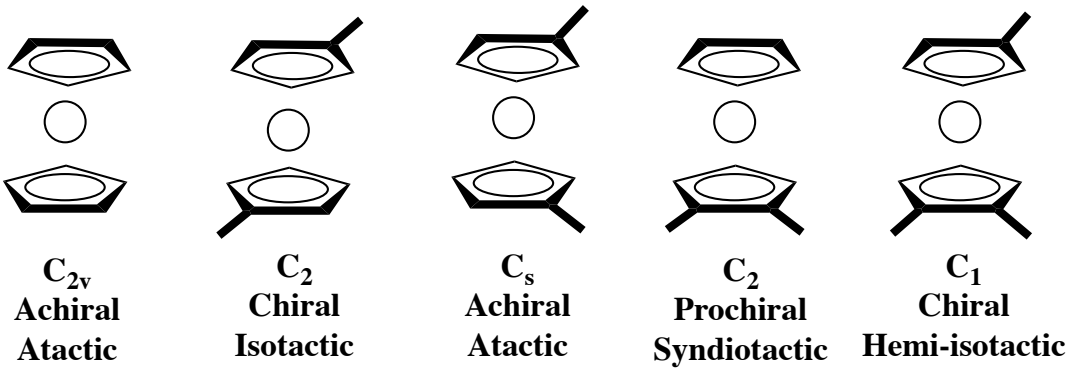

Figure 4. Summary of Ewen's Symmetry rules.

1.2.1 C_2 symmetric *ansa*-metallocenes

The general structure of an *ansa*-metallocene is shown in Figure 5. The symmetry of the metallocene is maintained by the rigidity of the bridging group (E) between the two cyclopentadienyl ligands blocking their rotation. The more common bridging groups include CH_2CH_2, Me_2C, and Me_2Si.[24] Position 1 on the Cp ring is classified as the connection to the bridging unit while positions 3 and 4 will contain the β-substituents. Positions 2 and 5 will contain the α-substituents. Substituents at positions 3 and 4 impart the most influence on stereoselectivity while the substituents at positions 2 and 5 have the most affect on the kinetics for chain release. *Ansa*-metallocenes are typically seen with zirconium due to its higher activity than hafnium, despite Hf's ability to produce polymers with higher molecular weights than those from the other group 4 metals.

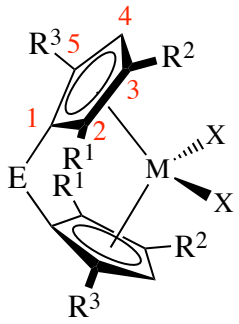

Figure 5. General *ansa*-metallocene structure

The simplest *ansa*-metallocene design **1** proved to be highly active and adept at producing isotactic polypropylene (Figure 6). Simple methyl substitutions to the Cp ring has allowed for the development of the commercially available catalyst **2**.[24] The addition of a *t*Bu substituent to the Cp ring, **3**, showed a dramatic decrease in the activity and the molecular weight of the polymers produced as a result of the increased sterics. However, the high activities were recovered with the removal of the silyl bridging group in **4**.[27]

The bridging group also allows for another synthetic stepping stone in which to tune the design. **5-8** in Figure 6 shows a series of unsubstituted bisindenyl zirconium complexes where the effect of the bridging group was studied. It was found that the stereoselectivity and molecular weight of the polymer increase in the order of H_2C < Me_2C < C_2H_4 < Me_2Si.[28-30] The ability to add substituents to the indenyl system has led to countless iterations of catalysts that can be used for polymerizations. With substitutions at the 2 and 4 position on the indenyl system, **9** and **10** have shown an increase in both activity and stereoselectivity compared to the more simple design strategies. Both of theses complexes can be found in industry where **9** and **10** produce isotactic polypropylenes of % *mmmm* > 0.93 and % *mmmm* > 0.99, respectively.[31,32]

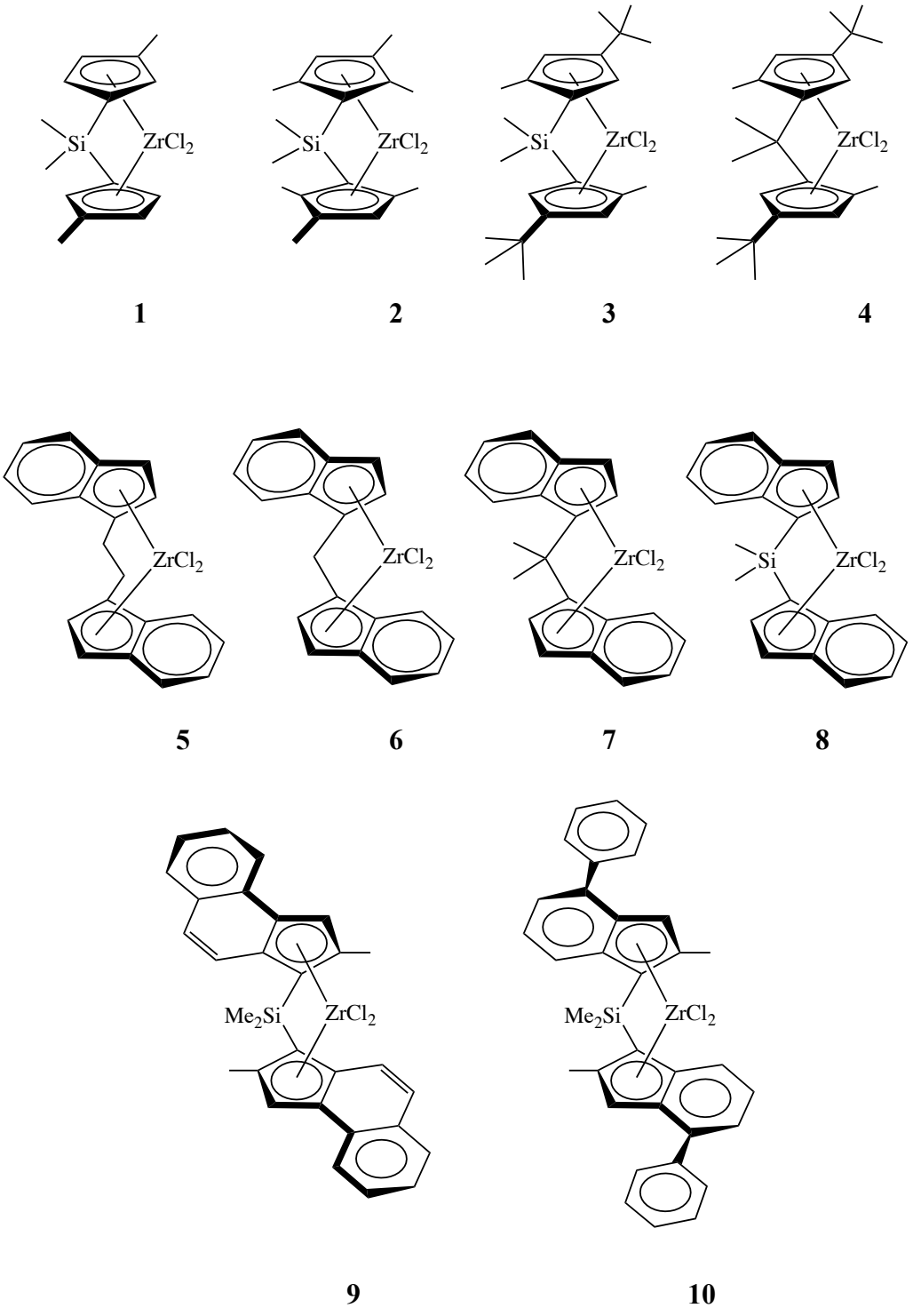

Figure 7. Selected *ansa*-metallocene catalysts.

1.2.2 C_2-*meso*-C_S metallocenes

Meso ansa-metallocenes are less active and produce only atactic polymers due to a lack of enantioselectivity that arises from the two achiral diastereotopic active sites. Waymouth and Coates developed *ansa*-metallocenes that combine the C_2-stereoselectiveness from the traditional *ansa* design with the C_S-nonstereoselective *meso ansa* design into a single catalyst design that has been dubbed 'C_2-*meso*-C_S' (Figure 7).[33-42] Catalysts using this design have the unique ability to switch symmetries as a result of the two indenyl systems being unbridged, allowing them to rotate. This switching between symmetries allows for the creation of stereoblock polymers, producing isotactic material in the C_2 conformation and atactic material in the C_S conformation. The first iteration of this new design strategy **11** was able to produce elastomeric materials with moderate stereoselectivity ($0.24 < \%\ mmmm < 0.40$).[33] Substitution to the phenyl group, **12**, resulted in a catalyst that was less stereoselective and produced lower molecular weight polymers.[34] However, substitution with the CF_3 group **13** increased the stereoselectivity ($0.45 < \%\ mmmm < 0.73$).[37]

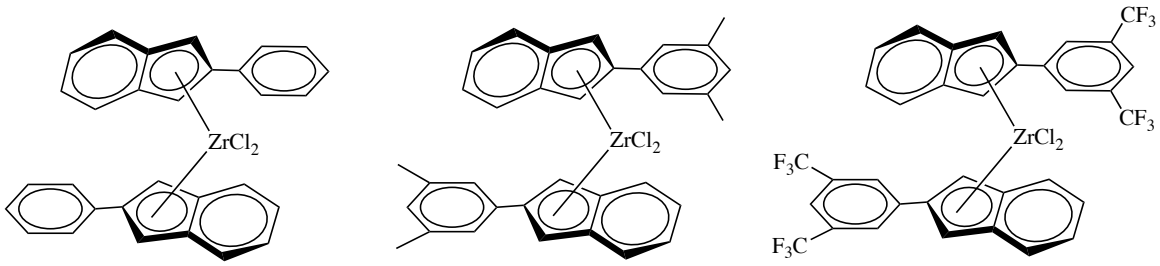

11 **12** **13**

Figure 8. Selected C_2-*meso*-C_S metallocenes.

1.2.3 C_S metallocenes

14 was the first reported catalyst to produce syndiotactic polypropylenes.[43] The species is C_S symmetric that results in two enantiotopic active sites. An interesting feature with this catalyst is that enantiomorphic site control governs propagation in that the pentad *rmmr* is seen, where the '*mm*' signals the correction of the misinsertion. This design appears to be less responsive to ligand variations, and the most success has been seen which substitutions to the bridging group. With the family of compounds shown in Figure 8, the syndiotacticity decreases from $Me_2C > Ph_2C > Ph_2Si > Ph_2C$ while the molecular weight decreases from $Ph_2C > Me_2C \sim Me_2Si > Ph_2Si$.[44,45] As with many of the other metallocene designs, titanium and hafnium are both reported to be considerably less active than zirconium.[46]

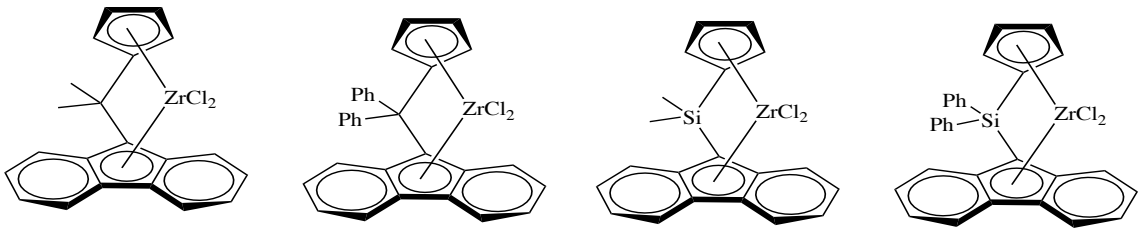

14 **15** **16** **17**

Figure 9. Selected syndiotactic producing catalysts.

1.2.4 C_1 symmetric metallocenes

The C_1 symmetric metallocenes are unique in that they are able to produce materials with a variety of microstructures including: hemi-isotactic (mostly isotactic and contains stereoerrors at regular intervals), partially isospecific, and completely isospecific.[13] Production of this type of metallocene can be advantageous in that stereoselectivity can still be achieved without the synthesis of the *meso* isomer that is

produced with synthesis of any *ansa*-C_2 species. The *meso* forms of *ansa*-metallocenes are typically unwanted products in that they produce low molecular weight atactic polymers, and are synthetically challenging to remove from the desired product. C_1 symmetric species are able to impart stereoselectivity as a result of their diastereotopic active sites, where tuning of the ligand environment can produce the desired microstructure. The hemi-isotactic microstructure is a result of a site switch between an isospecific active site and an aspecific active site.[47,48] Generally, the molecular weights and activities are lower than what is reported for C_2 designs, but they are able to access a wider range of materials.

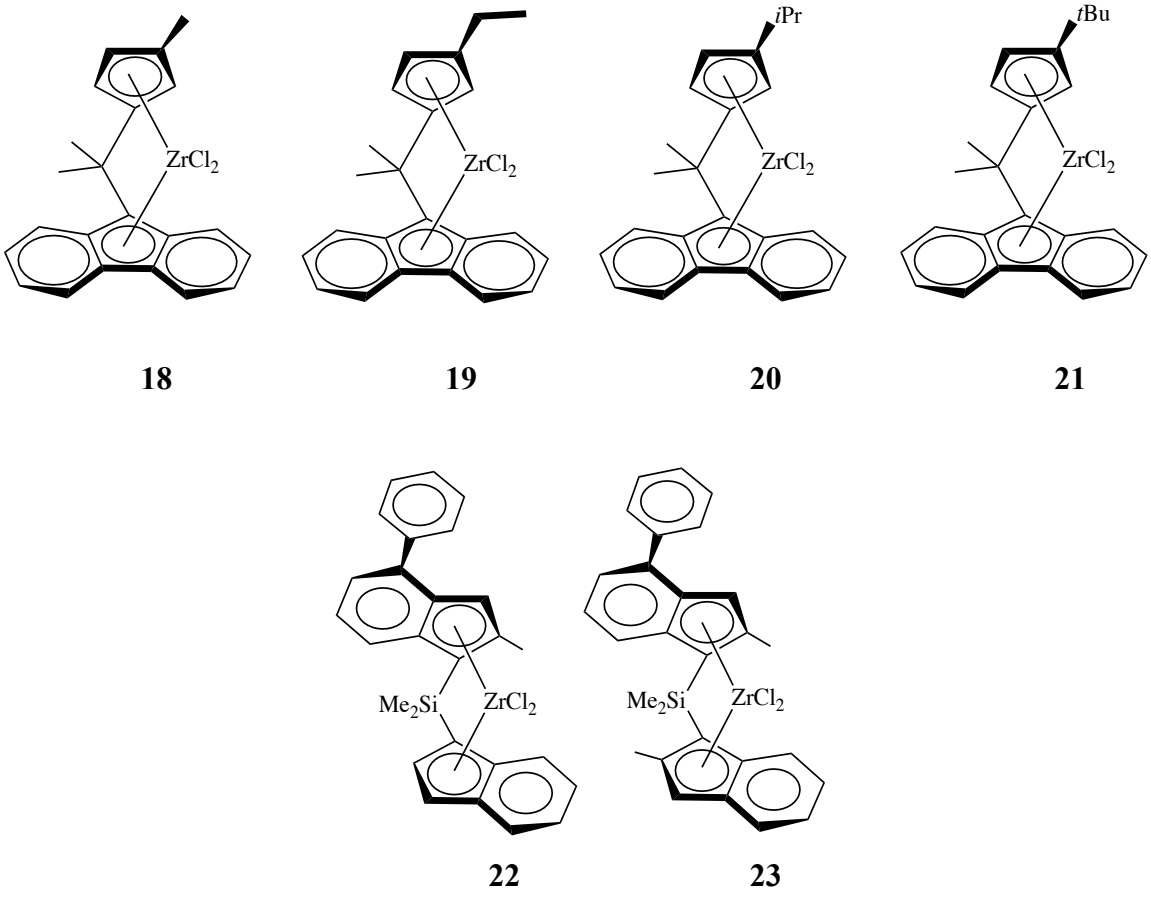

18 **19** **20** **21**

22 **23**

Figure 10. Selected C_1 symmetric metallocenes.

18 (Figure 9) was the first reported by the Hoechst and Fina groups, and the first complex to produce hemi-isotactic polypropylene (*mmmm* = 0.1875).[49-52] This complex exhibits a remarkable ability to tune sterics and electronics. Changing methyl group on the Cp ring to an ethyl group (**19**) resulted in nearly hemi-isotactic material; however, increasing the group to an isopropyl group and a *tert*-butyl group increased the stereoselectivity to *mmmm* = 0.44 and *mmmm* = 0.76, respectively.[53] Spaleck and coworkers have reported the highest performing design strategy, **22** and **23**, where they substitute the C_2 symmetric indenyl systems previously developed by the Hoechst group that are currently used for industrial polymerizations.[54] These C_1 symmetric catalysts produce high molecular weight (M_w = 530 kDa) and highly isotactic polypropylenes (*mmmm* > 0.96).

1.3 The Post-Metallocene Era

Although revolutionary to the field of olefin polymerization and still the most widely used catalyst designs in industry, metallocenes are still crippled by their β-hydride termination pathways that prevent the production of polymers with extremely tight molecular weight control or block polyolefins. In a living polymerization the ability to self terminate has been removed, and the active site will continue to remain active as long as there is a continuous supply of monomer. Typical characteristics of living polymerizations include:

(1) the polymerization will proceed such that there is complete consumption of the monomer;

(2) the molecular weight (M_n) increases linearly;

(3) the active centers remain active and constant;

(4) exact control over molecular weight through stoichiometry;

(5) narrow polydispersities (<1.10);

(6) ability to synthesize block copolymers through sequential additions;

(7) ability to end functionalize.[55]

Living polymerizations have been well documented for anionic and radical polymerizations, and the first reported living Ziegler-Natta polymerization occurring with a $V(acac)_3/Et_2AlCl$ catalyst/cocatalyst system.[56]

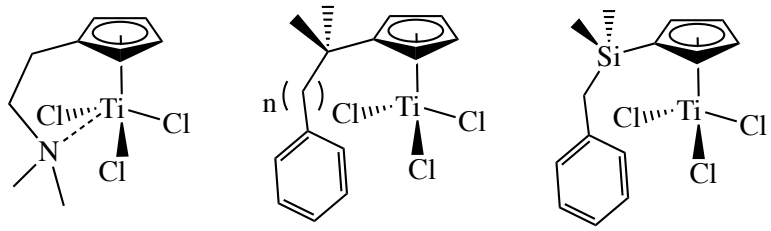

24 **25a:** n = 0 **25b:** n = 1 **26**

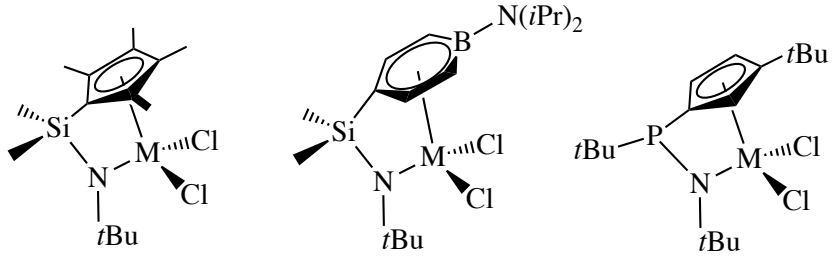

27a: M = Ti **27b:** M = Zr **28a:** M = Ti **28b:** M = Zr **29a:** M = Ti **29b:** M = Zr

Figure 12. Cp related catalysts.

1.3.1 Cp Derived Catalysts

There is precedent for non-group 4 metals being used for living polymerizations, but it remains the most popular group of metals in use. A less radical redesign of the metallocene structure led to the development of complexes containing only a single cyclopentadienyl unit coordinated to the metal center to create 'piano-stool' complexes such as **24-26** (Figure 10). Activities of these complexes were found to exhibit low polymerization activities until donor ligands were coordinated to the metal center and then success was seen with a radical increase in activity, and not surprisingly, air and thermal stability.[57-63] In the case of **25** and **26**, coordination of the arene substituent is not seen until after the trichloride species has been activated with a Lewis acid.

Linkage of the cyclopentadienyl system to the metal center via anionic amide substituents have also gained popularity and have spawned off another subset of catalysts known as constrained geometry catalysts (CGCs) **27-29** (Figure 10). One of the simplest CGCs, **27**, was shown to be highly active at copolymerizing ethylene and α,ω-functionalized olefins.[64-66] It was found that modification of the steric environment at the cyclopentadienyl unit could tune the amount of comonomer incorporated in copolymerizations with ethylene and 1-octene when **28** was employed.[67] Another example of one of the many CGCs available is **29** where a phosphorous bridge was used instead of the traditional silyl bridge to produce linear high molecular weigh polyethylene.[68]

1.3.2 Diamido Complexes

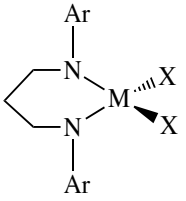

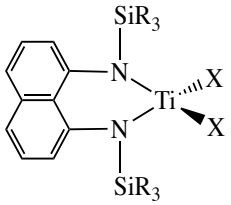

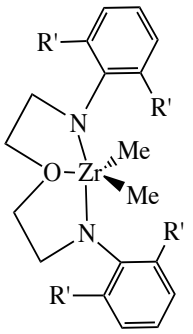

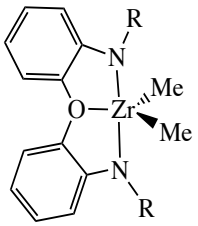

30a: M=Ti, X =Me
30b: M=Ti, X =Cl
30c: M=Zr, X =CH_2Ph

31 **32** **33**

Figure 13. Diamido catalysts

In a radical departure from the previous design strategies, McConnville and coworkers reported the synthesis and successful living homopolymerizations of 1-hexene at room temperature using the diamido titanium complex **30a** in a polar solvent.[69,70] Using the dichloride analogue, **30b**, Uozumi and coworkers were able to synthesize isotactic polypropylene (%*mmmm* < 0.83) due to enantiomorphic site control from coordination of the solvent cyclohexene or a second propylene unit.[71,72] The dibenzyl derivative, **30c**, showed low activity towards ethylene polymerization.[73] It is interesting to note that much higher polymerization activities were seen with the more rigid silyl-diamide titanium complex **31**.[74,75]

Schrock and coworkers designed **32** and **33** in an effort to stabilize the cationic active species through the use of an additional donor in the ligand frame.[76-81] Both of these complexes were active towards 1-hexene homopolymerizations, but **32** was found to terminate via β-hydride elimination.[82] However, with slight modifications to the

structure they were able to obtain living polymerizations of 1-hexene at 0 ^{o}C using **33**.[76,79,81,83] Extensive stability studies showed an obvious correlation between their polymerization activities and the stability of their respective active species. There is competition between the decomposition of the active species with the insertion of the olefin, resulting in a nonliving polymerization in the case of **32** where the decomposition occurs more rapidly than the polymerization.[83,84]

1.3.3 Amidinate Complexes

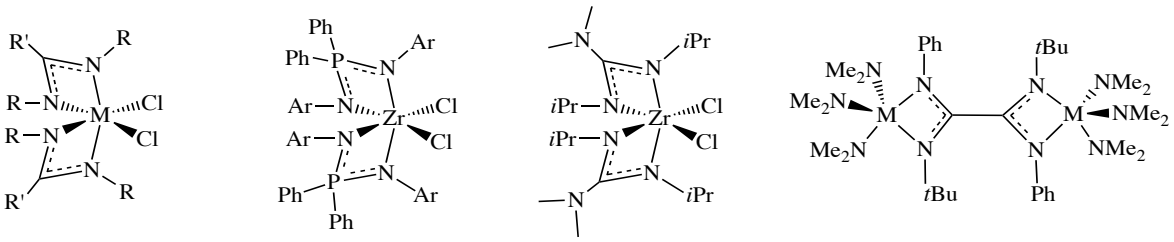

34 **35** **36** **37**

Figure 14. Amidinate based catalysts.

Moving towards the amidinate design, steric equivalent to a cyclopentadienyl ligand, Eisen and coworkers first reported the synthesis of isotactic polypropylene via living polymerization using a catalyst containing two monoanionic amidinate ligands **34**. However at lower pressures of propylene, the epimerization with regard to the amidinate proceeded much faster than the propagation of the propylene creating an atactic polymer.[85,86] The related bis(iminophosphonamide) complex, **35**, reported by Collins and coworkers had a much higher activity towards ethylene polymerization than the bisamidinate complexes reported by Eisen.[87] The N-bearing guanidinate framework **36** has also been proven to be successful with ethylene polymerizations.[88] Interestingly,

Green and coworkers have reported moderate activities for a novel binuclear amidinate design **37**.[89]

1.3.4 Alkoxide Based Complexes

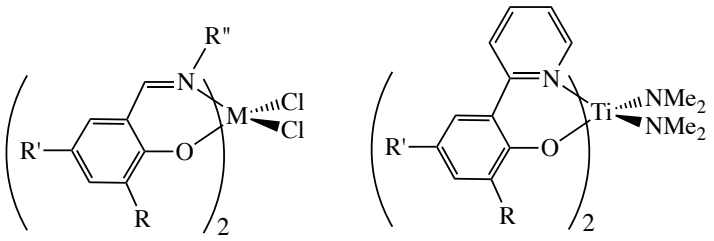

38 **39**

Figure 15. General structure of salicylaldiminato catalysts.

Fujita and coworkers at Mitsui Chemicals reported highly active catalysts based on the salicylaldiminato ligand frame with the general structure shown in Figure 13.[90] An interesting component of this system is that when titanium is used for the metal in **39**, syndio-rich polypropylene is produced, but when zirconium or hafnium is used only atactic to slightly syndiotactic polymers are produced.[91-93] It has been proposed by Cavallo and coworkers that the unusal 2,1-insertion to produce syndiotacic material is a result of the stereochemistry influencing the configuration of a fluxional octahedral active site.[94]

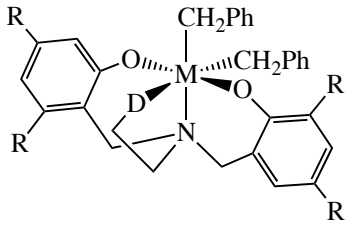

40a: M=Ti, R=*t*Bu, D=OMe
40b: M=Zr, R=*t*Bu, D=OMe
40c: M=Zr, R=*t*Bu, D=NMe_2
40d: M=Ti, R=*t*Bu, D=NMe_2

Figure 16. General structure of bis(phenoxy)amino catalysts.

Another group of highly successful alkoxide based catalysts are the bis(phenoxy)-amino catalysts developed by Kol and coworkers (Figure 14).[95,96] When activated with $B(C_6F_5)$ they proved to be extremely adept at polymerizing 1-hexene at room temperature. Between the series, the catalysts that contained D = OMe_2 showed more activity over those with D=NMe_2, and the zirconium analogues were considerably more active than the titanium analogues.[86,97,98]

1.4 Coordinative Chain Transfer

With the advancements in single-site catalysts over the last few decades, there has been one major hurdle that is finally being addressed and that is the cost associated with using transition metal species for catalysts. Single-site catalysts are only able to grow one chain per metal site, making the process inherently expensive with regard to the amount of transition metal catalysts needed in order to produce large quantities of polymeric materials. By enabling the growth of multiple polymer chains per metal site, the high cost of the process can be reduced while maintaining control over the polymerization, making single-site catalysts even more profitable. Over the last two decades, a type of polymerization known as coordinative chain transfer polymerization (CCTP), involving the addition of a main group metal alkyl species to enable the growth

of multiple polymer chains, has been developed.[99-107] With CCTP, the growing polymer chain transfers from the active transition metal species to the main group metal alkyl species that is acting as the chain transfer agent (CTA), whereupon the transition metal species begins to propagate a different polymer chain. It is important to consider the amount of CTA used as increasing the amount of the transfer agent will allow for an increase in the number of polymer chains allowed to grow at the more expensive transition metal species.

Scheme 6. Traditional coordinative polymerization and coordinative chain transfer polymerization.

Traditional Coordinative Polymerization

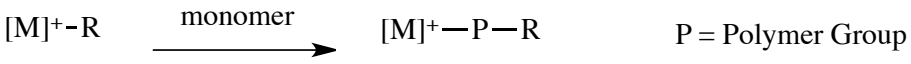

CCTP

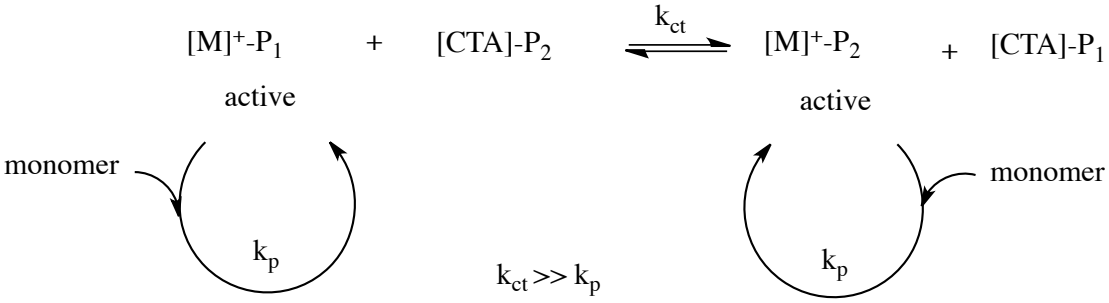

CCTP can be considered a degenerative group transfer process in that a dynamic equilibrium that exists between the active transition metal species and the CTA.[108] This transfer must occur more rapidly than the propagation and be reversible so that multiple polymer chains are allowed to grow (Scheme 6). Also, β-hydride elimination and other termination pathways must not occur to ensure that there is strict control over the

molecular weight of the polymer. This process also allows for facile functionalization given that the polymer chains are capped with the CTA, which could access an entirely new area of materials and applications.

1.4.1 CCTP of Propene

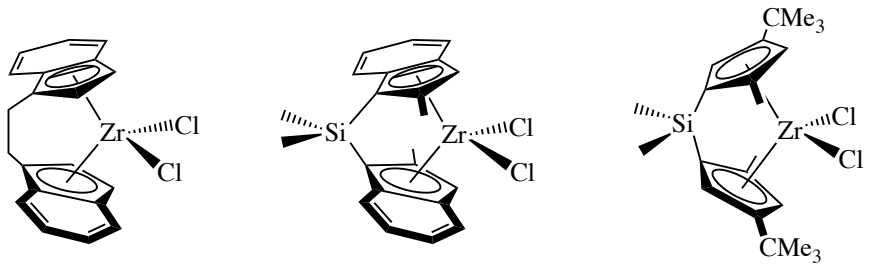

41 **42** **43**

Figure 17. Zirconium initiators for CCTP of propene

A majority of the initiators used with CCTP of propylene are zirconium based; however, the first example of CCTP of propylene was reported by Sita and coworkers using a non-stereoselective hafnium amidinate initiator **53**.[107,109-115] Isospecific polypropylene was obtained under CCTP conditions using both **41** and **42** after activation with $[Ph_3C][B(C_6F_5)_4]$ using either $AlEt_3$ or Al*i*Bu_3 as a chain transfer agent.[111] As expected with coordinative chain transfer polymerization, it was found that the molecular weight of the resulting polymers decreased as the amount of chain transfer agent was increased. It was also found that the $AlEt_3$ was a more efficient chain transfer agent than Al*i*Bu_3. Evidence of β-hydride transfer to the metal center and subsequent reinsertion into the metal-hydride was seen in the form of *n*-propyl groups by ^{13}C NMR end group analysis. This β-hydride transfer was suppressed with a change in the reaction conditions: lowering the polymerization temperature and activation with $AlEt_3$ containing

MAO.[113] Complex **43** also afforded highly stereoregular (*mmmm* = 0.99-0.95) and regioregular (100% 1,2-insertion) under CCTP conditions using $AlMe_3$/MAO.[112] Increased amounts of $AlEt_3$ resulted in lower molecular weight polymers.

1.4.2 Random Copolymer Production

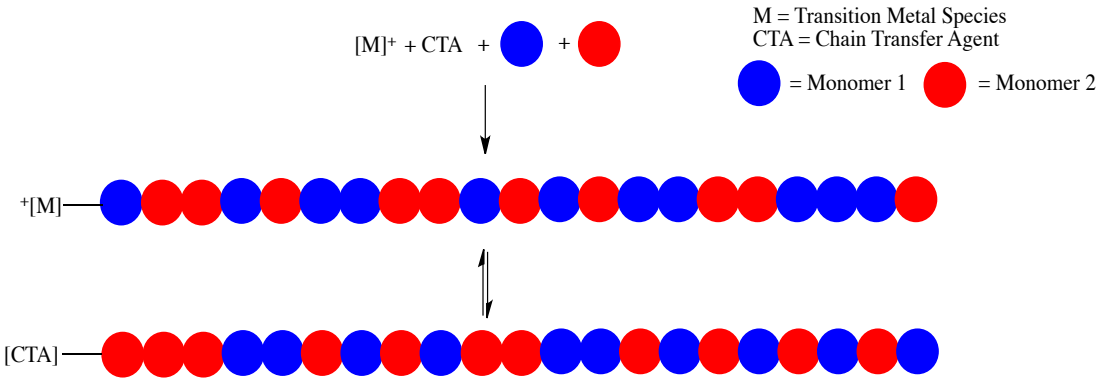

Figure 18. Random copolymer production with CCTcoP.

Statistical coordinative chain transfer copolymerization (CCTcoP) (Figure 16), which has mainly been used to produce ethylene based random copolymers, involves the use of one catalyst and one chain transfer agent to produce random copolymers.[108] The first reported use of CCTcoP was the copolymerization of ethylene and allylbenzene using **18** (Figure 9).[116] After activation with MAO at 80 ^{o}C under 1.2 bar of ethylene, the maximum amount of comonomer incorporated was 20.0%. It was determined that chain transfer to the aluminum species was more favored after end group analysis and the molecular weight reduction as the MAO was increased. Chain transfer was also seen as the preferred termination pathway for this combination of allylbenzene and catalyst.

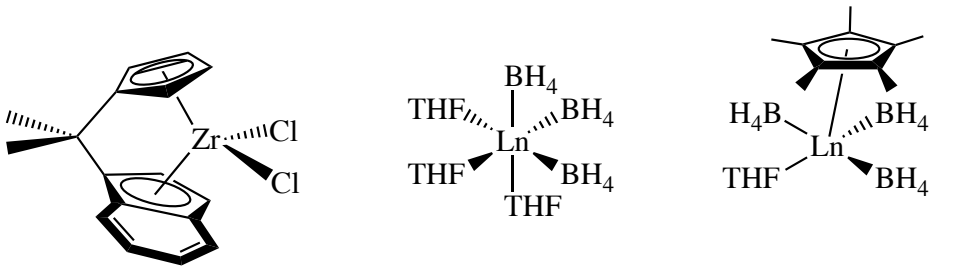

44

45a: Ln = Nd
45b: Ln = La
45c: Ln = Sm

46a: Ln = Nd
46b: Ln = La

Figure 19. Catalysts for CCTcoP.

Interesting ethylene-co-norbornene materials were synthesized via CCTcoP using **44**/MAO in combination with aluminum and zinc alkyls.[117] Chain transfer from the zirconium to the main group metals was proved with the decreasing molecular weights of the polymeric materials. Modest additions of CTA were able to increase the comonomer incorporation by ~4x but large accesses of CTA would decrease the level of incorporation. It was found that the bulkier aluminum alkyl species were ineffective in that they were too sterically hindered and would not react with cationic active species.[118,119]

In a rare departure from group 4 catalysts, remarkable control over comonomer control and stereocontrol between isoprene, styrene, and 1-hexene was achieved through the use of a series of lanthanide-based catalysts **45** and **46** (Figure 17) by tuning the amounts of either the magnesium or aluminum alkyl CTAs.[120-122] Valente and coworkers were able to obtain precise microstructure control over the resulting styrene-co-isoprene material when using equimolar amounts of both monomers with **46b** by controlling the amount of $MgEt_2$ (Scheme 7). With 1 equivalent of CTA they were able to obtain a

material with 12% styrene incorporation, but an increase of the CTA to 10 equivalents increases the styrene incorporation to 32% while maintaining high stereoselectivity for the polymerization of the isoprene.[122] There is also a decrease in the molecular weights of the polymers from 45.2 kDa to 3.3 kDa with the increased amount of $MgEt_2$. The addition of aluminum alkyls showed a moderate 1.5x increase in the styrene incorporation while retaining stereoselectivity over the isoprene. However, the larger molecular weights were indicative that the chain transfer process to the aluminum species was not as efficient as it is with the magnesium CTA. The process was successfully adapted for the first example of styrene/1-hexene copolymerizations as increasing the magnesium-CTA was able to produce an increase in the amount of 1-hexene that was incorporated into the polymeric material.[121]

Scheme 7. CCTP controlled comonomer incorporation.

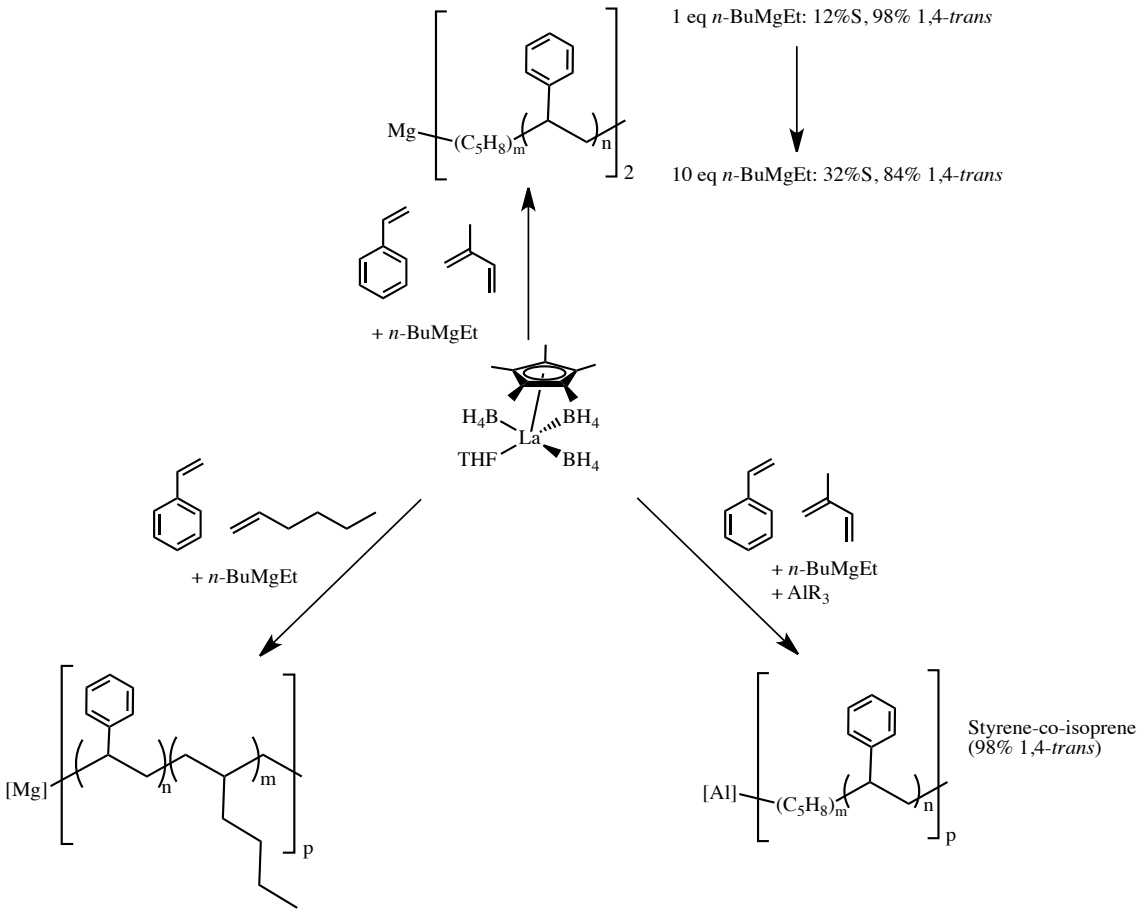

1.4.3 Chain Shuttling for Block Copolymers

Arriola and coworkers reported the first case of using CCTcoP with two catalysts to create a new class of thermoplastic elastomers *via* a process dubbed 'chain shuttling'.[106] These novel materials were comprised of a random copolymer of sequential low 1-octene containing crystalline segments ('hard' blocks) and low ethylene containing non-crystalline ('soft' blocks) segments. These materials are invaluable in that the hard blocks with low 1-octene incorporation have high melting temperatures whereas the soft blocks with high 1-octene incorporation display low glass transition temperatures.[123] Also, the resulting microstructures of these materials led to better organization with regard to their crystalline morphologies than random ethylene/1-octene copolymers.

These materials are synthesized via the presence of two catalysts, a pyridylamide hafnium (**47**) and a bis(phenoxyimine) zirconium (**48**) complex with $ZnEt_2$ added to serve as the chain shuttling agent (CSA) transferring the polymer chains between the two propagating species (Scheme 8). The zirconium species has a lower affinity for the propagation of the 1-octene than the hafnium species enabling the production of two polymer chains with different levels of comonomer incorporation. As seen previously with other CCTP examples, increasing the amount of the CSA led to shortened polymer chains.[124]

Scheme 8. Chain shuttling polymerization with ethylene and 1-octene.

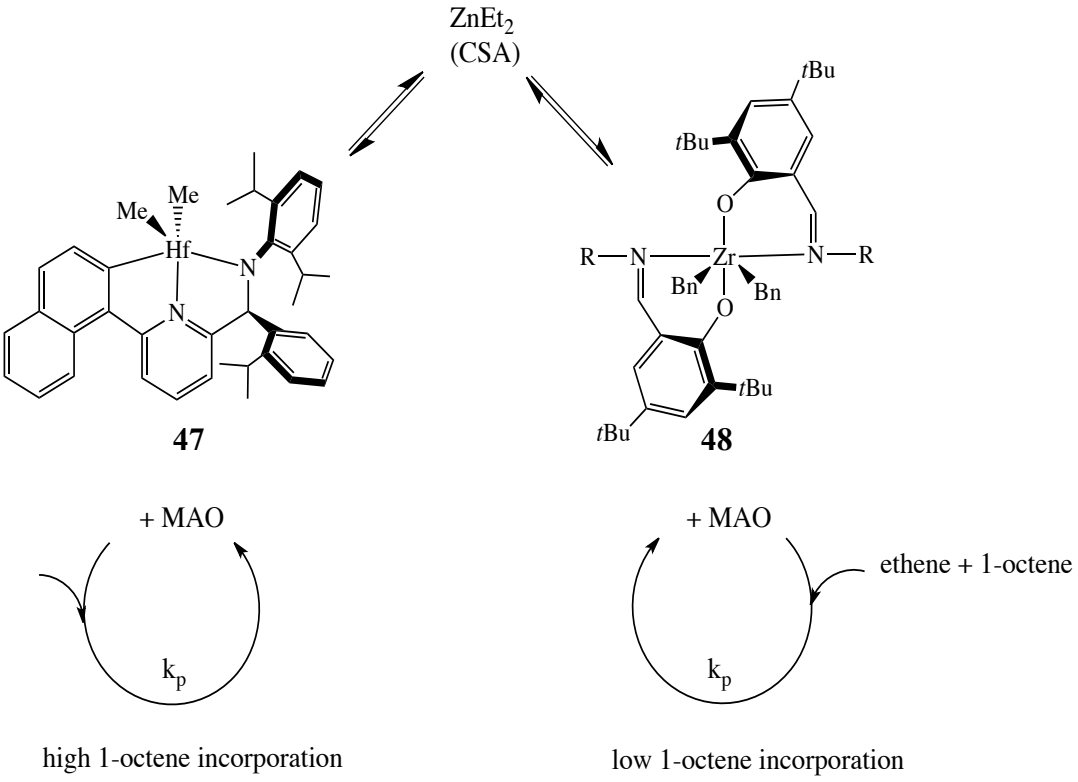

1.5 'CpAm' System – A Closer Look

1.5.1 Discovery

Scheme 9. 'One pot' synthetic route for amidinate precatalysts.

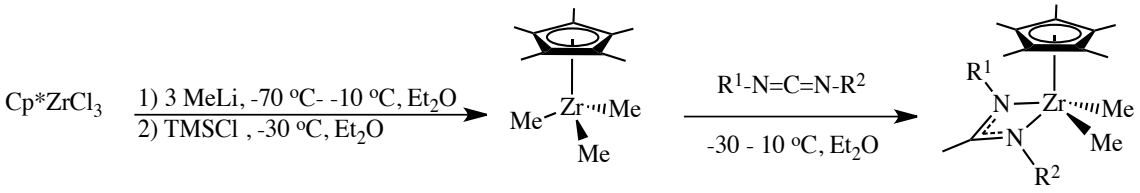

In 2000, the Sita group first reported the use of a novel zirconium amidinate precatalyst for the use in living polymerizations.[125] Once activated by $[PhNHMe_2][B(C_6F_5)_4]$ (**49**) or $[Ph_3C][B(C_6F_5)_4]$ (**50**) the C_1 symmetric active species **51**, R^1 = Et and R^2 = *t*Bu, proved adept at polymerizing 1-hexene in a stereospecific fashion. This system has been successful with several α-olefins including: propene, 1-butene, 1-octene, 4-methyl-1-pentene, 1,6-hexadiene, and other higher olefins. Due to the living nature of the polymerizations, block copolymers and stereo-block polymers have been able to be synthesized using a single initiator. An impressively wide range of initiators can be synthesized via a 'one pot' synthesis through the insertion of a carbodiimide into a Zr-Me bond after creating the $(\eta^5\text{-}C_5Me_5)ZrMe_3$ species in situ upon methylation of the commercially available $(\eta^5\text{-}C_5Me_5)ZrCl_3$.

Scheme 10. Metal-centered epimerization of the amidinate frame of **51**.

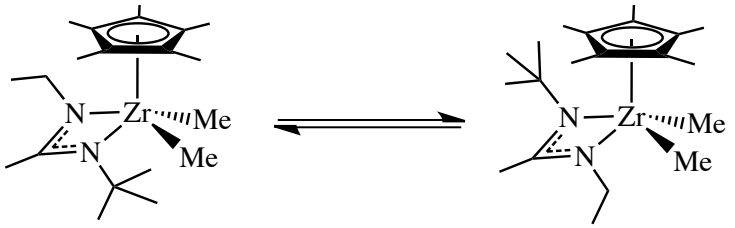

The cationic active species is configurationally stable; however, it has been found that the neutral precatalyst species is not configurationally stable and suffers from metal-centered epimerization with regard to the amidinate frame (Scheme 10). The coalescence temperature was found to be 223 K with a $\Delta G^{\neq}$ of 10.9 kcal/mol.[126] The stereoselectivity of the active species arises from its inherent C_1 symmetry as a result of $R^1 \neq R^2$. Once the neutral species is activated by demethylation, two enantiomers (R and S manifolds) are produced and both will produce an isotactic polymer under the reaction conditions via enantiomorphic site control (Scheme 11). With each of these manifolds, the growing polymer chain will isomerize to the *t*Bu side and allow for the insertion of the incoming olefin to occur on the less sterically hindered ethyl side. This rate of this isomerization is much more rapid than the rate of the propagation.

This polymerization occurs in a living fashion in that no termination β hydride elimination is detected via ^{1}H analysis of the vinylic region. It has been found that this species will β hydride eliminate, but will hold onto the vinyl terminated chain and subsequently reinsert into the active metal center.[127] Because this is a living process, the molecular weight of the polymer has been shown to increase linearly in regard to the consumption of the monomer and the resulting polydispersities are quite narrow (PDI < 1.10).

Scheme 11. Enantiomorphic site control of **51** during the polymerization of propene.

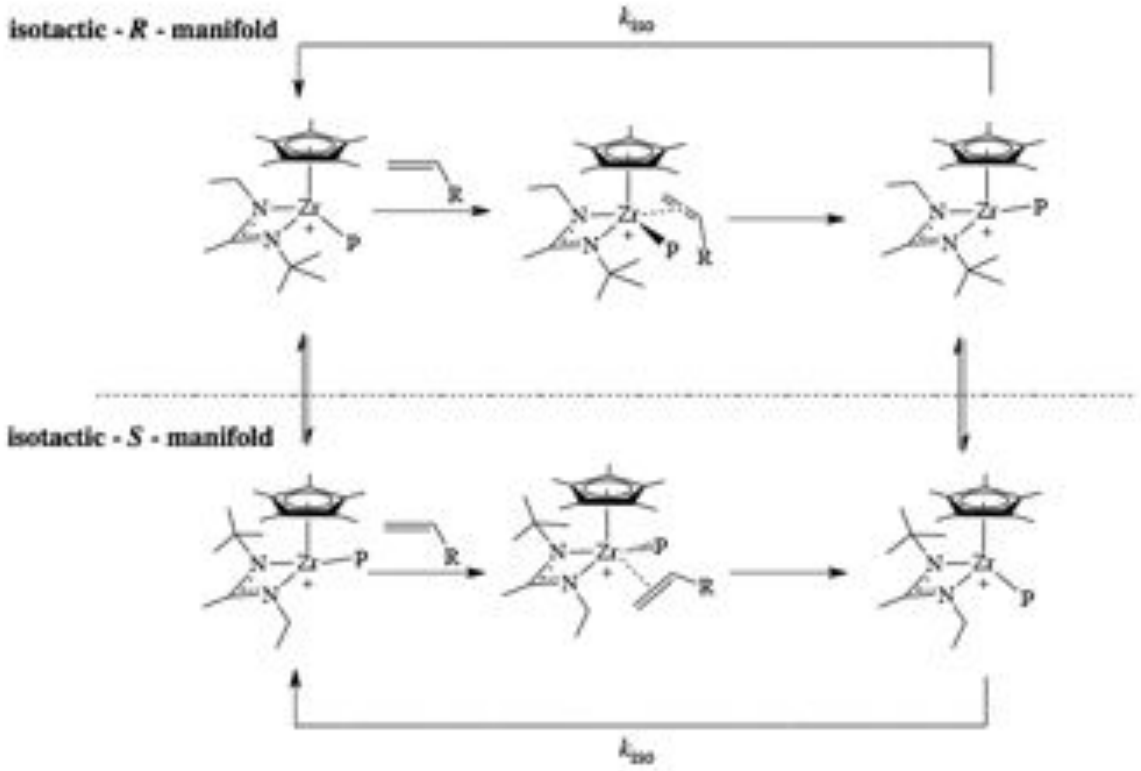

1.5.2 Degenerative Group Transfer Polymerizations

In an effort to widen the range of materials available from the 'CpAm' system, the Sita group executed the first example of a living degenerative group-transfer coordinative polymerization.[128] With substoichiometric activation of **51**, a cationic active species and a neutral dormant species will both be present in the polymerization solution. As stated previously, the cationic species is configurationally stable; however, the neutral dormant species undergoes rapid metal-centered epimerization. This epimerization of the dormant species allows for the precise insertion of stereoerrors into the polymer microstructure once it is reengaged in polymerization with the transfer of a methyl group to an active species (MeDeT). It is a statistical likelihood that the species has changed conformations due to the rapid epimerization, R to S or S to R, upon reactivation thus

introducing a stereoerror. This group transfer can also be employed with a configurationally stable alkyl chloride species where the chloride group will be transferred between the active and dormant species (Scheme 12). In the case of this chloride degenerative transfer (ChloDeT) process, the resulting alkyl chloride species is configurationally stable and will not introduce stereoerrors into the microstructure.[129]

1.5.3 Reversible Chain Transfer Coordination Polymerizations

Scheme 12. General proposed mechanism of degenerative group transfer polymerization (X= Me for MeDeT, X= Cl for ChloDeT).

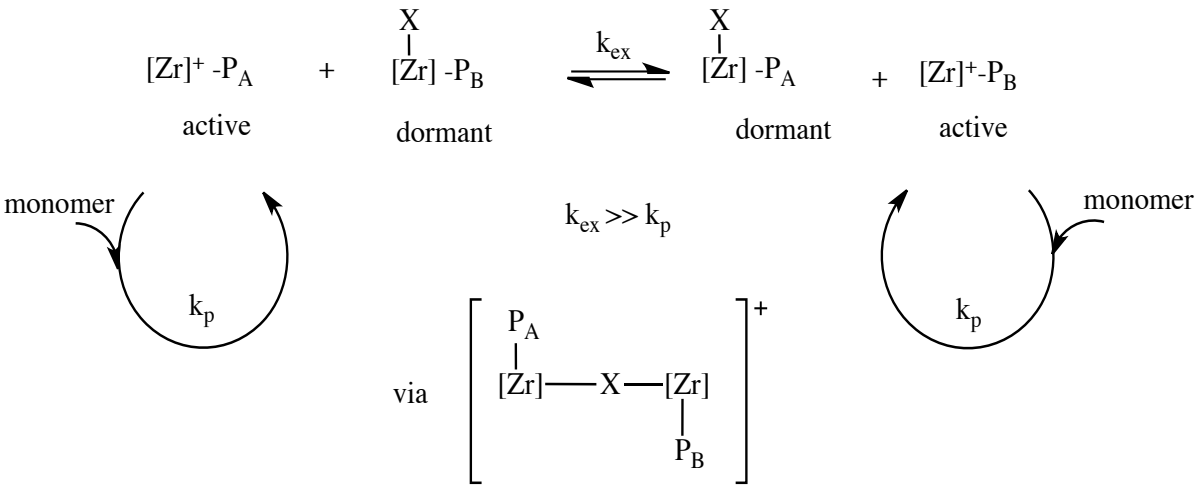

Living coordinative chain transfer polymerization (LCCTP) has been employed by the Sita group to overcome the inherent 'one chain per metal' site limitation that prevents large-scale production for commercial applications. This issue can be side stepped through the addition of a main group metal species to act as a surrogate chain growth site during the polymerization. The main group metal species, in this case diethyl zinc (DEZ), acts as a surrogate chain growth site with the amount of polymer that can be produced showing dependency on the amount of the chain transfer agent.[130] The main

draw back to this process is that stereocontrol from the initiator is lost due to the transfer process on and off the propagating transition metal species. By using **51** there is a statistical likelihood that the incoming polymer group will transfer onto an active manifold that is of a different conformation (R vs. S) than the one it originated from (Scheme 13). This introduces a stereoerror into the polymer chain and the rapid transfer between the two different manifolds of the initiator will result in a stereoerror rich, atactic, polymer.

Scheme 13. Proposed mechanism of LCCTP.

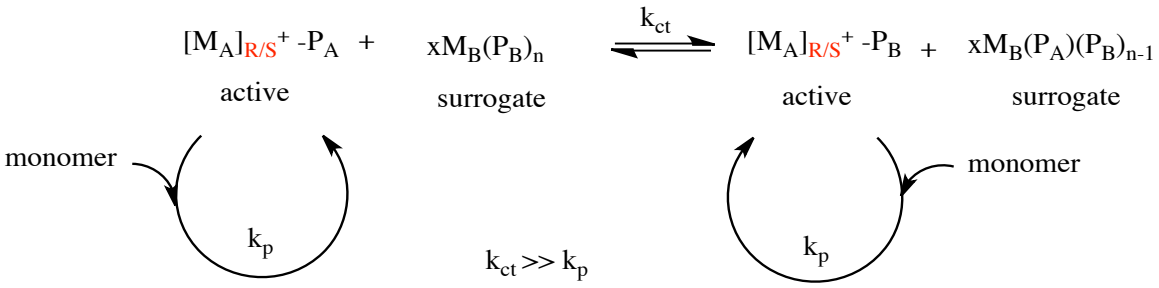

1.5 References

(1) Natta, G.; Corradini, P. *Makromol. Chem.* **1955**, *16*, 77-80.

(2) Ziegler, K.; Holzkamp, E.; Breil, H.; Martin, H. *Angew. Chem.* **1955**, *67*, 426.

(3) Nexant, I. 2007; Vol. 2012.

(4) Natta, G.; Pino, P.; Corradini, P.; Danusso, F.; Mantica, E.; Mazzanti, G.; Moraglio, G. *J. Am. Chem. Soc.* **1955**, *77*, 1708-1710.

(5) Natta, G. *Angew. Chem.* **1956**, *68*, 393-403.

(6) Natta, G.; Mazzanti, G.; Crespi, G.; Moraglio, G. *Chim. Ind. (Milan, Italy)* **1957**, *39*, 275-283.

(7) Natta, G.; Pino, P.; Mazzanti, G.; Giannini, U. *J. Am. Chem. Soc.* **1957**, *79*, 2975-2976.

(8) Cossee, P. *Tetrahedron Lett.* **1960**, 12-16.

(9) Cossee, P. *Tetrahedron Lett.* **1960**, 17-21.

(10) Arlman, E. J. *J. Catal.* **1964**, *3*, 89-98.

(11) Arlman, E. J.; Cossee, P. *J. Catal.* **1964**, *3*, 99-104.

(12) Cossee, P. *J. Catal.* **1964**, *3*, 80-88.

(13) Maier, C.; Calafut, T. *Polypropylene: A Definitive User's Guide and Handbook* Norwich, NY, 1998.

(14) Hillman, M.; Weiss, A. J.; Hahne, R. M. A. *Radiochim. Acta* **1969**, *12*, 200-202.

(15) Chen, E. Y.-X.; Marks, T. J. *Chem. Rev. (Washington, D. C.)* **2000**, *100*, 1391-1434.

(16) Pedeutour, J.-N.; Radhakrishnan, K.; Cramail, H.; Deffieux, A. *Macromol. Rapid Commun.* **2001**, *22*, 1095-1123.

(17) Baugh, L. S.; Canich, J. A. M.; Editors *Stereoselective Polymerization with Single-Site Catalysts*; CRC Press LLC, 2008.

(18) Herwig, J.; Kaminsky, W. *Polym. Bull. (Berlin)* **1983**, *9*, 464-469.

(19) Kaminsky, W.; Miri, M.; Sinn, H.; Woldt, R. *Makromol. Chem., Rapid Commun.* **1983**, *4*, 417-421.

(20) Schneider, M. J.; Suhm, J.; Muelhaupt, R.; Prosenc, M.-H.; Brintzinger, H.-H. *Macromolecules* **1997**, *30*, 3164-3168.

(21) Grassi, A.; Zambelli, A.; Resconi, L.; Albizzati, E.; Mazzocchi, R. *Macromolecules* **1988**, *21*, 617-622.

(22) Cheng, H. N.; Ewen, J. A. *Makromol. Chem.* **1989**, *190*, 1931-1943.

(23) Mizuno, A.; Tsutsui, T.; Kashiwa, N. *Polymer* **1992**, *33*, 254-258.

(24) Resconi, L.; Cavallo, L.; Fait, A.; Piemontesi, F. *Chem. Rev. (Washington, D. C.)* **2000**, *100*, 1253-1345.

(25) Ewen, J. A. *J. Am. Chem. Soc.* **1984**, *106*, 6355-6364.

(26) Kaminsky, W.; Kuelper, K.; Brintzinger, H. H.; Wild, F. R. W. P. *Angew. Chem.* **1985**, *97*, 507-508.

(27) Resconi, L.; Piemontesi, F.; Nifant ev, I. E.; Ivchenko, P. V.; Montell Technology Company B.V., Neth. . 1996, p 39.

(28) Herrmann, W. A.; Rohrmann, J.; Herdtweck, E.; Spaleck, W.; Winter, A. *Angew. Chem.* **1989**, *101*, 1536-1538.

(29) Winter, A.; Antberg, M.; Spaleck, W.; Rohrmann, J.; Dolle, V.; Hoechst A.-G., Germany . 1992, p 19.

(30) Han, T. K.; Woo, B. W.; Park, J. T.; Do, Y.; Ko, Y. S.; Woo, S. I. *Macromolecules* **1995**, *28*, 4801-4805.

(31) Spaleck, W.; Kueber, F.; Winter, A.; Rohrmann, J.; Bachmann, B.; Antberg, M.; Dolle, V.; Paulus, E. F. *Organometallics* **1994**, *13*, 954-963.

(32) Stehling, U.; Diebold, J.; Kirsten, R.; Roell, W.; Brintzinger, H. H.; Juengling, S.; Muelhaupt, R.; Langhauser, F. *Organometallics* **1994**, *13*, 964-970.

(33) Coates, G. W.; Waymouth, R. M. *Science (Washington, D. C.)* **1995**, *267*, 217-219.

(34) Hauptman, E.; Waymouth, R. M.; Ziller, J. W. *J. Am. Chem. Soc.* **1995**, *117*, 11586-11587.

(35) Bruce, M. D.; Coates, G. W.; Hauptman, E.; Waymouth, R. M.; Ziller, J. W. *J. Am. Chem. Soc.* **1997**, *119*, 11174-11182.

(36) Kravchenko, R.; Masood, A.; Waymouth, R. M. *Organometallics* **1997**, *16*, 3635-3639.

(37) Petoff, J. L. M.; Bruce, M. D.; Waymouth, R. M.; Masood, A.; Lal, T. K.; Quan, R. W.; Behrend, S. J. *Organometallics* **1997**, *16*, 5909-5916.

(38) Bruce, M. D.; Waymouth, R. M. *Macromolecules* **1998**, *31*, 2707-2715.

(39) Kravchenko, R.; Masood, A.; Waymouth, R. M.; Myers, C. L. *J. Am. Chem. Soc.* **1998**, *120*, 2039-2046.

(40) Petoff, J. L. M.; Agoston, T.; Lal, T. K.; Waymouth, R. M. *J. Am. Chem. Soc.* **1998**, *120*, 11316-11322.

(41) Lin, S.; Waymouth, R. M. *Macromolecules* **1999**, *32*, 8283-8290.

(42) Tagge, C. D.; Kravchenko, R. L.; Lal, T. K.; Waymouth, R. M. *Organometallics* **1999**, *18*, 380-388.

(43) Ewen, J. A.; Jones, R. L.; Razavi, A.; Ferrara, J. D. *J. Am. Chem. Soc.* **1988**, *110*, 6255-6256.

(44) Razavi, A.; Atwood, J. L. *J. Organomet. Chem.* **1993**, *459*, 117-123.

(45) Shiomura, T.; Kohno, M.; Inoue, N.; Asanuma, T.; Sugimoto, R.; Iwatani, T.; Uchida, O.; Kimura, S.; Harima, S.; et, a. *Macromol. Symp.* **1996**, *101*, 289-299.

(46) Yamaguchi, M.; Ohba, K.; Tomonaga, H.; Yamagishi, T. *J. Mol. Catal. A: Chem.* **1999**, *140*, 255-258.

(47) Farina, M.; Di Silvestro, G.; Sozzani, P. *Macromolecules* **1993**, *26*, 946-950.

(48) Herfert, N.; Fink, G. *Makromol. Chem., Macromol. Symp.* **1993**, *66*, 157-178.

(49) Antberg, M.; Dolle, V.; Klein, R.; Rohrmann, J.; Spaleck, W.; Winter, A. *Catalytic Olefin Polymerization, Studies in Surface Science and Catalysis* Tokyo, 1990.

(50) Dolle, V.; Rohrmann, J.; Winter, A.; Antberg, M.; Klein, R.; Hoechst A.-G., Germany . 1990, p 15.

(51) Ewen, J. A.; Elder, M. J.; Harlan, C. J.; Jones, R. L.; Atwood, J. L.; Bott, S. G.; Robinson, K. *Polym. Prepr. (Am. Chem. Soc., Div. Polym. Chem.)* **1991**, *32*, 469-470.

(52) Ewen, J. A.; Elder, M. J.; Jones, R. L.; Haspeslagh, L.; Atwood, J. L.; Bott, S. G.; Robinson, K. *Makromol. Chem., Macromol. Symp.* **1991**, *48-49*, 253-295.

(53) Spaleck, W.; Antberg, M.; Aulbach, M.; Dolle, V.; Rohrmann, J.; Winter, A.; Kuber, F.; Haftka, S. *Ziegler Catalysts*, 1995.

(54) Spaleck, W.; Kuber, F.; Bachmann, B.; Fritze, C.; Winter, A. *J. Mol. Catal. A: Chem.* **1998**, *128*, 279-287.

(55) Coates, G. W.; Hustad, P. D.; Reinartz, S. *Angew. Chem., Int. Ed.* **2002**, *41*, 2236-2257.

(56) Doi, Y.; Ueki, S.; Keii, T. *Macromolecules* **1979**, *12*, 814-815.

(57) Foster, P.; Rausch, M. D.; Chien, J. C. W. *J. Organomet. Chem.* **1997**, *527*, 71-74.

(58) Van Der Zeijden, A. A. H.; Mattheis, C. *J. Organomet. Chem.* **1999**, *584*, 274-285.

(59) Chien, J. C.; Yu, Z.; Marques, M. M.; Flores, J. C.; Rausch, M. D. *J. Polym. Sci., Part A: Polym. Chem.* **1998**, *36*, 319-328.

(60) Blais, M. S.; Chien, J. C. W.; Rausch, M. D. *Organometallics* **1998**, *17*, 3775-3783.

(61) Flores, J. C.; Chien, J. C. W.; Rausch, M. D. *Organometallics* **1994**, *13*, 4140-4142.

(62) Skoog, S. J.; Mateo, C.; Lavoie, G. G.; Hollander, F. J.; Bergman, R. G. *Organometallics* **2000**, *19*, 1406-1421.

(63) Bochmann, M.; Lancaster, S. J. *Organometallics* **1993**, *12*, 633-640.

(64) Marques, M. M.; Correia, S. G.; Ascenso, J. R.; Ribeiro, A. F. G.; Gomes, P. T.; Dias, A. R.; Foster, P.; Rausch, M. D.; Chien, J. C. W. *J. Polym. Sci., Part A: Polym. Chem.* **1999**, *37*, 2457-2469.

(65) Ioku, A.; Hasan, T.; Shiono, T.; Ikeda, T. *Macromol. Chem. Phys.* **2002**, *203*, 748-755.

(66) Santos, J. M.; Ribeiro, M. R.; Portela, M. F.; Cramail, H.; Deffieux, A.; Antinolo, A.; Otero, A.; Prashar, S. *Macromol. Chem. Phys.* **2002**, *203*, 139-145.

(67) Klosin, J.; Kruper, W. J., Jr.; Nickias, P. N.; Roof, G. R.; De Waele, P.; Abboud, K. A. *Organometallics* **2001**, *20*, 2663-2665.

(68) Kotov, V. V.; Avtomonov, E. V.; Sundermeyer, J.; Harms, K.; Lemenovskii, D. A. *Eur. J. Inorg. Chem.* **2002**, 678-691.

(69) Scollard, J. D.; McConville, D. H. *J. Am. Chem. Soc.* **1996**, *118*, 10008-10009.

(70) Scollard, J. D.; McConville, D. H.; Payne, N. C.; Vittal, J. J. *Macromolecules* **1996**, *29*, 5241-5243.

(71) Tsubaki, S.; Jin, J.; Ahn, C.-H.; Sano, T.; Uozumi, T.; Soga, K. *Macromol. Chem. Phys.* **2001**, *202*, 482-487.

(72) Uozumi, T.; Tsubaki, S.; Jin, J.; Sano, T.; Soga, K. *Macromol. Chem. Phys.* **2001**, *202*, 3279-3282.

(73) Ziniuk, Z.; Goldberg, I.; Kol, M. *Inorg. Chem. Commun.* **1999**, *2*, 549-551.

(74) Nomura, K.; Naga, N.; Takaoki, K.; Imai, A. *J. Mol. Catal. A: Chem.* **1998**, *130*, L209-L213.

(75) Nomura, K.; Oya, K.; Imanishi, Y. *Polymer* **2000**, *41*, 2755-2746.

(76) Baumann, R.; Davis, W. M.; Schrock, R. R. *J. Am. Chem. Soc.* **1997**, *119*, 3830-3831.

(77) Baumann, R.; Stumpf, R.; Davis, W. M.; Liang, L.-C.; Schrock, R. R. *J. Am. Chem. Soc.* **1999**, *121*, 7822-7836.

(78) Schrock, R. R.; Liang, L. C.; Baumann, R.; Davis, W. M. *J. Organomet. Chem.* **1999**, *591*, 163-173.

(79) Baumann, R.; Schrock, R. R. *J. Organomet. Chem.* **1998**, *557*, 69-75.

(80) Goodman, J. T.; Schrock, R. R. *Organometallics* **2001**, *20*, 5205-5211.

(81) Schrock, R. R.; Baumann, R.; Reid, S. M.; Goodman, J. T.; Stumpf, R.; Davis, W. M. *Organometallics* **1999**, *18*, 3649-3670.

(82) Aizenberg, M.; Turculet, L.; Davis, W. M.; Schattenmann, F.; Schrock, R. R. *Organometallics* **1998**, *17*, 4795-4812.

(83) Schrock, R. R.; Bonitatebus, P. J., Jr.; Schrodi, Y. *Organometallics* **2001**, *20*, 1056-1058.

(84) Schrock, R. R.; Casado, A. L.; Goodman, J. T.; Liang, L.-C.; Bonitatebus, P. J., Jr.; Davis, W. M. *Organometallics* **2000**, *19*, 5325-5341.

(85) Averbuj, C.; Tish, E.; Eisen, M. S. *J. Am. Chem. Soc.* **1998**, *120*, 8640-8646.

(86) Volkis, V.; Shmulinson, M.; Averbuj, C.; Lisovskii, A.; Edelmann, F. T.; Eisen, M. S. *Organometallics* **1998**, *17*, 3155-3157.

(87) Vollmerhaus, R.; Shao, P.; Taylor, N. J.; Collins, S. *Organometallics* **1999**, *18*, 2731-2733.

(88) Duncan, A. P.; Mullins, S. M.; Arnold, J.; Bergman, R. G. *Organometallics* **2001**, *20*, 1808-1819.

(89) Chen, C.-T.; Rees, L. H.; Cowley, A. R.; Green, M. L. H. *J. Chem. Soc., Dalton Trans.* **2001**, 1761-1767.

(90) Makio, H.; Fujita, T. *Bull. Chem. Soc. Jpn.* **2005**, *78*, 52-66.

(91) Ishii, S.-I.; Mitani, M.; Saito, J.; Matsuura, S.; Kojoh, S.-I.; Kashiwa, N.; Fujita, T. *Chem. Lett.* **2002**, 740-741.

(92) Saito, J.; Mitani, M.; Mohri, J.-I.; Ishii, S.-I.; Yoshida, Y.; Matsugi, T.; Kojoh, S.-I.; Kashiwa, N.; Fujita, T. *Chem. Lett.* **2001**, 576-577.

(93) Ishii, S.; Saito, J.; Matsuura, S.; Suzuki, Y.; Furuyama, R.; Mitani, M.; Nakano, T.; Kashiwa, N.; Fujita, T. *Macromol. Rapid Commun.* **2002**, *23*, 693-697.

(94) Milano, G.; Cavallo, L.; Guerra, G. *J. Am. Chem. Soc.* **2002**, *124*, 13368-13369.

(95) Tshuva, E. Y.; Versano, M.; Goldberg, I.; Kol, M.; Weitman, H.; Goldschmidt, Z. *Inorg. Chem. Commun.* **1999**, *2*, 371-373.

(96) Tshuva, E. Y.; Goldberg, I.; Kol, M.; Weitman, H.; Goldschmidt, Z. *Chem. Commun. (Cambridge)* **2000**, 379-380.

(97) Tshuva, E. Y.; Goldberg, I.; Kol, M.; Goldschmidt, Z. *Inorg. Chem. Commun.* **2000**, *3*, 611-614.

(98) Tshuva, E. Y.; Groysman, S.; Goldberg, I.; Kol, M.; Goldschmidt, Z. *Organometallics* **2002**, *21*, 662-670.

(99) Olonde, X.; Mortreux, A.; Petit, F.; Bujadoux, K. *J. Mol. Catal.* **1993**, *82*, 75-82.

(100) Pelletier, J.-F.; Mortreux, A.; Olonde, X.; Bujadoux, K. *Angew. Chem., Int. Ed. Engl.* **1996**, *35*, 1854-1856.

(101) Britovsek, G. J. P.; Cohen, S. A.; Gibson, V. C.; van Meurs, M. *J. Am. Chem. Soc.* **2004**, *126*, 10701-10712.

(102) Chenal, T.; Olonde, X.; Pelletier, J.-F.; Bujadoux, K.; Mortreux, A. *Polymer* **2007**, *48*, 1844-1856.

(103) Kempe, R. *Chem. - Eur. J.* **2007**, *13*, 2764-2773.

(104) Zinck, P.; Valente, A.; Mortreux, A.; Visseaux, M. *Polymer* **2007**, *48*, 4609-4614.

(105) Amin, S. B.; Marks, T. J. *Angew. Chem., Int. Ed.* **2008**, *47*, 2006-2025.

(106) Arriola, D. J.; Carnahan, E. M.; Hustad, P. D.; Kuhlman, R. L.; Wenzel, T. T. *Science (Washington, DC, U. S.)* **2006**, *312*, 714-719.

(107) Sita, L. R. *Angew. Chem., Int. Ed.* **2009**, *48*, 2464-2472.

(108) Valente, A.; Mortreux, A.; Visseaux, M.; Zinck, P. *Chem. Rev. (Washington, DC, U. S.)* **2013**, *113*, 3836-3857.

(109) Barsties, E.; Schaible, S.; Prosenc, M.-H.; Rief, U.; Roell, W.; Weyand, O.; Dorer, B.; Brintzinger, H.-H. *J. Organomet. Chem.* **1996**, *520*, 63-68.

(110) Leino, R.; Luttikhedde, H. J. G.; Lehmus, P.; Wilen, C.-E.; Sjoeholm, R.; Lehtonen, A.; Seppaelae, J. V.; Naesman, J. H. *Macromolecules* **1997**, *30*, 3477-3483.

(111) Naga, N.; Mizunuma, K. *Polymer* **1998**, *39*, 5059-5067.

(112) Lieber, S.; Brintzinger, H.-H. *Macromolecules* **2000**, *33*, 9192-9199.

(113) Fan, G.; Dong, J.-Y. *J. Mol. Catal. A: Chem.* **2005**, *236*, 246-252.

(114) Hild, S.; Cobzaru, C.; Troll, C.; Rieger, B. *Macromol. Chem. Phys.* **2006**, *207*, 665-683.

(115) Tynys, A.; Eilertsen, J. L.; Rytter, E. *Macromol. Chem. Phys.* **2006**, *207*, 295-303.

(116) Byun, D.-J.; Shin, D.-K.; Kim, S. Y. *Macromol. Rapid Commun.* **1999**, *20*, 419-422.

(117) Bhriain, N. N.; Brintzinger, H.-H.; Ruchatz, D.; Fink, G. *Macromolecules* **2005**, *38*, 2056-2063.

(118) Hoffmann, E. G. *Trans. Faraday Soc.* **1962**, *58*, 642-649.

(119) Yamamoto, O.; Hayamizu, K. *J. Phys. Chem.* **1968**, *72*, 822-828.

(120) Valente, A.; Zinck, P.; Mortreux, A.; Visseaux, M. *Macromol. Rapid Commun.* **2009**, *30*, 528-531.

(121) Valente, A.; Zinck, P.; Mortreux, A.; Bria, M.; Visseaux, M. *J. Polym. Sci., Part A: Polym. Chem.* **2011**, *49*, 3778-3782.

(122) Valente, A.; Zinck, P.; Mortreux, A.; Visseaux, M. *J. Polym. Sci., Part A: Polym. Chem.* **2011**, *49*, 1615-1620.

(123) Khariwala, D. U.; Taha, A.; Chum, S. P.; Hiltner, A.; Baer, E. *Polymer* **2008**, *49*, 1365-1375.

(124) Wang, H. P.; Khariwala, D. U.; Cheung, W.; Chum, S. P.; Hiltner, A.; Baer, E. *Macromolecules (Washington, DC, U. S.)* **2007**, *40*, 2852-2862.

(125) Jayaratne, K. C.; Sita, L. R. *J. Am. Chem. Soc.* **2000**, *122*, 958-959.

(126) Koterwas, L. A.; Fettinger, J. C.; Sita, L. R. *Organometallics* **1999**, *18*, 4183-4190.

(127) Harney, M. B.; Keaton, R. J.; Sita, L. R. *J. Am. Chem. Soc.* **2004**, *126*, 4536-4537.

(128) Zhang, Y.; Keaton, R. J.; Sita, L. R. *J. Am. Chem. Soc.* **2003**, *125*, 9062-9069.

(129) Zhang, Y.; Sita, L. R. *J. Am. Chem. Soc.* **2004**, *126*, 7776-7777.

(130) Zhang, W.; Sita, L. R. *J. Am. Chem. Soc.* **2008**, *130*, 442-443.

Chapter 2

Stereoengineering of Poly(1-Butene)

2.1 Background

By using several strategies, involving reversible group transfers, in combination with the pentamethylcyclopentadienyl amidinate complexes, one can use a single initiator to create a wide range of poly(1-butene) materials. The first strategy in achieving the ability to stereoengineer poly(1-butene) is use of the previously developed stereomodulated degenerative transfer living (SDTL) Ziegler-Natta polymerization process.[1] This technique allows for the precise control of the amount of *mmrm* stereoerrors introduced into the resulting polymer's microstructure using a single initiator by controlling the level of concentration of the epimerizing dormant species through the use of substoichiometric activations with the cocatalyst **49**. Second, living coordinative chain transfer polymerization (LCCTP) can be engaged to side-step the 'one chain per metal site' limitation that is attached to using single site catalysts to produce scalable quantities of stereoerror rich materials.[2] Lastly, novel olefin block copolymers can be synthesized by controlling the degree of 1-butene and ethylene incorporation with the use of two active ion pairs in solution.[3]

2.2 Methyl Degenerative Transfer

Scheme 14. Methyl group degenerative transfer polymerization.

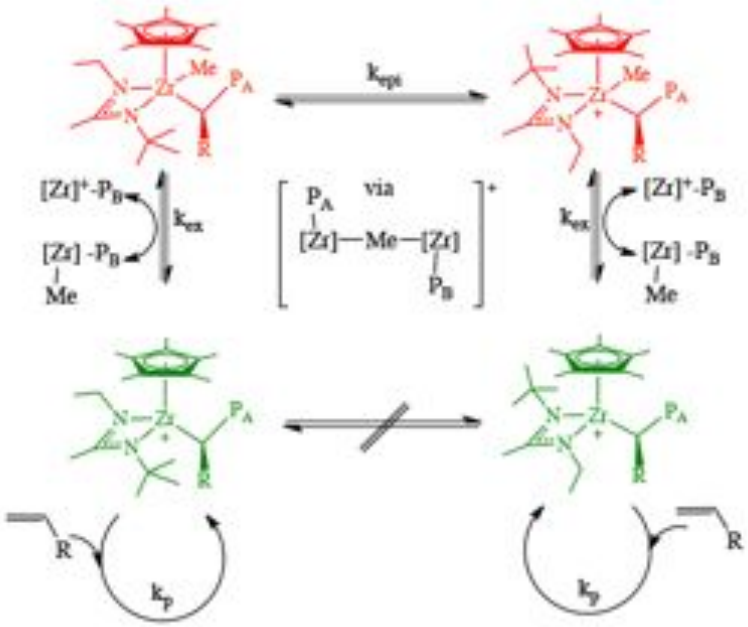

It has been previously reported that both mononuclear and dinuclear analogues of group (IV) initiators with the general formula $(\eta^5\text{-}C_5Me_5)MMe_2[N(R^1)C(R^2)N(R^3)]$ and $[(\eta^5\text{-}C_5Me_5)MMe_2]_2[N(R^1)C(R^2)N\text{-}(CH_2)_6\text{-}NC(R^2)N(R^1)]$ are adept at controlling stereoselectivity in propene (%*mmmm* = 0.72) and other long chain α-olefins (1-hexene, %*mmmm* > 0.98) under living polymerization conditions.[4] When substoichiometric amounts of **49** are used to activate the precatalyst **51**, a mixture of the cationic active species (green) and a dormant non-propagating species (red) are present in the solution (Scheme 14). This exchange process involves a fast and reversible transfer of a methyl group, via a methyl-bridged dinuclear adduct, between the propagating and dormant species. Programmable stereoerrors are possible due to the fact that the dormant non-propagating species is not configurationally stable and will undergo rapid metal

centered epimerization.[5] Once the dormant species is reengaged in polymerization, it is a statistical likelihood ($k_{epi} > k_{ex}$) that the conformation of the active species has changed, thus creating a stereoerror in the growing polymer chain that will continue to propagate until a conformation change reoccurs in the exchange process. Since it's been established that $k_{ex} >> k_p$, the exchange and epimerization will occur more frequently than the propagation of the inserting monomer unit. This will lead to a shortening of the stereoblock length of the resulting polymer. This programmable nature of the stereoerrors can be harnessed and used to produce polymers with specific microstructures and material properties.

Scheme 15. General poly(1-butene) polymerization scheme.

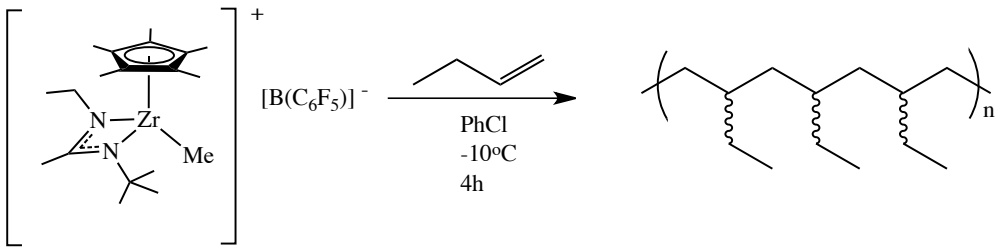

Table 1. Polymerizations with 1-butene[a]

Entry	Precatalyst	[**49**]/[**5-**]	M_n[b] (kDa)	M_w[b] (kDa)	PDI[b]	T_g[c] (°C)	T_m[c] (°C)	T_c[c] (°C)	Yield (g)	% mmmm[d]
1	**51**	1.0	29.5	46.5	1.58	-31.5	93.9	52.6	0.72	0.91
2	**51**	.95	29.4	46.2	1.58	-32.2	94.7	61.0	0.83	0.90
3	**51**	.90	33.4	48.3	1.45	-32.7	84.2	--	0.99	0.73
4	**51**	.80	21.6	31.8	1.47	-28.6	--	--	0.52	0.55
5	**51**	.70	21.5	30.7	1.43	-28.3	--	--	0.53	0.49
6	**52**	1.0	23.2	37.9	1.63	-37.4	87.9	45.7	0.49	0.89
7	**52**	.70	22.4	33.7	1.50	-33.0	78.3	--	0.48	0.72

[a] Polymerizations were terminated at precipitation into acidic MeOH. [b] Determined by gel permeation chromatography (GPC) analysis. [c] Determined by differential scanning calorimetry (DSC) analysis. [d] Determined by ^{1}H (600 MHz) and ^{13}C (150 MHz) NMR at 110 °C in 1,1,2,2-tetrachloroethane-d_2

1-butene polymerizations were conducted using this methyl group exchange process with both the mononuclear **51** and C6-dinuclear precatalyst **52** using $[PhNHMe_2][B(C_6F_5)_4]$ (**49**) as the activating cocatalyst in chlorobenzene at -10 ^{o}C per Scheme 15. Polymerizations were conducted such that the concentration of the metal centers were held constant while the concentrations of the cocatalyst **49** were varied so that 100, 95, 90, 80, or 70% levels of activation of the initiator were achieved to produce the desired concentration of dormant species available in the solution to engage in methyl group transfer. The polymerizations were allowed to proceed over a time period of 4 h to ensure the complete consumption of the 1-butene.

As expected, both **51** and **52**, proved to be adept at polymerizing 1-butene in a living process. GPC analysis of the resulting polymers confirmed that the molecular

weight distributions were monomodal. The polydispersities obtained from the analysis do not agree with values <1.10 that are typically expected from living polymerizations but ^{1}H NMR analysis (600 MHz in1,1,2,2-tetrachlorethane-d_2 at 110 °C) did not reveal any vinylic resonances that would result from β-hydride elimination thus confirming the living nature of the polymerizations. The cause of this broadening phenomenon is unknown and needs further investigation. Based on the results in Table 1, the results are in agreement with previously reported polymerizations using propene in that the degree of isotacticity (% *mmmm*) decreases with the increasing amount of dormant species present for both the mononuclear and dinuclear analogues of the precatalyst. It's worth noting that there is little effect in the properties of the materials produced by only a slight decrease in the level of activation of the mononuclear initiator **51** from 1.0 to 0.95 (Table 1, entries 1-2). Also, in agreement with results using propene, the dinuclear precatalyst **52** produced comparable materials at 100% activation, where no dormant species are present. The interesting feature of the dinuclear initiator is that it was able to retain a higher degree of stereoselectivity under a lower percentage of activation as its mononuclear analogue (Table 1, entries 6-7). This can be attributed to the fact that it is known that **52** is more configurationally stable and is thusly more resilient in terms of its ability to epimerize.

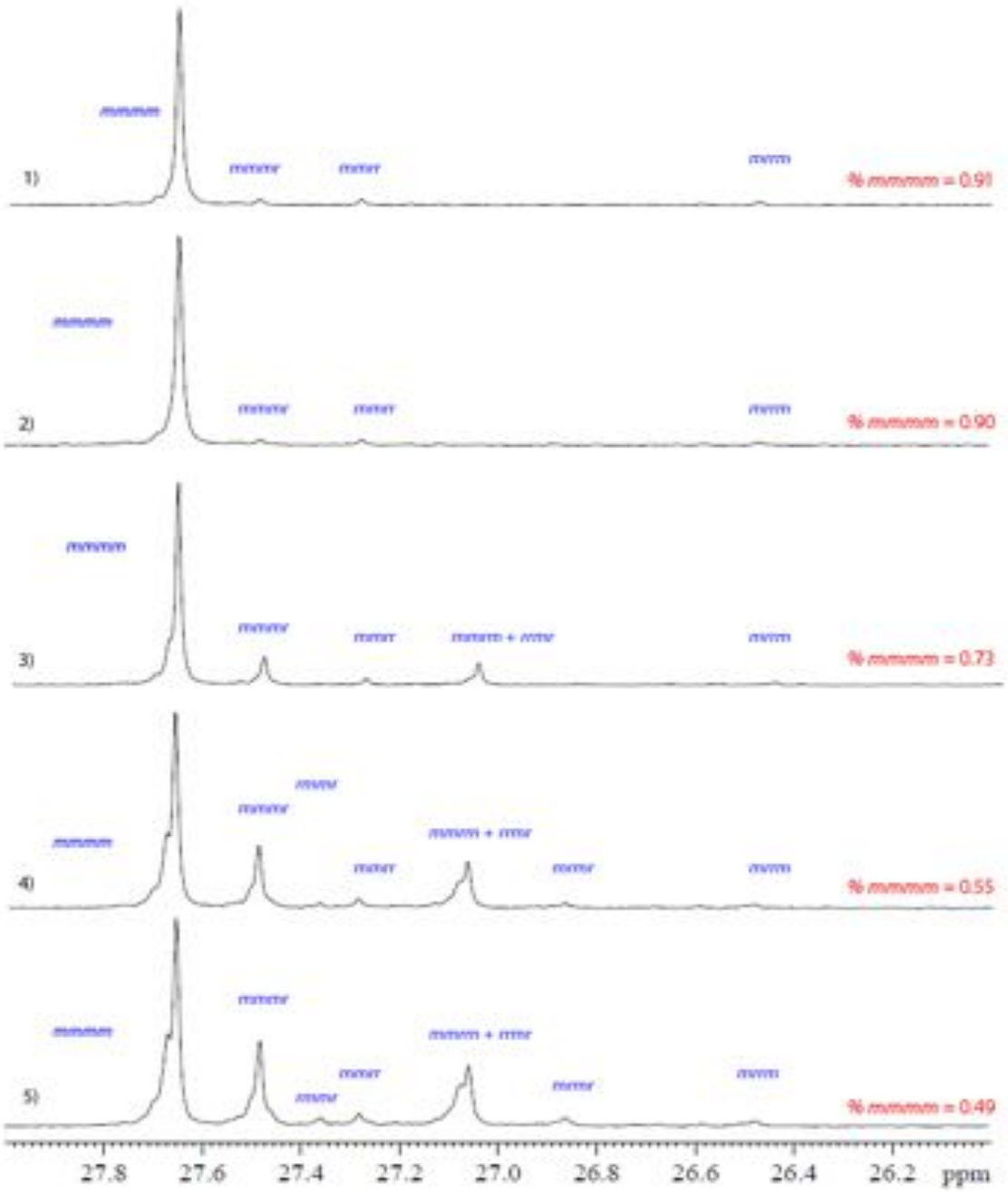

Figure 18. Partial ^{13}C NMR: 150 MHz, 1,1,2,2-tetrachloroethane-d_2, 110°C of polybutylene (entries 1-5 from Table 1) using **51**.

2.2.1 Microstructure Analysis

A detailed ^{13}C NMR analysis (150 MHz in 1,1,2,2-tetrachlorethane-d_2 at 110 °C) reveals more information regarding the microstructure of the resulting materials in relation to the level of precatalyst activation. Initially, it is apparent that there are significant differences in the resulting polymers' microstructure as a result of the level of activation used. Figure 18 represents the ^{13}C NMR of the methylene region and the amount of stereoerrors noticeably increases with the decreasing level of activation of the initiator. There is not an observable difference between entry 1 and 2 as both polymers contain the same errors as well as have the same %*mmmm*. As the level of activation decreases further, from 0.95 to 0.90, *mmrm* + *rrmr* stereoerrors appear and the %*mmmm* decreases rather substantially from 0.90 to 0.73. Both the *rmmr* and *mrmr* stereoerrors can be found in entry 4 and 5 with activations of .80 and .70. There is no appreciable difference when comparing the stereoselectivity of the complete activation of the mononuclear initiator and the dinuclear initiator. More remarkably, the dinuclear initiator **52** shows more resilience to decreasing the level of activation (Figure 19) as it retains more stereoselectivity, %*mmmm* of 0.72 vs. 0.49, upon a lower activation than it's mononuclear counterpart.

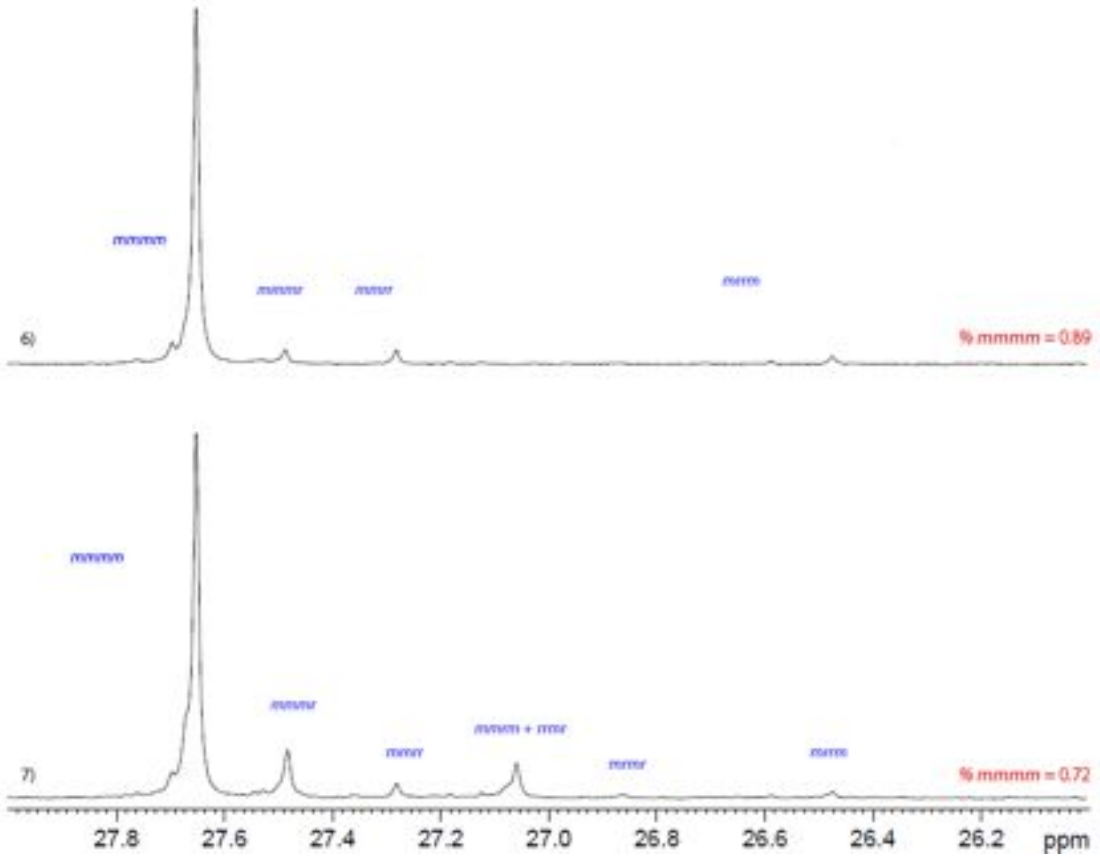

Figure 19. Partial ^{13}C NMR: 150 MHz, 1,1,2,2-tetrachloroethane-d_2, 110°C of polybutylene (entries 6-7 from Table 1) using **52**.

2.2.2 Crystalline Structure

Wide-angle X-ray diffraction (WAXD) was used to study the solid-state structures of the poly(1-butene) materials obtained from both **51** and **21** under MeDeT conditions due to potential commercial applications. The materials synthesized using **51** adopt a mixture of crystalline forms II and I, with the reflection peaks occurring for form I at 2θ = 9.9, 17.3, and 20.5 ° for $(110)_I$, $(300)_I$, and $(220)_I$+$(211)_I$ respectively (Figure 20). The reflection peaks for form II are identified at 2θ = 11.9, 16.9, and 18.3 ° for $(200)_{II}$, $(220)_{II}$, and $(213)_{II}$+$(311)_{II}$ respectively.[6] With the baseline removed to see the crystalline reflections more clearly, it is evident that the resulting crystallinity of the polymeric materials shows a noticeable decrease in crystallinity as the number of the epimerizing

dormant species is increased through substoichiometric activation of the initiator **51**. By the time only .70 of **51** have been activated, no crystallinity is detected by WAXD.

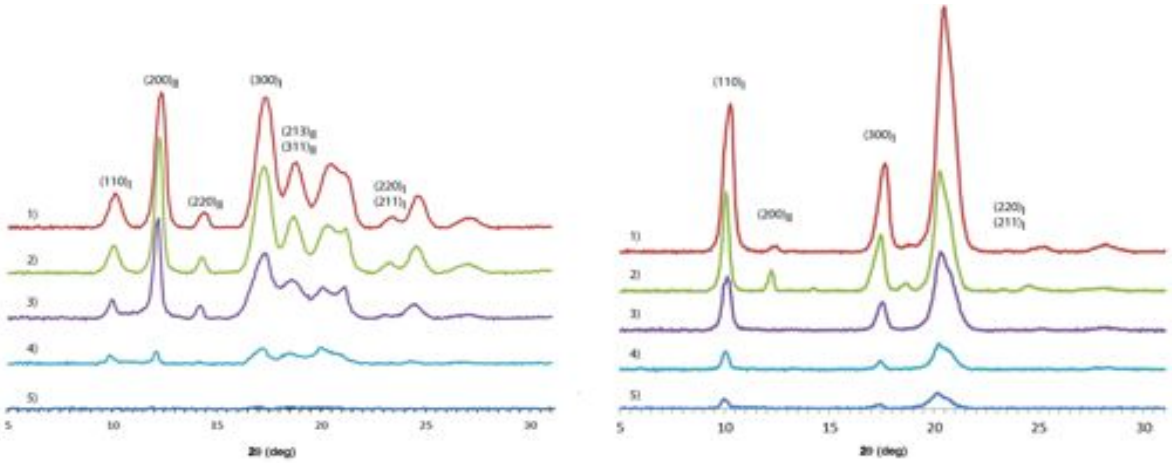

Figure 20. Partial WAXD profiles of unannealed (left) and annealed (right) poly(1-butene) materials using **51** from Table 1.

Upon thermally aging the polymers at 75 ºC and cooling down to room temperature over the course of 12 hours in a vacuum oven revealed a change in the crystalline form of the polymers. The polymeric materials now contain only the crystalline form I as evidence by the reflections at 2θ = 9.9, 17.3, and 20.5 º for $(110)_I$ $(300)_I$ and $(220)_I$+$(211)_I$.[6] Minor peaks are seen in the case of entry 5, the 'atactic' material, due to crystallization as the polymer chains cool from the molten state.

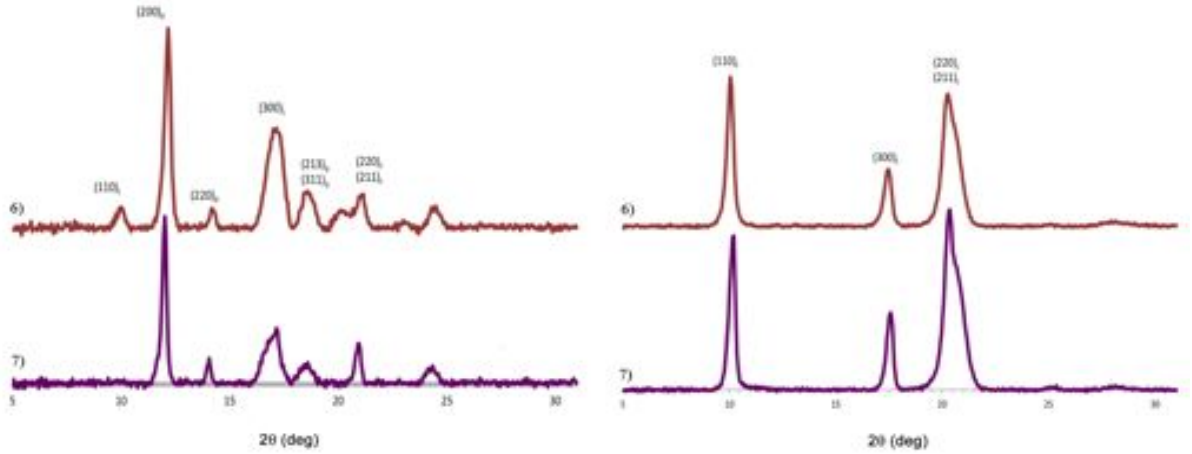

Figure 21. Partial WAXD profiles of unannealed (left) and annealed (right) poly(1-butene) materials using **52** from Table 1.

The same WAXD studies were carried out on the materials synthesized using the dinuclear initiator, **52**. As seen with the materials produced from the mononuclear analogue, reflections for both crystalline forms I and II can be seen with peaks at 2θ = 9.9, 17.3, and 20.5 ° for $(110)_I$, $(300)_I$, and $(220)_I$+$(211)_I$ respectively for form I and peaks at 2θ = 11.9, 16.9, and 18.3 ° for $(200)_{II}$, $(220)_{II,}$ and $(213)_{II}$+$(311)_{II}$ respectively for form II (Figure 21).[6] It is interesting to note here that there is a reduced loss of crystallinity with the same degree of activation, .70, using the dinuclear initiator compared to its mononuclear analogue (entry 6 vs. entry 7, Figure 21). This phenomenon has been previously attributed to regional and steric influences from the tether in the dinuclear design of the initiator.[7]

Again, as seen with the mononuclear initiator, there is a definite change in the crystalline properties of the artificially aged materials. The poly(1-butene) materials only contain form I crystals as evident by the reflections at 2θ = 9.9, 17.3, and 20.5 ° for $(110)_I$ $(300)_I$ and $(220)_I$+$(211)_I$ respectively.

2.3 Living Coordinative Chain Transfer Polymerization

Scheme 16. Living Coordinative Chain Transfer Polymerization (LCCTP).

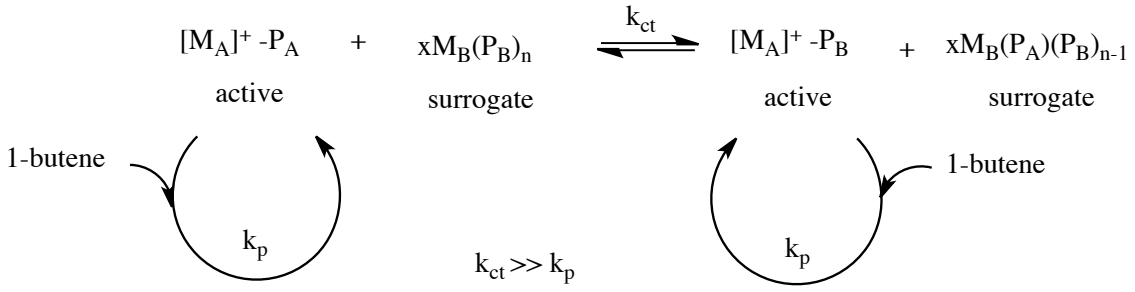

LCCTP has enabled us to overcome the 'one polymer chain per metal site' limitation that is associated with single site catalysts through the addition of a main group metal alkyl species. This main group species, in this case diethyl zinc (DEZ), acts as a surrogate chain growth site with the amount of polymer that can be produced showing dependency on the amount of the chain transfer agent. It is important to note that this surrogate chain growth site does not contain the potential to engage in polymerization and cannot be classified as a dormant species. As seen in Scheme 16 the key feature to this being a viable option is the rapid *and* reversible chain transfer of the polymeric group that occurs between the active transition metal species and the main group metal surrogate species. If the rate constant of the chain transfer between the two metals, k_{ct}, is several orders of magnitude greater than the rate of propagation, k_p, it will seem that the metal centers are undergoing propagation at the same rate.[2,3,8] This process has allowed for the retention of desirable living polymerization characteristics such as narrow polydispersities (shown in the equation below where N_i is the number of molecules of mass M_i) from strict molecular weight control, facile chain end functionalization, and the production of block co-polymers.[4] The addition of a surrogate species allows for the

production of the polymer to be scaled up such that the amount produced will depend on the amount of surrogate growth sites that are present in the solution.

$$\mathrm{PDI} = \frac{M_\mathrm{w}}{M_\mathrm{n}} \approx 1 + \frac{k_\mathrm{p}}{k_\mathrm{CT}}$$

$$M_\mathrm{w} = \frac{\Sigma M_\mathrm{i} N_\mathrm{i}}{\Sigma N_\mathrm{i}}$$

$$M_\mathrm{n} = \frac{\Sigma M_\mathrm{i}^2 N_\mathrm{i}}{\Sigma M_\mathrm{i} N_\mathrm{i}}$$

The main draw back to this process, and the focus of the remaining chapters of this thesis, is that stereocontrol from the initiator is lost due to the transfer process on and off the propagating transition metal species. With using **51** there is a statistical likelihood that the incoming polymer group will transfer onto an active manifold that is of a different conformation (R vs. S) than the one it originated from. This introduces a stereoerror into the polymer chain and the rapid transfer between the two different manifolds of the initiator will result in a stereoerror rich, atactic, polymer.

Scheme 17. LCCTP of 1-butene using **53**.

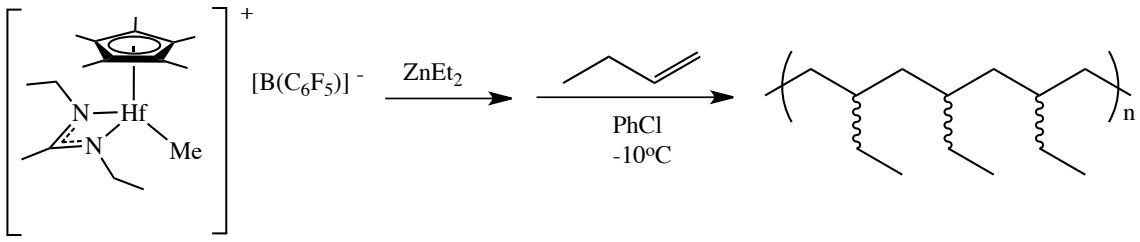

Table 2. Polymerizations with 1-butene under LCCTP conditions using **53**.

Entry	$ZnEt_2$ (eq.)	t_p [a] (h)	Yield (g)	M_n [b] (KDa)	PDI[b]	T_m [c] (°C)	T_c [c] (°C)	T_g [c] (°C)	% *mmmm*[d]
1	0	20	1.03	35.7	1.33	--	--	-24.0	0.18
2	10	16	1.40	4.42	1.03	--	--	-38.4	0.16

[a] Polymerizations were terminated at precipitation into acidic MeOH. [b] Determined by gel permeation chromatography (GPC) analysis. [c] Determined by differential scanning calorimetry (DSC) analysis. [d] Determined by ^1H (600 MHz) and ^{13}C (150 MHz) NMR at 110 °C in 1,1,2,2-tetrachloroethane-d_2

The polymerizations were conducted as shown in Scheme 17 using diethyl zinc as the chain transfer agent in chlorobenzene at -10 ^oC. An initial screen using the initiator (η^5-C_5Me_5)$HfMe_2$[N(Et)C(Me)N(Et)] (**53**) under non-LCCTP conditions revealed the successful homopolymerization of 1-butene (Table 2). As expected, due to the C_s-symmetric initiator, the resulting polymer had a very low degree of stereoregularity (% *mmmm* = 0.18) as calculated by ^{13}C NMR analysis (150 MHz in 1,1,2,2-tetrachlorethane-d_2 at 110 °C). Under LCCTP conditions with 10 equivalents of $ZnEt_2$ (Table 2, entry 2) **53** was also an effective initiator, and ^1H NMR analysis (600 MHz in 1,1,2,2-tetrachlorethane-d_2 at 110 °C) confirmed that this was a living process via the absence of vinylic protons that would result from β-hydride elimination. Also, Table 2 shows a decrease in the M_n and the PDI that is expected from the rapid chain transfer processes. ^{13}C NMR analysis of the resulting polymer's microstructure under LCCTP conditions is highly stereoerror rich, atactic, as expected with a % *mmmm* = 0.16.

2.4 Controlled Comonomer Incorporation

Scheme 18. Proposed mechanism of LCCTP mediated comonomer incorporation of ethene-co-1-butene.

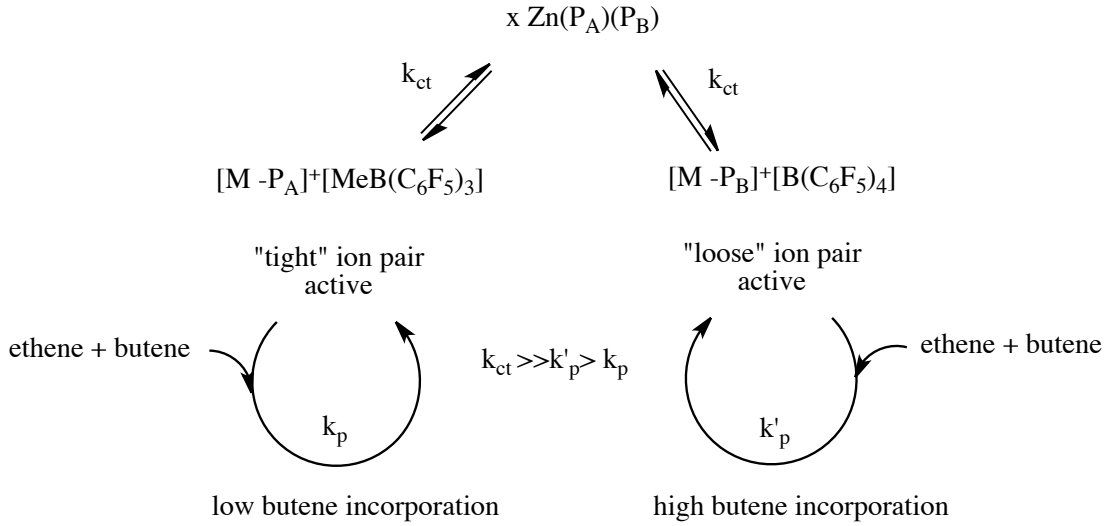

The reversible polymer chain transfer between “tight” and “loose” ion pairs has been previously documented and has successfully been adapted to control the amount of 1-butene that can be incorporated through copolymerization with ethene to open up a new range of materials available from one initiator.[9] Per Scheme 18, the dialkyl zinc species is able to act as a mediator between the ‘tight’ ion pair formed from activation of the (η^5-C_5Me_5)$HfMe_2$[N(Et)C(Me)N(Et)] (**53**) with the borate cocatalyst, [$PhNHMe_2$][$B(C_6F_5)_4$] (**49**) and the ‘loose’ ion pair formed from activation with the borane cocatalyst, $B(C_6F_5)_3$ (**63**). The key to this process is the rapid *and* reversible transfer, mediated by the diethyl zinc, of the polymeric group between the two propagating ion pairs. There is no direct exchange of the polymeric group observed between the two ion pairs in the absence of a

chain transfer agent.[9] This technology will allow for precise control of comonomer addition through the use of a *single* initiator.

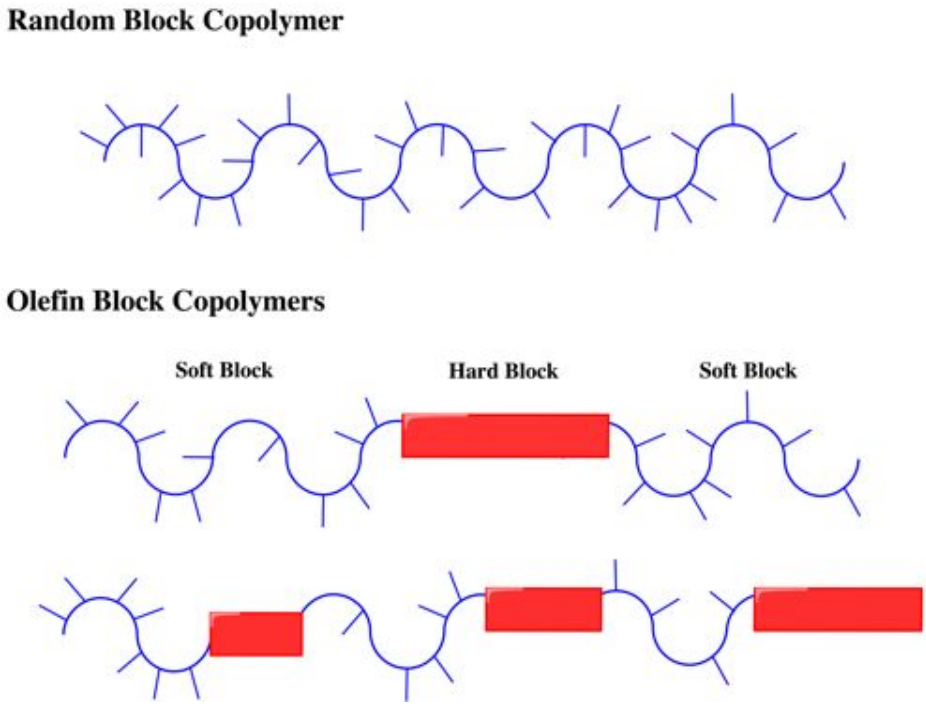

Figure 22. Random block copolymer and olefin block copolymer structure.

This new class of materials created from controlling the comonomer incorporation, dubbed 'olefin block copolymers', were first reported by Arriola and coworkers via a chain shuttling process involving two different catalysts and a chain shuttling agent (CSA) transferring the polymer chain between the different propagating catalysts in the copolymerization of ethene and 1-octene.[10] One catalyst has an affinity for inserting the large comonomer units while the second catalyst was less likely to insert and propagate 1-octene. The final product is then a blocky material composed of 'hard' blocks from long runs of polyethylene and 'soft' blocks from runs of the longer poly(α-olefin) (Figure 22). This process has been replicated here via the use of only *one* catalyst by creating

the two affinities for comonomer insertion through the use of two different ion pairs. The 'tight' ion pair has a lower affinity for the 1-butene insertions, and the other 'loose' ion pair has a greater affinity for the 1-butene insertions creating this blocky structure.

Table 3. Controlled comonomer incorporation of 1-butene (B) and ethene (E) using precatalyst Cp*Hf(Me)$_2$[N(Et)C(Me)N(Et)] (**53**) via LCCTP.

Entry	Cocatalyst[a] **49**:**63**	$ZnEt_2$ (eq.)	t_p (min)	Yield (g)	M_n[b] (KDa)	PDI[b]	%B[c] (^{13}C)	%B[c] (^{1}H)
1	1:0	10	20	1.75	7.87	1.13	20.0	24
2	1:1	10	20	1.02	5.76	1.14	15.5	17
3	1:3	10	20	1.00	--[d]	--[d]	8.7	10
4	0:1	10	10	0.52	--[d]	--[d]	6.0	7

[a]Conditions: precatalyst **53** (0.020 mmol), cocatalyst (**49** + **63** = 0.020 mmol, toluene at 0 °C, pressure of ethene (~5 psi), terminated at precipitation into acidic MeOH. [b] Determined by gel permeation chromatography (GPC) analysis. [c]Determined by ^{1}H (600 MHz) and ^{13}C (150 MHz) NMR at 110 °C in 1,1,2,2-tetrachloroethane-*d2*. [d] Insoluble for GPC analysis

2.4.1 Microstructure

The results summarized in Table 3 and entries 1-4 reveal that the 'looser' the ion pair, obtained through use of a higher ratio of borate to borane, incorporates more 1-butene than with the 'tighter' ion pair (higher ratio of borane to borate). For copolymerizations without a mixture of the cocatalysts (entries 1 and 4) there is a significant drop, by ^{13}C NMR (150 MHz in 1,1,2,2-tetrachlorethane-d_2 at 110 °C) triad analysis (Figure 23), in the amount of (1-butene) that is incorporated into the polymer, from 20.0% with exclusively using the borate and 6.0% with exclusively using the borane

cocatalysts.[11] This is also confirmed from the inability of the polymers with high ethylene incorporation (entries 3 and 4) to be solubilized enough for gel permeation chromatography.

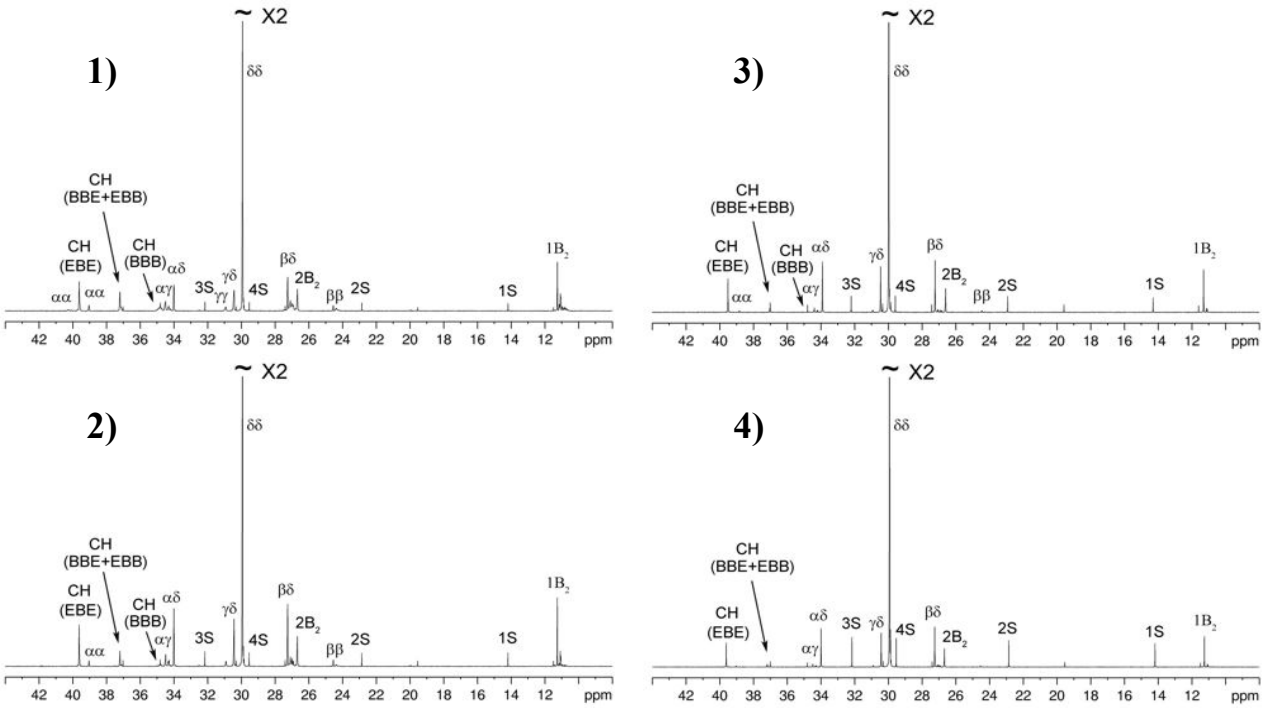

Figure 23. Partial ^{13}C NMR: 150 MHz, 1,1,2,2-tetrachloroethane-d_2, 110 ^{o}C spectrum and resonance assignments of poly(ethene-*co*-1-butene) of materials from Table 3.

2.4.2 Thermal Analysis

Table 4. Physical properties of poly(ethylene-co-butene) materials.

Entry	Cocatalyst[a] **49**:**63**	$ZnEt_2$ (eq.)	T_m [a] (°C)	T_c [a] (°C)	X_c [a] (%)	ΔH_m [a] (J/g)
1	1:0	10	106.5; 73.2	93.9; 55.8	13.6	39.8
2	1:1	10	101.1; 70.0	87.1; 70.1	19.7	57.7
3	1:3	10	111.2; 95.7	100.5; 83.7	11.9	34.9
4	0:1	10	106.1; 96.1	96.7; 76.0	14.0	40.9

[a] Determined by differential scanning calorimetry (DSC) analysis.

The thermal behavior of the copolymers is shown in Figure 24 with the second heating and cooling cycles obtained by differential scanning calorimetry (DSC). The peak temperatures, for both the T_m and T_c, increased slightly with the decreasing 1-butene content of the materials. The material that contains the highest percentage of 1-butene incorporated (entry 1, Table 4) using the 'loose' ion pair is seen to show considerable broadening in the melting and cooling thermograms (1, Figure 24). This is expected given the greater disruption of the crystallinity of the polyethylene segments from the greater amount of 1-butene incorporated into the polymer chains. Subsequently the material that contains the lowest amount of 1-butene from using the 'tight' ion pair shows the sharpest peaks in both the melting and cooling thermograms from the higher concentration of the more crystalline polyethylene. The percent crystallinity and ΔH_m was calculated from the thermograms using 100 % crystalline polyethylene homopolymer as a reference with a heat capacity of 293.0 J/g.[12] It is curious that the samples containing the higher amount of polyethylene display a lower percent crystallinity, but it

is reasonable to assume that these differences can be accounted for by the molecular weights of the materials given that they were too insoluble for GPC analysis.

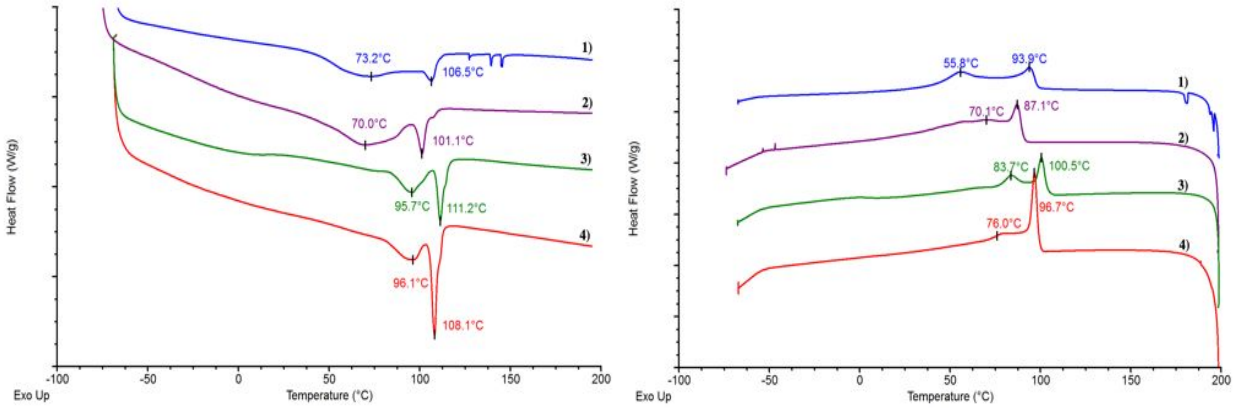

Figure 24. DSC thermograms of ethylene-co-1-butene materials from Table 4.

The presence of two temperatures for each material gives rise to the likelihood that these materials are not true random copolymers, but instead they could be classified as 'blocky' copolymers. Only one temperature would be observed on the thermograms should the materials be random copolymers. Instead T_c's and T_m's are seen for both a polyethylene segment (the second, higher peaks) and a poly(1-butene) segment (the first, lower peak).

2.4.3 WAXD Profile

Wide-angle X-ray diffraction (WAXD) was used to study the solid-state structures of the poly(ethylene-co-1-butene) materials obtained from controlling the comonomer incorporation. The orthorhombic unit cell of the crystalline polyethylene can be identified by the peaks at 2θ = 21.5 23.9, and 30.0 ° for (110), $(200)_I$, and (210) respectively.[13] The reflections of the crystalline polyethylene, although decreased

significantly, can still be seen through the increased amorphous halo caused by the increased poly(1-butene) content.

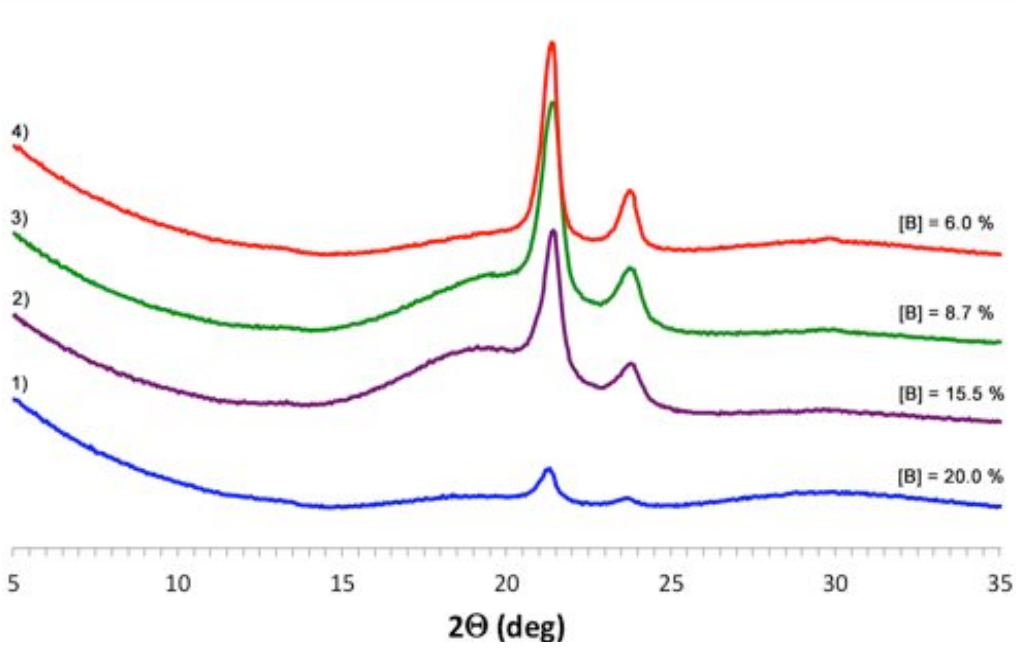

Figure 25. WAXD profiles of poly(ethylene-co-1-butene) materials from Table 3.

2.4.4 Rheological Behavior

A comparison of the storage moduli in Figure 26 show that the material containing 8.7% 1-butene exhibits a storage modulus higher than that of the material containing 20.0% 1-butene and 15.5% 1-butene indicating that the material was fully in the liquid state at 100 ^{o}C, which is expected given the increased concentration of polyethylene in the polymer structure. Figure 27 represents the viscoelastic properties of the poly(ethylene-co-1-butene) materials (entries 1-3, Table 3) that were determined via rheology at a frequency sweep of 0.1 rad/sec at 100 ^{o}C. For material 1, it is interesting to note that the slope is ~0. This indicates that the material displays a spherical morphology

at 100 °C with 1.0 % strain at low frequencies.[14] At 120 °C the material is fully in the molten state and shows no ordering with regard to morphology. A log G' slope of ~0.5 is seen for material 2 at low frequencies to indicate that the polymer has adopted a lamellae structure at 100 °C with 1.0 % strain. If these materials were random copolymers, as expected, then the slope of the storage modulus (log G') vs. frequency (log ω) would be ~2 representing the homogenous phase of the material from the molten state.[14] However, rheological analysis further supports the hypothesis that these materials can be considered 'blocky' instead of true random copolymers. For material 3 the log G' curve at 4.0 % strain displays an inversion of the log G' and log G" which is indicative that the material is still highly crystalline despite the high degree of strain and temperature. Material 4 was not characterized due to the liquid nature expressed by the material 3; it would display more liquid characteristics given its highest concentration of polyethylene in the series.

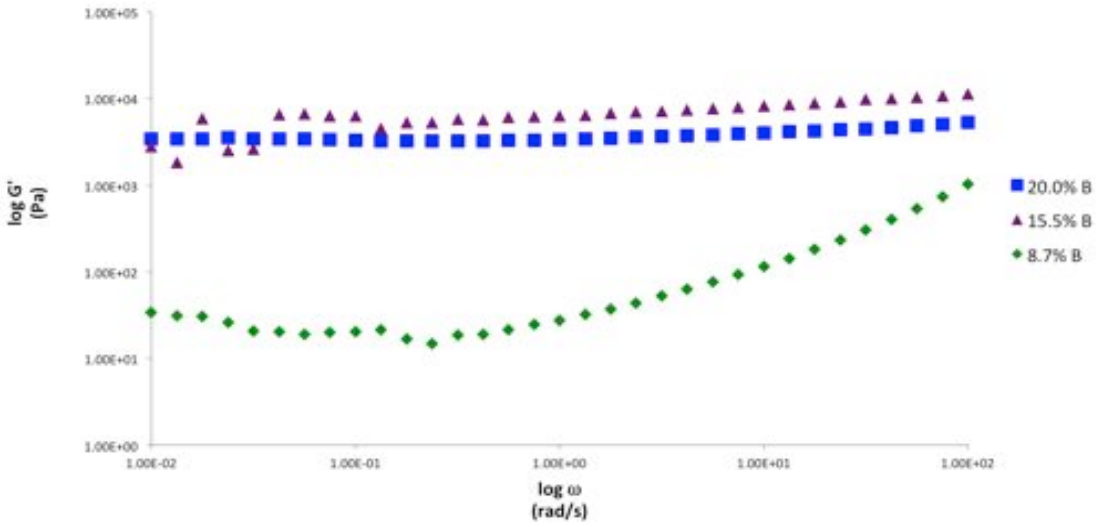

Figure 26. Comparison of storage modulus (log G') for poly(ethylene-co-1-butene) materials (entries 1-3, Table 3) with 0.1 rad/sec frequency sweep at 100 °C.

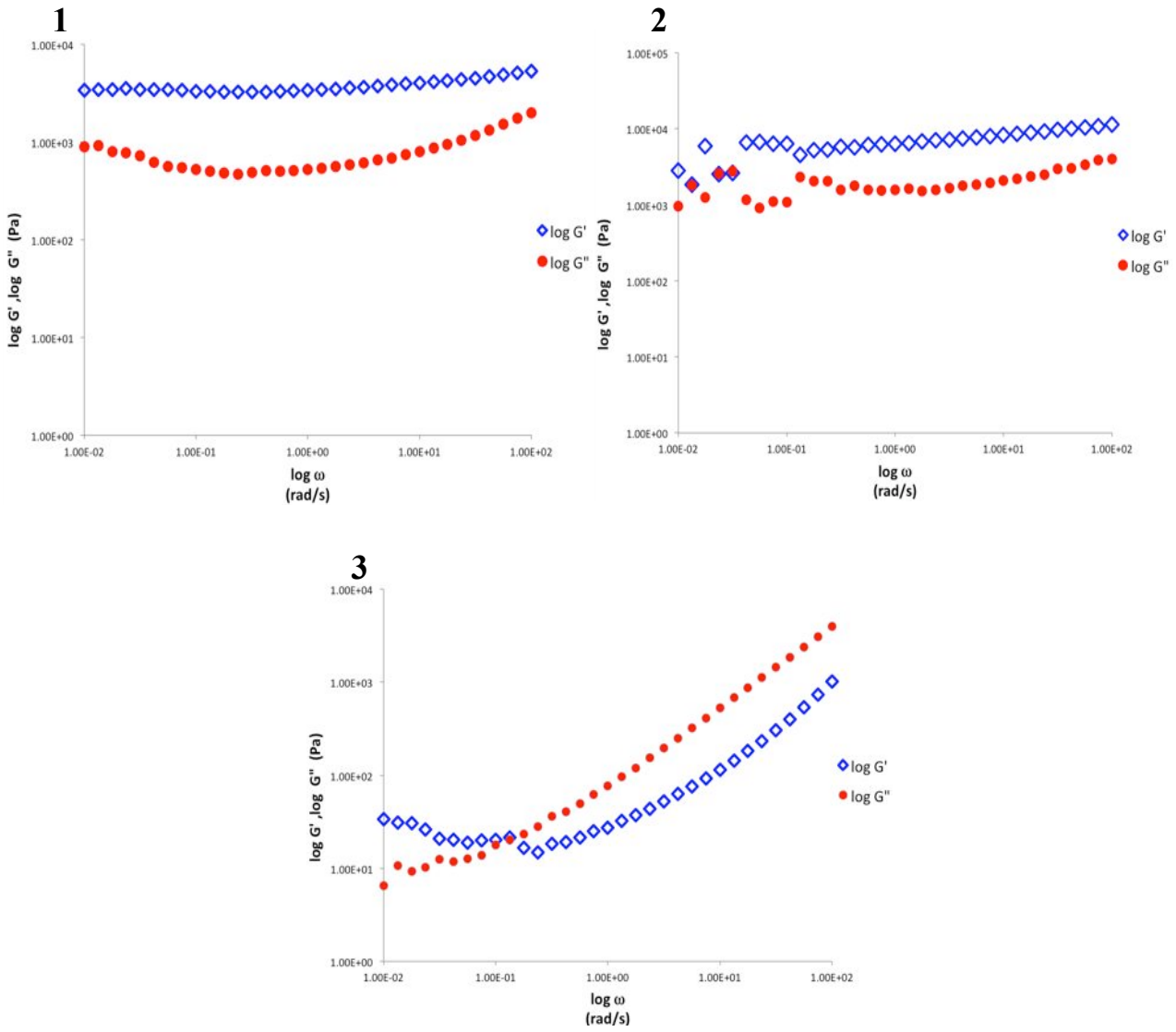

Figure 27. Strain sweep tests for poly(ethylene-co-1-butene) materials (entries 1-3, Table 3) with 0.1 rad/sec at 100 ^{o}C.

2.4.5 Phase Imaging

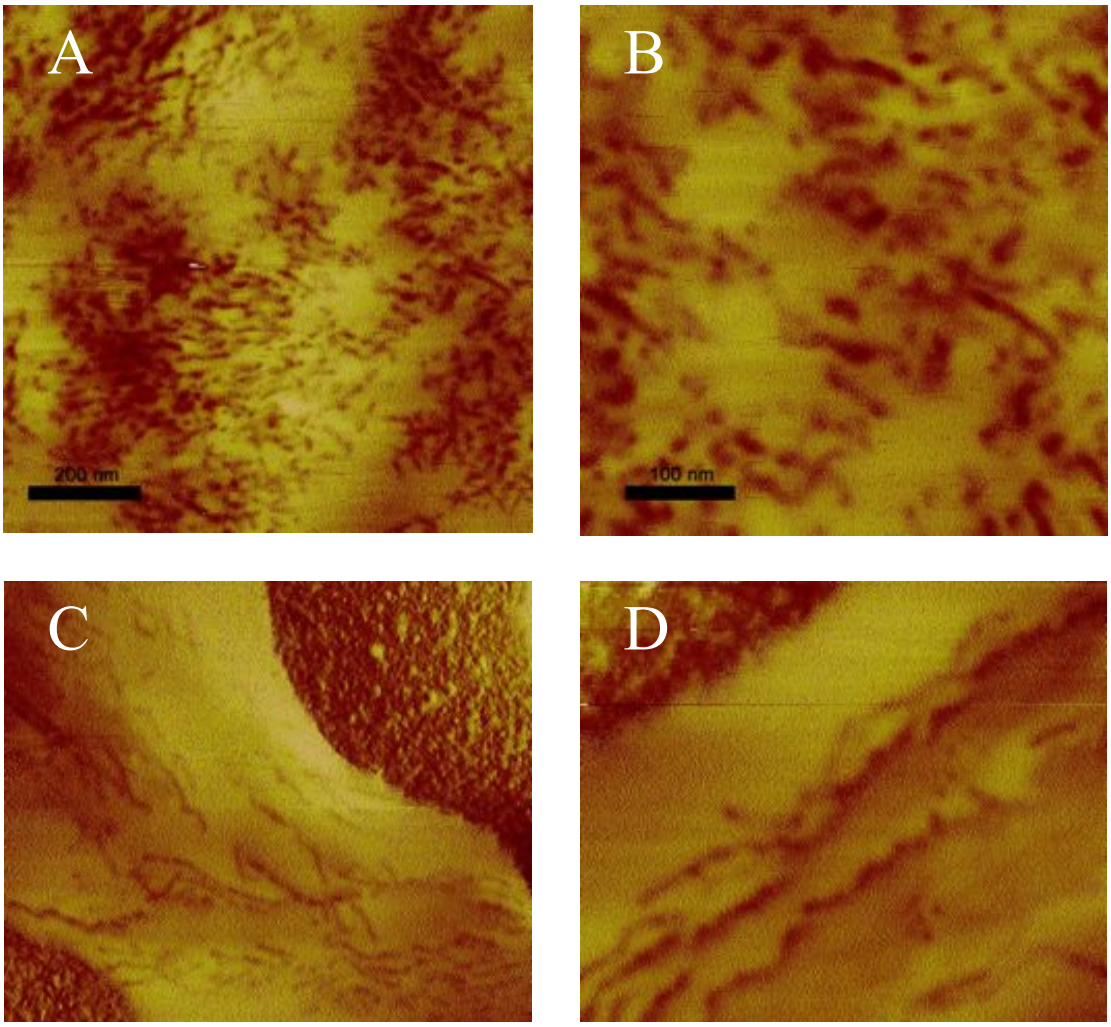

Figure 28. ps-tm-AFM phase maps of 20.0 % B material (entry 1, Table 3) as cast (A,B) and thermally annealed (C,D).

With the rheological data suggesting order in the crystalline morphologies of the materials containing 20.0% and 15.5% 1-butene (entries 1 & 2, Table 3), samples of the materials were imaged, as cast and thermally annealed, using phase-sensitive tapping-mode atomic force microscopy (ps-tm-AFM).[15-18] In the phase maps of both the spin cast and thermally annealed samples of the poly(ethylene-co-1-butene) containing 20.0% 1-

butene (entry 1, Table 3) show large crystalline domains from weak ordering of crystalline lamellae morphologies. Rheological analysis at 100 ^{o}C suggested a spherical morphology, but room temperature analysis of the material suggests lamellae ordering. Should these materials be truly random copolymers, no phase separation would be visible. Typically, ultra low-density polyethylene (ULDPE) contains 10-30 wt% of comonomer. Entry 1 and 2 might be the ULDPE and the small fraction of PE crystalline lamellar structures would be expected. However, the viscoelastic behaviors at low frequencies of the 15.5 and 20.0 % 1-butene materials show the ordered microphase separation that is well known phenomena in block copolymer phase separation. As the temperature increases to the melting point, microphase separation occurs between pure PE block and PE-co-PB block. Similar features are seen in the images in Figure 29 of both the spin cast and thermally annealed samples of the poly(ethylene-co-1-butene) containing 15.5% 1-butene (entry 2, Table 3). The phase imaging for this material is in agreement with rheological analysis in that lamellae morphologies are observed.

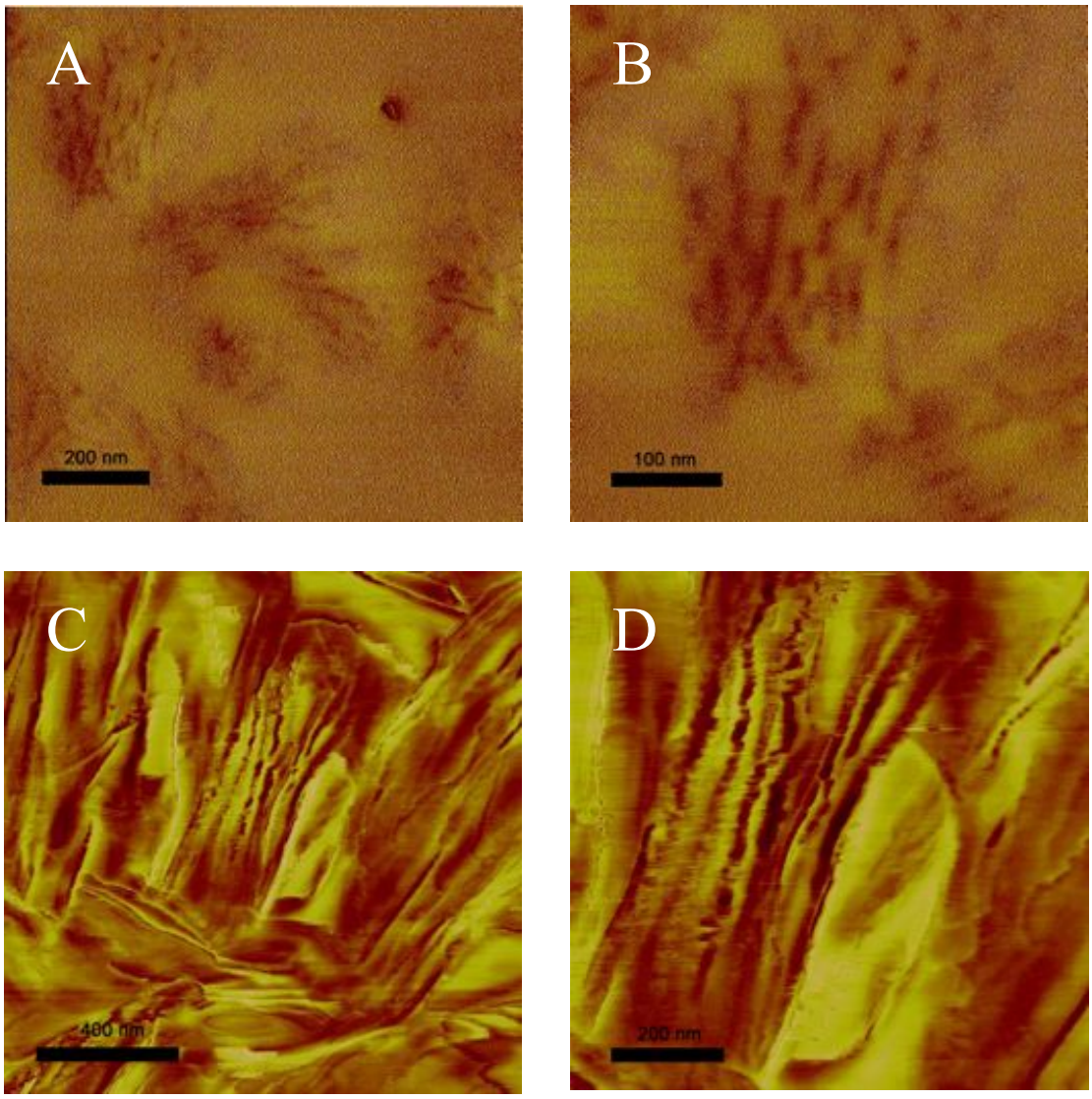

Figure 29. ps-tm-AFM phase maps of 15.5 % B material (entry 2, Table 3) as cast (A,B) and thermally annealed (C,D). Note the different scale in the thermally annealed (C,D) images.

2.5 Conclusions

Upon substoichiometric activation of **51** and **53** with **49**, living methyl group degenerative transfer polymerization is achieved for the use of programming stereorrors

in a controlled fashion into the resulting poly(1-butene) materials. The resulting dormant species present in solution from the incomplete activation of the initiators undergo metal centered epimerization, which results in a stereoerror introduced into the growing polymer chain upon reactivation with the transfer of the methyl group. A clear decrease in the isotacticity of the resulting materials was seen as the number of epimerizing dormant species was increased through decreased activation of the initiator. Secondly, the limitation of 'one chain per metal site' was negated with the addition of diethyl zinc to act as a surrogate growth site in living coordinative chain transfer polymerization. The rapid and reversible polymer group transfer between the active transition metal species and the main group metal species resulted in materials of a lower molecular weight due to the polymer group transfer occurring more frequently than propagation. Also a decrease in the polydispersity of the materials was seen due to the inverse relationship between the PDI and the rate constant for chain transfer. Lastly, novel OBC's containing ethylene and 1-butene were created and fully characterized via controlling the 1-butene incorporation into polyethylene with the presence of two active ion pairs, from the same initiator, that was mediated by the presence of diethyl zinc acting as a chain transfer agent. These two active pairs, created by activation with mixtures of **49** and **63**, experience different affinities for the propagation of the two olefins therefore creating 'blocky' structures.

2.6 Experimentals

Materials:

All manipulations were performed under an inert atmosphere of N_2 using standard Schlenk-line or glove-box techniques. All solvents were dried (Na for toluene and CaH_2

for chlorobenzene) and distilled under N_2 prior to use. (η^5-C_5Me_5)$ZrMe_2$[N(*t*Bu)C(Me)N(Et)] (**51**), [(η^5-C_5Me_5)$ZrMe_2$]$_2$[N(*t*Bu)C(Me)N-$(CH_2)_6$-NC(Me)N(*t*Bu)] (**52**), and (η^5-C_5Me_5)$HfMe_2$[N(*Et*)C(Me)N(Et)] (**53**) were prepared from previously reported procedures. 1-butene was purchased from Sigma Aldrich and used as received. Polymer grade ethene was purchased from Matheson Trigas and passed through activated Q5 and molecular sieves (4 Å) before use. [$PhNHMe_2$][$B(C_6F_5)_4$] (**49**) was purchased from Boulder Scientific while $B(C_6F_5)_3$ (**63**) was obtained from Strem Inc. and used without further purification. $ZnEt_2$ was purchased from Sigma Aldrich and added to the reaction as a 1.1M (15% wt) solution in toluene.

Instrumental:

GPC analyses were performed using a Viscotek GPC system equipped with a column oven and a differential refractometer both maintained at 45 °C and four columns also maintained at 45 °C. THF was used as the eluent at a flow rate of 1.0 mL/min. M_n, M_w, and M_w/M_n values were obtained using a Viscotek GPC with OmniSEC software and ten polystyrene standards (M_n=580 Da to 3150 kDa) (Polymer Laboratories).

^{13}C NMR spectra were recorded at 600 MHz and 150 MHz, respectively, using 1,1,2,2-tetrachlorethane-d_2 at 110 °C with a Bruker AVIII-600MHz spectrometer equipped with a Bruker 5 mm C13/H1 dual probe with Z gradient. Spectra were recorded under the following conditions: 45° pulse; without NOE; acquisition time, 1.2 s; relaxation delay, 2.0 s; >10K transients.

Differential Scanning Calorimetry (DSC) thermograms were collected on a TA DSC Q1000 system with a heating and cooling rate of 5 or 10 ^oC/min. All samples were prepared in hermetically sealed pans (8 – 10 mg/sample) and were run using an empty

pan as a reference and empty cells as a subtracted baseline. The samples were scanned for multiple cycles to remove recrystallization differences between the samples and the results reported are of the second and third scans in the cycles.

Wide-angle X-ray diffraction (WAXD) measurements were carried out with all the samples measured in an as-prepared state with and without thermal annealing at 85 ^{o}C with a cool down of 12 hours in a 1400E VWR Vacuum Oven. 0.5 g of each material was mounted on the sample holder and the measurement was performed on Bruker D8 Advance system with LynxEye detector. The wavelength of Cu *Kα* radiation was selected $\lambda = 1.54$ Å and the scan angle was 5~60˚with 0.05˚step. The data was collected at room temperature and the amorphous halo of each material was subtracted by amorphous material with arbitrary scale. The obtained profiles were fitted with built-in software (Advanced TOPAS).

Dynamic mechanical shear modulus analysis was conducted using RSA III Analyzer (Rheometric Scientific Inc.) with parallel plates (diameter : 7.9 mm, gap : ca. 1 mm). Dynamic storage and loss shear moduli, G' and G'', were obtained with a shear oscillation of 0.1 rad/sec and a low strain amplitude of 2-4% keeping in the linear viscoelastic regime of each sample. The frequency was adjusted to 10 and 100 rad/sec for homo materials to detect enough mechanical response, keeping in the linear viscoelastic regime of each sample. The temperature range was 25-120 ˚C with 1 ˚C/min ramp in order to obtain order-disorder transition temperatures (T_{ODT}) under nitrogen gas purging to prevent thermal oxidation. The storage modulus, loss modulus, and tan δ were monitored and analyzed using TA Orchestrator software version 7.2.

The topological analysis was performed on a Multimode AFM with Nanoscope IIIa controller (Digital Instrument) in tapping mode. Both height and phase-shift data were obtained with a silicon etched tip (Nanosensors, spring constant k = 25-55 N/m, resonance frequency f = 292-377 KHz) under ambient conditions. All samples were dissolved in toluene (1 wt %) and spin-coated at 2000 rpm onto Si substrates. Si substrates surfaces were cleaned with 7:3, H_2SO_4 : H_2O_2 "pirahna" solution (CAUTION). Film thickness was obtained by using Gaertner ellipsometer for 3 different spots on each sample. Spin-coated film thicknesses were remained between 30 to 35 nm. All AFM samples were measured before and after annealing at 85 ˚C for 12 hours.

Typical procedure for polymerization of 1-butene:

A solution of 0.050 mmol precatalyst **51** or 0.025 mmol of precatalyst **52** in 0.5 mL chlorobenzene at -10 °C was added to the $[PhNMe_2][B(C_6F_5)_4]$ (% activation x 0.050 mmol) and agitated until a clear light yellow solution formed. The resulting mixture was added to 29.5 mL chlorobenzene and 400eq 1-butene at -10 °C in a 250 mL Schlenk flask. The stirring and temperature was maintained at -10 ± 2 ºC for the duration of the reaction where upon it was quenched with 1.0 mL of methanol and precipitated into 600 mL acidic methanol to isolate the polymer. The final poly(1-butene) was collected by filtration and washed with 5 mL × 4 methanol before being dried under vacuum. The resulting polymers were characterized by DSC, GPC, $^{1}H/^{13}C$ NMR, WAXD, Rheology, and AFM.

Typical procedure for LCCTP polymerization of 1-butene:

A solution of 9.1 g (0.020 mmol) of precatalyst **53** in 0.5 mL of pre-cooled (-10 ºC) chlorobenzene was added to a solution of 16.8 g (0.020 mmol) of co-catalyst **49** in

0.5 mL of pre-cooled (-10 ºC) chlorobenzene, and mixed until a clear light yellow solution formed. This solution was then rapidly added to a 250-mL Schlenk flask loaded with 20 mL of chlorobenzene, 165 mg (10 equivalents relative to **53**) of $ZnEt_2$ (15 % wt in toluene) and 2.24 g (2000 equivalents relative to **53**) of 1-butene at -10 ºC. Polymerization temperature was maintained at -10 ± 2 ºC. After 16 h, polymerization was quenched with 1.0 mL of methanol. The polymerization solution was then precipitated into 600 mL methanol to isolate the polymer. The final poly(1-butene) was collected by filtration and washed with 5 mL × 4 methanol before being dried under vacuum.

Typical procedure for LCCTP copolymerization of ethene with 1-butene :

A solution of 9.1 g (0.020 mmol) of precatalyst **53** in 0.5 mL of pre-cooled (-10 ºC) chlorobenzene was added to a solution of 16.8 g (0.020 mmol) of co-catalyst **49** in 0.5 mL of pre-cooled (-10 ºC) chlorobenzene, and mixed until a clear light yellow solution formed. This solution was then rapidly added to a 250-mL Schlenk flask loaded with 20 mL of toluene, 165 mg (10 equivalents relative to **53**) of $ZnEt_2$ (15 wt% in toluene) and 2.24 g (2000 equivalents relative to **53**) of 1-butene at -10 ºC., which was previously pressurized to 5 psi with ethene. The pressure was maintained for the desired polymerization time with polymerization temperature maintained at -10 ± 2 ºC. Polymerization was quenched with 1.0 mL of methanol, and then precipitated into 600 mL methanol to isolate the polymer. The final copolymer was collected by filtration and washed with 5 mL × 4 methanol before being dried under vacuum.

2.7 References

(1) Zhang, W.; Sita, L. R. *Adv. Synth. Catal.* **2008**, *350*, 439-447.

(2) Zhang, W.; Sita, L. R. *J. Am. Chem. Soc.* **2008**, *130*, 442-443.

(3) Sita, L. R. *Angew. Chem., Int. Ed.* **2009**, *48*, 2464-2472.

(4) Jayaratne, K. C.; Sita, L. R. *J. Am. Chem. Soc.* **2000**, *122*, 958-959.

(5) Jayaratne, K. C.; Sita, L. R. *J. Am. Chem. Soc.* **2001**, *123*, 10754-10755.

(6) De Rosa, C.; Auriemma, F.; Ruiz de Ballesteros, O.; Esposito, F.; Laguzza, D.; Di Girolamo, R.; Resconi, L. *Macromolecules (Washington, DC, U. S.)* **2009**, *42*, 8286-8297.

(7) Wei, J.; Hwang, W.; Zhang, W.; Sita, L. R. *J. Am. Chem. Soc.* **2013**, *135*, 2132-2135.

(8) Zhang, W.; Wei, J.; Sita, L. R. *Macromolecules (Washington, DC, U. S.)* **2008**, *41*, 7829-7833.

(9) Wei, J.; Zhang, W.; Wickham, R.; Sita, L. R. *Angew. Chem., Int. Ed.* **2010**, *49*, 9140-9144.

(10) Arriola, D. J.; Carnahan, E. M.; Hustad, P. D.; Kuhlman, R. L.; Wenzel, T. T. *Science (Washington, DC, U. S.)* **2006**, *312*, 714-719.

(11) Sahoo, S. K.; Zhang, T.; Reddy, D. V.; Rinaldi, P. L.; McIntosh, L. H.; Quirk, R. P. *Macromolecules* **2003**, *36*, 4017-4028.

(12) Wunderlich, B.; Academic: **1981**, p 91.

(13) McFaddin, D. C.; Russell, K. E.; Wu, G.; Heyding, R. D. *J. Polym. Sci., Part B: Polym. Phys.* **1993**, *31*, 175-183.

(14) Kossuth, M. B.; Morse, D. C.; Bates, F. S. *J. Rheol. (N. Y.)* **1999**, *43*, 167-196.

(15) Leclere, P.; Lazzaroni, R.; Bredas, J. L.; Yu, J. M.; Dubois, P.; Jerome, R. *Langmuir* **1996**, *12*, 4317-4320.

(16) Hobbs, J. K.; Register, R. A. *Macromolecules* **2006**, *39*, 703-710.

(17) Stocker, W.; Beckmann, J.; Stadler, R.; Rabe, J. P. *Macromolecules* **1996**, *29*, 7502-7507.

(18) van Dijk, M. A.; van den Berg, R. *Macromolecules* **1995**, *28*, 6773-6778.

Chapter 3

Guanidinate Based Initiators for Stereocontrol During LCCTP

3.1 Background

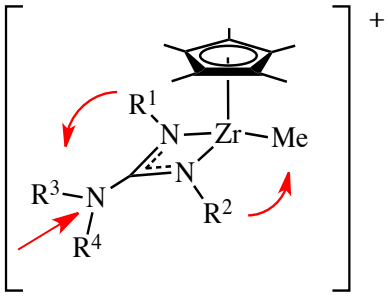

Figure 30. Proposed steric effects from a distal substituent

It has been well documented by our group that the C_1 symmetric precatalyst Cp*Zr[N(tBu)C(Me)N(Et)]Me_2 (**51**), when activated by [PhNHMe_2][B(C_6F_5)$_4$], produces polymers with a highly stereoregular microstructure (%*mmmm* = 0.72 for propene and %*mmmm* = 0.98 for 1-hexene).[1-3] The stereoselectivity achieved by using **51** is a result of an asymmetric amidinate, with *t*-butyl and ethyl side arms that emphasize the asymmetry allowing for more enantiofacial selective insertion of the incoming olefin. However, under living coordinative chain transfer polymerization (LCCTP) conditions, the stereoselectivity of the initiator is lost due to the statistical likelihood that the polymer group will transfer onto a propagating metal species of opposite handedness as it returns from the surrogate site due to $\nu_{CT} >> \nu_P$ (Chapter 1). This situation should be remedied through the use of an enantiopure active species so only one conformation is available as the polymer group transfers back onto a propagating species.[4]

An attractive option to solve this problem is to utilize a guanidinate, $[R_2NC(NR')_2]^{1-}$ instead of an amidinate, $[RC(NR')_2]^{1-}$ as it will provide another position from which the ligand framework can be tuned.[5-9] Since **51** has a limit to the amount of stereoselectivity it can impart, the objective is to use the distal substituent as a buttress against the side groups to provide more steric influence. The added steric influence from the side groups would theoretically create an active species with a greater influence on the stereoselectivity and provide a more isotactic polymer under non-LCCTP conditions. Additionally, the use of an enanitiomerically pure substituent would lead to a species that is unsusceptible to the loss of stereocontrol from the rapid chain transfer process in LCCTP conditions as only one conformation would be available for propagation.

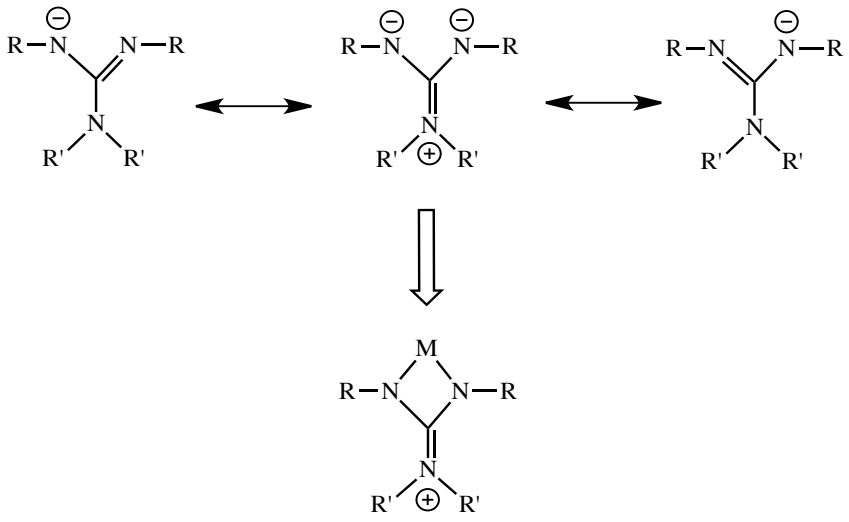

Figure 31. Resonance structures and bonding of the general guanidinate ligand

Unlike the mono-anionic amidinate ligand, the guanidinate ligand has been shown by the Bergman group to contribute more electron density to a metal center through a

zwitterionic resonance form that is a result of increased electron donation to the central carbon of the ligand (Figure 31).[5] The increased electron donation from the guanidinato ligand is expected to increase the stabilization of the cationic metal center, such as the one found in the active species during a living polymerization using **51**. A minimal loss in the activity of the species is expected due to this increased stabilization of the cationic metal center, but the increased stereoselectivity will counteract any decline in the usefulness of the initiator.

As mentioned in the previous paragraph, the guanidinate mono-anion has the ability to contribute more electron density to the metal center, therefore potentially changing the electronic nature of the pre-catalyst. The Bergman group found success in the non-living polymerization of ethylene and 1-hexene/ethylene with their Cp bisguanidinato complexes, but no previous attempt to substitute an amidinate ligand with a guanidinate ligand for the use of living coordinative polymerization has been found, and if successful, would prove to be the first reported case.[5]

3.2 Synthesis

3.2.1 Synthesis of 'Cp*ZrGuCl$_2$'

Scheme 19. Synthetic route to 'Cp*GuZrCl$_2$'

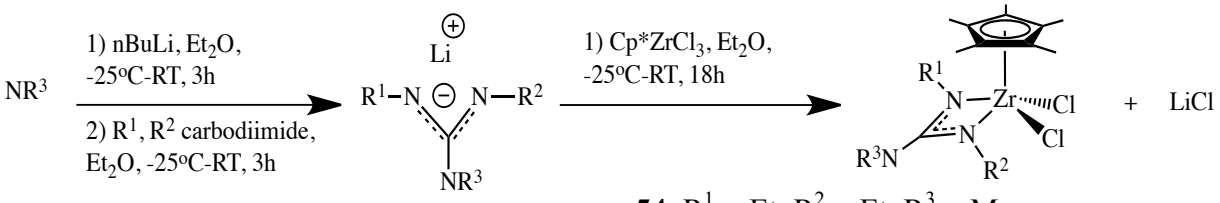

54 R^1 = Et, R^2 = Et, R^3 = Me_2
55 R^1 = Et, R^2 = Et R^3 = 2-methylpyrrol.
56 R^1 = Et, R^2 = tBu, R^3 = 2-methylpyrrol.
57 R^1 = Et, R^2 = tBu, R^3 = Me_2

The 'Cp*GuZrCl$_2$' complexes were synthesized in good yields by generating the guanidinate salt via addition of lithium dimethylamide with the desired carbodiimide, which was then subsequently added to the commercially available Cp*ZrCl$_3$ in ether at -25 ^{o}C (Scheme 19). In the case of the 2-methylprryolidine species, the amine was deprotonated with 1.1 equivalents of *n*-BuLi before the addition of the desired carbodiimide. The resulting compounds were easily purified by filtering with toluene to remove LiCl impurities followed by recrystallization at -25 °C using a solution of minimal toluene layered with pentane.

3.2.2 Synthesis of 'Cp*ZrGuMe$_2$'

Although typical methylation procedures involve reacting the corresponding dichloride complex with 2 equivalents of methyl lithium, this method proved to be unsuccessful with these complexes. To solve this problem, MeMgCl was targeted as an alternative methylating reagent.[5] Despite multiple attempts with both MeMgCl and MeLi, the dialkylation of **56** only resulted in the generation of a monomethyl species (**60**). The methylation of only one of the chlorides was confirmed via ^{1}H NMR and x-ray diffraction of single crystals.

Scheme 10. Synthetic route to 'Cp*GuMe$_2$'

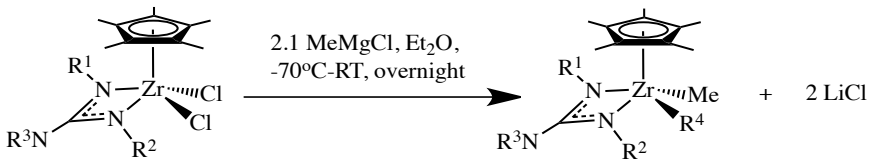

58 R^1 = Et, R^2 = Et, R^3 = Me_2 , R^4 = Me
59 R^1 = Et, R^2 = Et R^3 = 2-methylpyrrolidine, R^4 = Me
60 R^1 = Et, R^2 = tBu, R^3 = 2-methylpyrrolidine, R^4 = Cl
61 R^1 = Et, R^2 = tBu, R^3 = Me_2, R^4 = Me

3.3 Solid State Analysis

3.3.1 Et, Et Derivatives

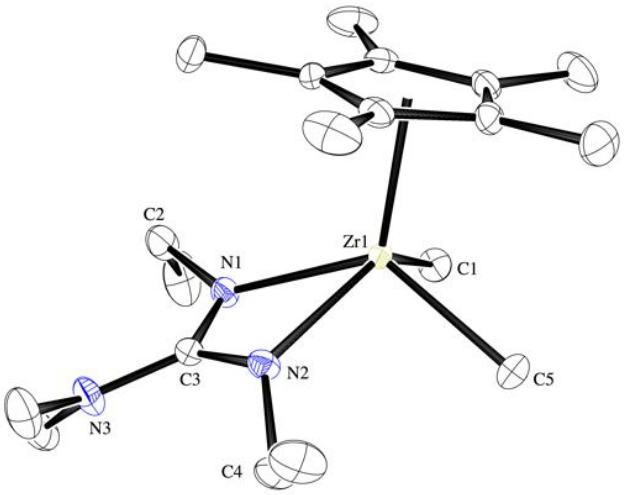

Figure 12. Crystal structure of **58** with hydrogen atoms omitted for clarity, ellipsoids for the non-hydrogen atoms are shown at the 30% probability level.

Table 5. Selected bond lengths and bond angles for the molecular structure of **58**.

Bond Angles (Å)	
Zr1-N1	2.2334(12)
Zr1-N2	2.2554(11)
Zr1-C1	2.2814(14)
Zr1-C5	2.2656(14)
C3-N1	1.3403(18)
C3-N2	1.3362(18)
C3-N3	1.3719(18)
Bond Angles (deg)	
N1-Zr1-N2	59.06(4)
Zr1-N2-C2	135.47(10)
Zr1-N1-C4	133.48(10)
C3-N2-C4	123.91(12)
C3-N1-C2	123.65(13)
N1-C3-N2	124.55(13)
ϕ[a]	-3.6(12)

[a] Angle between the mean planes defined by the following: Zr1-N1-C10 and Zr1-N2-C10.

Pure samples of **59** were able to be synthesized in 44% yield, as confirmed by ^{1}H NMR; however, multiple attempts at obtaining single crystals suitable for X-ray diffraction were unsuccessful. Single crystals of the C_s symmetric **58** were obtained and thus able to shed some insight into its behavior. Due to the symmetry of the complex, the bond lengths from the metal center to the guanidinato nitrogens, 2.2334(12) Å for Zr-N1 and 2.2554(11) Å for Zr-N2, are comparable to each other. The same applies to the metal-methyl group bond distances, 2.2814(14) Å for Zr-C1 and 2.2656(14) Å for Zr-C5. The guanidinate's C3-N3 bond distance is measured at 1.3719(18) Å, which is representative of a carbon-nitrogen single bond. The guanidinate's N1-C3 and N2-C3 bond lengths are 1.3402(18) Å and 1.3362(18) Å respectively, which are less than the expected 1.28 Å for a C=N. This is indicative that there is delocalization present in the guanidinato frame. The fairly large N1-C3-N2 angle, 124.55(13) °, provides evidence that the side ethyl groups will be able to 'relax' away from the metal center. It is expected that this initiator will be highly active without providing stereocontrol due to the openness of the guanidinate frame and the lack of enantiomorphic site control from it's high degree of symmetry.

3.3.2 *t*-Butyl, Ethyl Derivatives

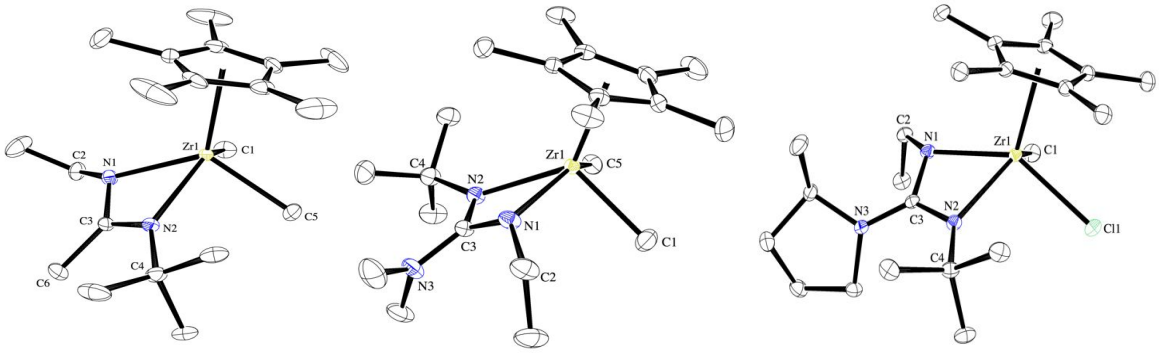

Figure 33. Crystal structure of (left) **51**, (middle) **60**, (right) **61** with hydrogen atoms omitted for clarity, ellipsoids for the non-hydrogen atoms are shown at the 30%

Table 6. Selected Bond Lengths and Bond Angles for the Molecular Structures of **51**, **60**, and **61**.

	51	**60**	**61**
		Bond Lengths (Å)	
Zr1-N1	2.251(3)	2.2624(15)	2.223(10)
Zr1-N2	2.265(2)	2.2543(14)	2.245(10)
Zr1-[X]	C1	C1	C1
	2.273(3)	2.2694(19)	2.2597(13)
Zr1-[Y]	C5	C5	Cl1
	2.272(3)	2.3320(18)	2.4691(3)
N1-C3	1.323(4)	1.334(2)	1.3490(14)
N2-C3	1.332(4)	1.338(2)	1.3447(14)
C3-C6/C3-N3	1.515(4)	1.382(2)	1.3738(15)
		Bond Angles (deg)	
N1-Zr1-N2	58.40(9)	58.78(5)	59.45(3)
Zr1-N1-C2	136.4(17)	132.22(12)	130.92(8)
Zr1-N2-C4	142.5(16)	137.49(11)	136.96(8)
C3-N1-C2	123.5(16)	122.44(15)	122.62(10)
C3-N2-C4	122(2)	125.75(14)	127.43(10)
N1-C3-N2	112.2(3)	112.11(14)	110.64(10)
ϕ[a]	18.3	10.0	7.6

[a] Angle between the mean planes defined by the following: Zr1-N2-C3 and Zr1-N1-C3.

The crystal structure for **51** has been previously reported in the literature with no unusual characteristics to note.[2] As expected with the asymmetry of the amidinate frame the ethyl side N1-C2 bond is 2.251(3) Å compared to a bond length of 2.2469(18) Å for the *t*-butyl side N2-C4 bond. The N1-C3/N2-C3 bonds are 1.323(4) Å and 1.332(4) Å which are in between 1.38 Å for a sp^2 C-N bond and 1.28 Å C=N bond indicating that there is only delocalization about the N1-C3-N2 fragment of the amidinate. It is also worth noting that the angle of the N1-C3-N2 fragment is 112.2(3) ° and the dihedral angle between the N1-C3-N2 segment and the N1-Zr1-N2 is 18.3 °.

Analysis of the solid-state structure of **60** reveals subtle structural differences of the neutral precatalyst species. As shown in Table 6, the lengths of the Zr-N bonds of 2.2624(15) Å for Zr1-N1 and 2.2543(14) Å for the Zr1-N2 bond are similar to those same bonds on **51**. The only obvious deviation between the two structures is the longer *t*-butyl side Zr1-C5 bond of 2.3320(18) Å for **60** and 2.272(3) Å for **51**, indicating that there is steric congestion on that side of the complex from the *t*-butyl group and the NMe_2 group, resulting in the metal-bound methyl group being pushed out further. The C3-N3 bond length of 1.382(2) Å is typical of an sp^2 C-N bond suggesting that there is not a significant contribution from the zwitterionic resonance structure of the guanidinate anion to the neutral complex. It is not expected that there would be a need for stabilization of the metal center from the guanidinate moiety as this is the solid-state structure for the neutral precatalyst - which lacks sufficient electron deficiency and is coordinatively saturated.

The solid-state structure for **61** is more interesting in that repeated attempts to synthesize the dialkylated species were unsuccessful due to the steric congestion on the *t*-

butyl side of the complex. The metal-nitrogen bonds, 2.223(10) Å for Zr1-N1 and 2.245(10) Å for Zr1-N2, are noticeably shorter in this derivative. Also, the C3-N3 bond length is 1.3738(15) Å, compared to a distance of 1.382(2) Å in the dimethylamino derivative, indicating that there may be more contribution from the zwitterionic resonance form of the guanidinate monoanion. This could also be a result of the steric bulk of the substituted pyrrolidine ring pushing up against the N1-C3-N2 fragment; the buttressing effect would also explain the shorter Zr-N distances. **61** also contains the smallest N1-C3-N2 angle of the series at 110.64(10) º. The smaller N1-C3-N2 angle is expected, as the N-alkyl substituents are less able to 'relax' away from the metal-alkyl groups creating a smaller N1-C3-N2 angle.

The buttressing effect from the distal substituents can be seen in the bond angles about the metal bound nitrogen atoms. The Zr1-N2-C4 angles decrease going from **51** [142.5(16) and 136.4(14) º] to **60** [137.49(11) and 132.22(13) º] to **61** [136.96(8) and 130.92(8) º] as the steric bulk increases. These decreasing bond angles causes an increase in the C3-N2-C4 angles going from **51** [122(2) and 123.5(16) º] to **60** [125.75(14) and 122.44(15) º] to **61** [127.43(10) and 122.62(10) º].

3.4 Polymerization Studies

Scheme 21. General activation procedure.

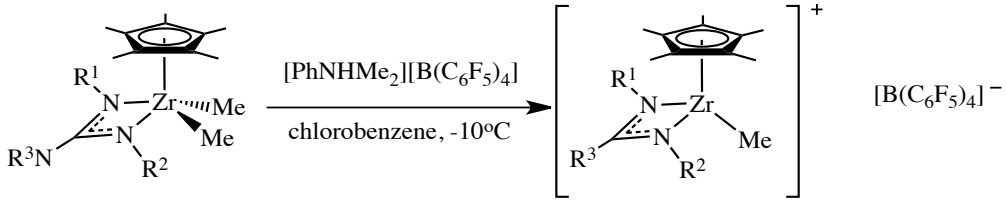

58 R^1 = Et, R^2 = Et, R^3 = Me_2
59 R^1 = Et, R^2 = Et R^3 = 2-methylpyrrol.
60 R^1 = Et, R^2 = tBu, R^3 = Me_2

Polymerizations were carried out based on the general activation procedure shown in Scheme 21 at -10 °C in chlorobenzene by reacting the dimethyl initiator with 1.05 equivalents of the cocatalyst, $[PhNHMe_2][B(C_6F_5)_4]$ (**49**) to create the active species. After the designated reaction time, the polymerizations were quenched, precipitated into acidic methanol and isolated by extraction into pentane. The resulting polymers were dried and characterized through the use of ^1H and ^{13}C NMR analysis. They were also characterized via differential scanning calorimetry (DSC) and gel permeation chromatography (GPC) to obtain information about their material characteristics including the T_m, T_c, T_g, molecular weight, and polydispersity.

Table 7. Polymerizations with propene with **51**, **58**, **59**.

Run	Precat.	Yield[a] (g)	M_n[b] (kDa)	PDI[c]	T_m[d] (°C)	% *mmmm*[e]
1	**51**	0.40	23.4	1.2	110.4	0.72
2	**58**	2.10	391.3	2.1	--	0.07
3	**59**	0.20	67.8	1.5	--	0.11

[a] Polymerizations were terminated at precipitation into acidic MeOH after 3 h. [b,c] Determined by gel permeation chromatography (GPC) analysis. [d]Determined by differential scanning calorimetry (DSC) analysis. [e] Determined by ^1H (600 MHz) and ^{13}C (150 MHz) NMR at 110 °C in 1,1,2,2-tetrachloroethane-d_2.

Visual and tactile observations of the resulting polymers indicated that they were highly amorphous and had very little crystallinity, while also having a rubbery and sticky feel. The values for the polydispersity index (PDI) are not in agreement with previously reported living polymerizations, indicating that these reactions did not proceed in a living manner. ^1H NMR analysis of the polymers confirmed the non-living character of the

polymerization with the presence of vinylic resonances indicating that these polymerizations terminated via β-hydride elimination. ^{13}C NMR of the microstructures of the resulting polymers show that there is no increase in isotacticity from what is expected of the C_s 'diethyl hafnium' species, and that these polymers are atactic.[10] The atactic nature of the microstructure is further confirmed by DSC analysis, which showed a lack of melting temperature (T_m) and a crystallization temperature (T_c), where here, it is noted that only polymers with a %*mmmm* > 0.15 will produce a melting temperature. The presence of these two distinguishing characteristic temperatures would have indicated a significant degree of isotacticity in the microstructure of the polymers.

It was expected that **58** would show little stereocontrol based on the lack of steric bulkiness on the distal substituents on the guanidinate frame based on previous work on the effect of stereoselectivity and size of substituents on an amidinate frame.[11] The high activity of the precatalyst was also expected due to the lack of steric bulk considering the two ethyl group side arms on the guanidinate. The smaller size of the NMe_2 distal group does not provide a 'buttressing effect' to the N-substituents, thus allowing them to bend away and create a more open active site compared **59**. Together, these two factors contributed to the predicted result of an ultra high molecular weight (>100KDa) polymer that was completely atactic. The lack of steric control from the distal position using ethyl groups as side-arm substituents prompted a return of the design strategy to use the *t*-butyl and ethyl group in the those positions. Here the distal substituent should increase the stereoselectivity by providing the same buttressing effect to the axial groups.

Table 8. Polymerizations with **51** and **60**.

Run	Monomer	Precat.	Equiv.	Yield[a] (g)	M_n[b] (kDa)	PDI[c]	T_m[d] (°C)	% *mmmm*[e]
1	Propylene	**51**	5 psi	0.40	23.4	1.2	110.4	0.72
2	1-hexene	**51**	200	0.28	20.3	1.0	--	0.98
3	Propylene	**60**	5 psi	0.03	1.98	1.1	83.2	0.37
4	1-hexene	**60**	200	0.04	1.93	1.1	--	0.72

[a] Polymerizations were terminated at precipitation into acidic MeOH after 3 h. [b,c] Determined by gel permeation chromatography (GPC) analysis. [d]Determined by differential scanning calorimetry (DSC) analysis. [e] Determined by ^{1}H (600 MHz) and ^{13}C (150 MHz) NMR at 110 °C in 1,1,2,2-tetrachloroethane-d_2. [e]Insoluble for GPC analysis.

To begin, the M_n and the amount of polymer produced are much lower than expected and is indicative of an active species with very low activity compared to **51** as seen in entries 1 and 3 in Table 8. Analysis of the polydispersity by GPC shows a larger value (1.1) than what is expected from a living polymerization process. ^{1}H NMR was used to detect the presence of vinylic resonances that would indicate termination from β-hydride elimination and in Figure 34 vinylic protons can be seen at 4.80 ppm. This confirms that the polymerization was indeed a non-living process. The non-living character is likely a result of the active species' increased ability to β-hydride eliminate from the increased electron donation to the metal center from the distal N in the guanidinato frame. The electronic stability and the increased steric crowding both contribute to the decrease in activity, as both of these issues will hinder the incoming olefin from binding to the metal center. Further investigation by ^{13}C NMR of the microstructure of the resulting polymer shows a decrease in the *%mmmm* value than what

is produced with **51**. A decrease from 0.70 with **51** to 0.37 with **60** indicates a dramatic loss of stereocontrol from the initiator.

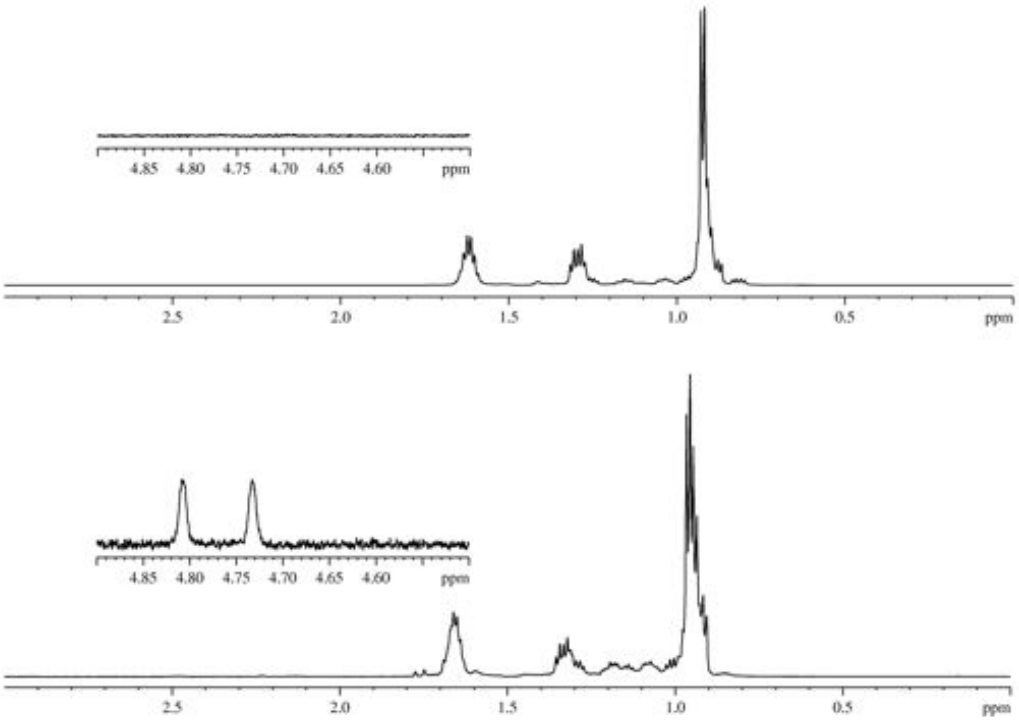

Figure 34. ^{1}H NMR: 600 MHz, 1,1,2,2-tetrachloroethane-d_2, 110°C of non-LCCTP polypropylene using **51** (top) and **60** (bottom).

The polymerization of 200 equivalents of 1-hexene was carried out in the same fashion by activation with 1.05 equivalents of the cocatalyst, $[PhNHMe_2][B(C_6F_5)_4]$ per Scheme 21. Despite the lack of stereocontrol seen with the use of **60** for the polymerization of propene, it is well known that more stereoselectivity can be imparted on a larger monomer; therefore, it was a logical choice to investigate the precatalyst using 1-hexene. As seen with the propene screening, the activity is much lower than what has been previously reported for **51.** Also, the PDI is broader than what would be accepted for a living polymerization process. Again the ^{1}H NMR was analyzed for vinylic

resonances to indicate termination via β-hydride elimination, and vinyl resonances were found at 4.15 ppm. Analysis of the ^{13}C NMR shows a decrease in the stereoselectivity with a *%mmmm* from 0.98 with **51** to 0.72 with **60**. The loss of stereocontrol of this initiator is likely due to the loss of steric discrimination from the side N-substituents as both of the groups are pushed forward from the buttressing effect seen by the increased size of the distal substituent.

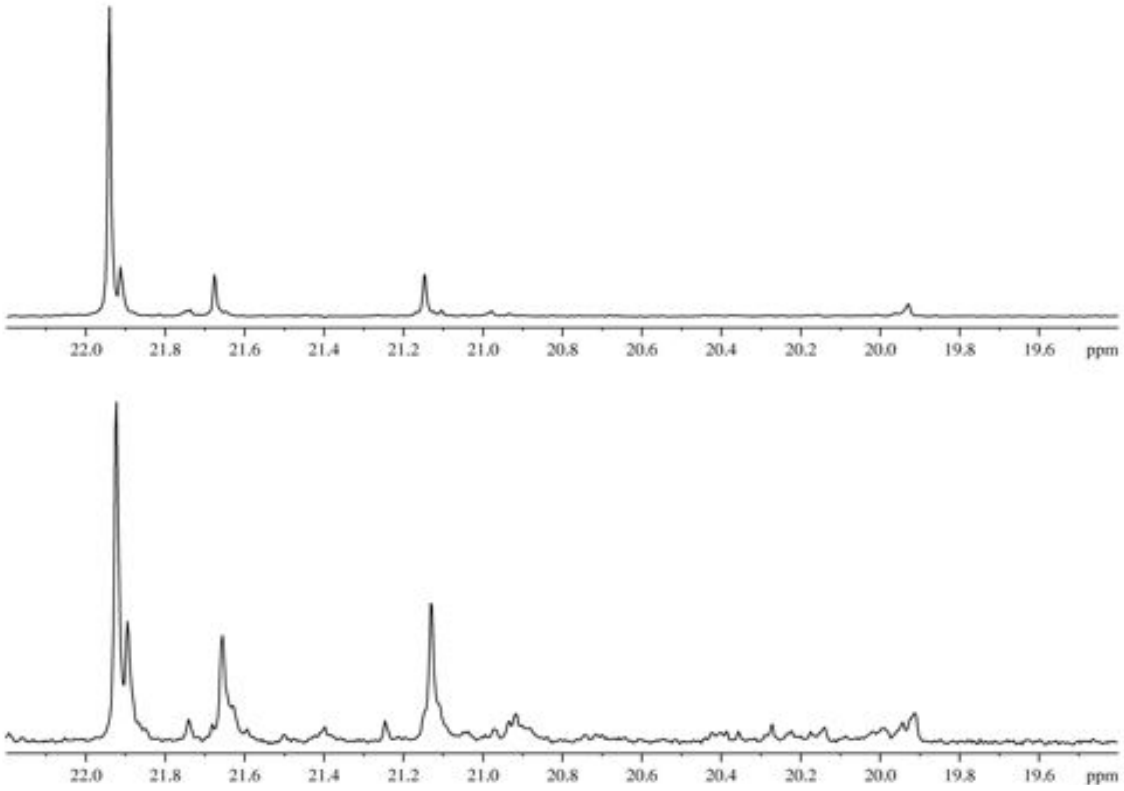

Figure 35. ^{13}C NMR: 150 MHz, 1,1,2,2-tetrachloroethane-d_2, 110°C of non-LCCTP polypropylene using **51** (top) and **60** (bottom).

3.5 Cation Stabilization

In an attempt to explain why the initiators did not perform as designed, efforts were focused on the isolation and characterization of the active cationic species. Attempts to crystallize [Cp*ZrMe{N(Et)C(NMe_2)N(^{t}Bu)}][$B(C_6F_5)_4$] in chlorobenzene at

-25 ºC were successful at producing a dicationic species, {Cp*Zr(μ-X)[N(Et)C(NMe_2)N(^{t}Bu)]}$_2$[B(C_6F_5)$_4$]$_2$ (X=Me or Cl), but the disorder was too great to resolve the bridging groups (Figure 36). It was found that the increased steric crowding at the metal center on the initiator results in a cationic active species that is more susceptible to chloride abstraction from the solvent, which lead to poor performance as an active species for living polymerizations.[6,12,13] Another attempt to explain the non-living nature of the polymerizations resulted in the synthesis of Cp*Zr(Me)(*i*Bu)[tBuNC(NMe_2)NEt] (**62**) in the hopes that evidence of β–hydride agostic interactions could be observed. The compound was successfully synthesized and activated using [PhNHMe_2][B(C_6F_5)$_4$]. However, attempts to isolate a single crystal of [Cp*Zr(*i*Bu){N(Et)C(NMe_2)N(^{t}Bu)}][B(C_6F_5)$_4$] suitable for x-ray diffraction were fruitless. The inability to produce crystals of the resulting cationic species led rise to the hypothesis that the active cations were unstable. Activation of the neutral species with cocatalysts, such as B(C_6F_5)$_3$ (**63**) to provide a tighter ion pair and stabilize the cationic species, was attempted.

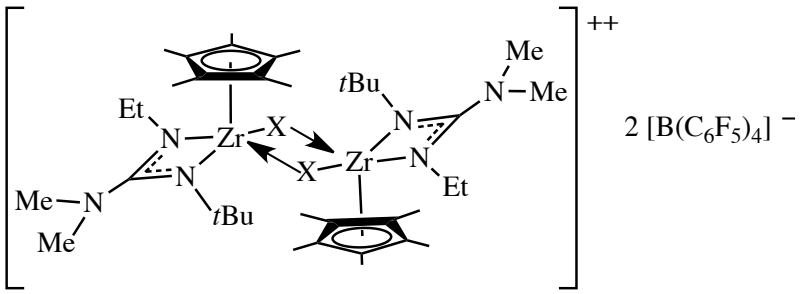

Figure 36. Proposed dicationic species, {Cp*Zr(μ-X)[N(Et)C(NMe_2)N(^{t}Bu)]}$_2$[B(C_6F_5)$_4$]$_2$ (X=Me or Cl).

Polymerizations with 1-hexene were repeated under the same conditions using a **63** as the cocatalyst to increase the cation-anion interaction and provide more stabilization to the cationic active species[14]. However, due to the 'tightness' of the ion pair, what little activity that was seen using the 'looser' interaction achieved by using the borate cocatalyst, $[PhNHMe_2][B(C_6F_5)_4]$, was completely compromised and no polymer was recovered. This was likely due to the combination of steric bulk at the metal center, the tighter cation-anion interaction, and the large monomer size. Polymerizations were repeated using propene, a smaller monomer compared to 1-hexene and again, the polymerizations resulted in the loss of all activity towards polymerization.

3.6 Conclusion

The solution to overcoming the loss of stereocontrol seems trivial in that only an enantiomerically pure initiator is needed, however execution of that idea is not as easy as expected. The distal position of the amidinate frame allows for ample opportunity to tune the catalyst, however the system experiences low tolerances for the combined increased electron donation and steric bulk of the guanidinate frame employed. It has been shown that mono-guanidinato Cp* zirconium complexes can be synthesized and isolated readily. Structural analyses show an increased steric crowding at the metal center that compromises the complex's ability to polymerize α-olefins in a living nature. The more crowded metal center resulted in a less stable cationic active species and therefore, the activity and stereocontrol towards living polymerizations was disrupted based on the specie's ability to terminate via β-hydride elimination. Efforts to isolate active cationic species were unsuccessful due to the decreased stability of the cationic active species, and attempts to stabilize the cationic species resulted in shutting down the complex's minimal

ability to polymerize. It is evident from this body of work that any future adjustments to the frame must occur elsewhere in the complex.

3.7 Experimentals

Materials:

All manipulations were performed under an inert atmosphere of N_2 using standard Schlenk-line or glove-box techniques. All solvents were dried (Na/benzophenone for pentane and diethyl ether, and Na for toluene) and distilled under N_2 prior to use. Benzene-d_6 was dried over Na/K alloy and was vacuum transferred prior to being used for NMR spectroscopy. Celite was oven dried at 150 °C for several days before use. Cooling for the reactions was performed in the internal freezer (-25 °C) of the glove box used. $(\eta^5\text{-}C_5Me_5)ZrCl_3$, $LiNMe_2$, and $[PhNMe_2][B(C_6F_5)_4]$ were purchased from Strem Chemicals, and used as received. 2-methylpyrrolidine, 2,5-transdiemethylpyrrolidine, and1-*tert*-butyl-3-ethylcarbodiimide were purchased from Sigma Aldrich and used as received *N,N*-diethylcarbodiimide was prepared according to previously reported procedures and dried over CaH_2 before use. 1-hexene was purchased from Sigma Aldrich and dried over Na/K alloy and was vacuum transferred prior to use. Polymer grade propene and ethene were purchased from Matheson Trigas, and passed over activated Q5 and molecular sieves.

Instrumental:

GPC analyses were performed using a Viscotek GPC system equipped with a column oven and a differential refractometer both maintained at 45 °C and four columns also maintained at 45 °C. THF was used as the eluent at a flow rate of 1.0 mL/min. M_n,

M_w, and M_w/M_n values were obtained using a Viscotek GPC with OmniSEC software and ten polystyrene standards (M_n=580 Da to 3150 kDa) (Polymer Laboratories).

^{1}H NMR spectra were recorded at 400MHz with benzene-d_6. For polymer samples ^{13}C NMR spectra were recorded at 600 MHz and 150 MHz, respectively, using 1,1,2,2-tetrachlorethane-d_2 at 110 °C with a Bruker AVIII-600MHz spectrometer equipped with a Bruker 5 mm C13/H1 dual probe with Z gradient. Spectra were recorded under the following conditions: 45° pulse; without NOE; acquisition time, 1.2 s; relaxation delay, 2.0 s; >10K transients.

Differential Scanning Calorimetry (DSC) thermograms were collected on a TA DSC Q1000 system with a heating and cooling rate of 5 or 10 ^{o}C/min. All samples were prepared in hermetically sealed pans (8 – 10 mg/sample) and were run using an empty pan as a reference and empty cells as a subtracted baseline. The samples were scanned for multiple cycles to remove recrystallization differences between the samples and the results reported are of the second and third scans in the cycles.

Elemental analyses (C, H, and N) were performed by Midwest Microlabs,LLC.

Synthesis of Cp*Zr[N(Et)C(NMe$_2$)N(Et)]Cl$_2$ (54):

A solution of 0.026 g (0.50 mmol) $LiNMe_2$ in 5 mL of Et_2O was cooled to -25 °C. A precooled solution, to -25 °C, of 0.049 g (0.5mmol) of *N.N*-diethylcarbodiimide in 5mL Et_2O was added and allowed to stir for 1h while warming up to ambient temperature. The resulting reaction mixture was re-cooled to -25 °C and then added to a suspension of 0.166 g (0.50 mmol) Cp^*ZrCl_3 in 20 mL of Et_2O, precooled to -25 °C. After stirring 16h at ambient temperature the reaction was filtered through a pad of celite whereupon the volatiles were removed. The product was extracted with minimal toluene and filtered

through a plug of celite. Approximately double the amount of pentane was layered on top and allowed to crystallize at -25 °C to give product as a orange crystalline material (0.115g, 52% yield). Anal. Calcd for $C_{17}H_{31}N_3Cl_2Zr$: C, 46.45; H, 7.11; N, 9.56. Found: C, 46.60; H, 7.10; N, 9.39. ^{1}H NMR (400MHz, benzene-*d*$_6$, 25 °C): δ 1.06 (t, 6H), 2.04 (s, 15H), 2.11 (s, 6H), 3.11 (q, 4H).

Synthesis of Cp*Zr[N(Et)C(NMe$_2$)N(Et)]Me$_2$ (58):

Methyl lithium, 0.21 mL (0.38 mmol, 1.84M in Et_2O), was added dropwise to a precooled solution, at -70 °C, of 0.080 g (0.18 mmol) (Et, Et, NMe_2)Cp*$ZrCl_2$ in 5mL of Et_2O. The reaction was stirred for 2h while warming up to ambient temperature whereupon the volatiles were removed. Minimal pentane was used to extract the product and filtered through a plug of celite. The solution was concentrated down by half and crystallized at -25 °C to give product as a white crystalline material (0.042g, 44%). Anal. Calcd for $C_{19}H_{37}N_3Zr$: C, 57.23; H, 9.35; N, 10.54. Found: C, 57.09; H, 9.21; N, 10.36. ^{1}H NMR (400MHz, benzene-*d*$_6$, 25 °C): δ 0.29 (s, 6H), 1.02 (t, 6H), 2.01 (s, 15H), 2.30 (s, 6H), 3.00 (q, 4H).

Synthesis of Cp*Zr[N(Et)C(2-methylpyrrolidine)N(Et)]Cl$_2$ (55):

A solution of 0.043 g (0.50 mmol) 2-methylpyrrolidine in 5mL of Et_2O was cooled to -25 °C. 0.25 mL of nBuLi (0.5 mmol, 2.0M in hexanes) was added dropwise to the chilled solution and allowed to stir for 3h while warming up to ambient temperature. A solution of 0.049 g (0.5 mmol) of, precooled to -25 °C, *N.N*-diethylcarbodiimide in 5mL Et_2O was added to the cooled reaction mixture and allowed to stir for 3h while warming up to ambient temperature. The resulting reaction mixture was re-cooled to -25 °C and then added to a suspension of 0.166 g (0.50 mmol) Cp*$ZrCl_3$ in 20 mL of Et_2O,

precooled to -25 °C. After stirring 16h at ambient temperature the reaction was filtered through a pad of celite whereupon the volatiles were removed. The product was extracted with minimal toluene and filtered through a plug of celite. Approximately double the amount of pentane was layered on top and allowed to crystallize at -25 °C to give product as a yellow crystalline material (0.139g, 58% yield). Anal. Calcd for $C_{20}H_{35}N_3Cl_2Zr$: C, 50.08; H, 7.36; N, 8.76. Found: C, 50.17; H, 7.41; N, 8.50. ^{1}H NMR (400MHz, benzene-*d*$_6$, 25 °C): δ 0.86 (d, 4H), 1.08 (t, 6H), 1.24 (m, 1H), 1.51 (p, 1H), 2.10 (s, 15H), 2.64 (t, 1H), 2.86 (m, 1H), 3.04 (sextet, 2H), 3.30 (m, 3H).

Synthesis of Cp*Zr[N(Et)C(2-methylpyrrolidine)N(Et)]Me$_2$ (59):

Methyl lithium, 0.28 mL (0.46 mmol, 1.66M in Et_2O), was added dropwise to a precooled solution, at -70 °C, of 0.106 g (0.22 mmol) (Et, Et, 2-methylpyrrolidine)Cp*$ZrCl_2$ in 5 mL of Et_2O. The reaction was stirred for 2h while warming up to ambient temperature whereupon the volatiles were removed. Minimal pentane was used to extract the product and filtered through a plug of celite. The solution was concentrated down by half and crystallized at -25 °C to give product as a white crystalline material (0.042g, 44%). ^{1}H NMR (400MHz, benzene-*d*$_6$, 25 °C): δ 0.21 (s, 3H), 0.37 (s, 3H), 1.01 (m, 10H), 1.60 (p, 1H), 2.06 (s, 15H), 2.90 (t, 1H), 3.06 (m, 6H), 3.39 (m, 1H).

Synthesis of Cp*Zr[N(*t*Bu)C(NMe$_2$)N(Et)]Cl$_2$ (56):

A solution of 0.10 g (2.0 mmol) $LiNMe_2$ in 5 mL of Et_2O was cooled to -25 °C. A precooled solution, to -25 °C, of 0.25 g (2.0mmol) of 1-*tert*-butyl-3-ethylcarbodiimide in 5 mL Et_2O was added and allowed to stir for 1h while warming up to ambient temperature. The resulting reaction mixture was re-cooled to -25 °C and then added to a

suspension of 0.67 g (2.0 mmol) Cp^*ZrCl_3 in 40 mL of Et_2O, precooled to -25 °C. After stirring 16h at ambient temperature all of the volatiles were removed and the solid was extracted with toluene before being filtered through a pad of celite. The solution was reduced to approximately three milliliters and allowed to crystallize at -25 °C to give product as a yellow crystalline material (0.831g, 89% yield). Anal. Calcd for $C_{19}H_{35}N_3Cl_2Zr$: C, 48.80; H, 7.54; N, 8.99. Found: C, 49.08; H, 7.62; N, 8.07. ^{1}H NMR (400MHz, benzene-d_6, 25 °C): δ 1.06 (t, 3H), 1.32 (s, 9H), 2.08 (s, 15H), 2.16 (s, 6H), 3.04 (q, 2H).

Synthesis of $Cp^*Zr[N(tBu)C(NMe_2)N(Et)]Me_2$ (60):

Methyl magnesium chloride, 0.67 mL (3.1M in THF), was added dropwise to a precooled solution of, at -70 °C, of 0.47 g (1.0 mmol) [*t*Bu, Et, NMe_2]Cp^*ZrCl_2 in 40 mL of Et_2O. The reaction was stirred for overnight while warming up to ambient temperature whereupon the volatiles were removed. Minimal pentane was used to extract the product and filtered through a pad of celite. The solution was concentrated down by half and crystallized at -25 °C to give product as a white crystalline material (0.182g, 45%). Anal. Calcd for $C_{21}H_{41}N_3Zr$: C, 59.10; H, 9.68; N, 9.85. Found: C, 59.01; H, 9.41; N, 9.86. ^{1}H NMR (400MHz, benzene-d_6, 25 °C): δ 0.37 (s, 6H), 1.15 (t, 3H), 1.4 (s, 9H), 2.14 (s, 15H), 2.52 (s, 6H), 2.94 (q, 2H).

Synthesis of $Cp^*Zr[N(tBu)C(2\text{-methylpyrrolidine})N(Et)]Cl_2$ (57):

A solution of 0.17 g (2.0 mmol) 2-methylpyrrolidine in 5 mL of Et_2O was cooled to -25 °C. 1.38 mL of nBuLi (1.6M in hexanes) was added dropwise to the chilled solution and allowed to stir for 3h while warming up to ambient temperature. A solution of 0.25 g (2.0 mmol) of, precooled to -25 °C, 1-*tert*-butyl-3-ethylcarbodiimide in 5 mL

Et_2O was added to the cooled reaction mixture and allowed to stir for 3h while warming up to ambient temperature. The resulting reaction mixture was re-cooled to -25 °C and then added to a suspension of 0.67 g (2.0 mmol) Cp^*ZrCl_3 in 40 mL of Et_2O, precooled to -25 °C. After stirring 16h at ambient temperature all of the volatiles were removed and the solid was extracted with toluene before being filtered through a pad of celite. The solution was reduced to approximately two milliliters and allowed to crystallize at -25 °C to give product as a yellow-orange crystalline material (0.703g, 69% yield).Anal. Calcd for $C_{22}H_{39}N_3Cl_2Zr$: C, 52.05; H, 7.74; N, 8.28. Found: C, 52.23; H, 7.62; N, 8.07. ^1H NMR (400MHz, benzene-d_6, 25 °C): δ 0.65(d, 3H), 1.02 (s broad, 3H), 1.40 (s, 9H), 1.50 (m, 1H), 2.12 (s, 15H), 2.69 (t, 1H), 3.33 (m, 3H).

Synthesis of Cp*Zr[N(*t*Bu)C(2-methylpyrrolidine)N(Et)]MeCl (61):

Methyl magnesium chloride, 0.67 mL (3.1M in THF), was added dropwise to a precooled solution, at -70 °C, of 0.47 g (1.0 mmol) (*t*Bu, Et, 2-methylpyrrolidine)Cp^*ZrCl_2 in 40 mL of Et_2O. The reaction was stirred for overnight while warming up to ambient temperature whereupon the volatiles were removed. Minimal pentane was used to extract the product and filtered through a pad of celite. The solution was concentrated down by half and crystallized at -25 °C to give product as a white/pale yellow crystalline material (0.421g, 88%). Anal. Calcd for $C_{23}H_{42}N_3ClZr$: C, 56.70; H, 8.69; N, 8.62. Found: C, 56.73; H, 8.32; N, 8.60. ^1H NMR (400MHz, benzene-d_6, 25 °C): δ 0.13 (s broad, 3H), 0.39 (s, 3H), 1.10 (m, 7H), 1.27 (s, 9H), 1.40 (m, 3H), 1.62 (m, 1H), 2.07 (s, 15H), 2.87 (p, 3H), 3.42 (m, 3H).

Synthesis of Cp*Zr[N(*t*Bu)C(NMe_2)N(Et)](iBu)Cl (62):

Isobutyl magnesium chloride, 1.0 mL (2.0 M in THF), was added dropwise to a precooled solution of, at -70 °C, of 0.93 g (2.0 mmol) [*t*Bu, Et, NMe_2]Cp*$ZrCl_2$ in 70 mL of Et_2O. The reaction was stirred for overnight while warming up to ambient temperature whereupon the volatiles were removed. Minimal toluene was used to extract the product and filtered through a pad of celite. The solution was concentrated down by half and crystallized at -25 °C to give product as a yellow crystalline material (0.770g, 79%). Anal. Calcd for $C_{23}H_{44}N_3ClZr$: C, 56.44; H, 9.07; N, 8.59. Found: C, 56.43; H, 8.78; N, 8.98. ^{1}H NMR (400MHz, benzene-*d*$_6$, 25 °C): δ 0.71 (m, 1H), 1.07 (s, 3H), 1.20 (d, 3H), 1.34 (s, 9H), 1.41 (d, 3H), 2.03 (s, 15H), 2.07 (s, 1H), 2.38 (m, 6H), 2.71 (sextet, 1H), 2.96 (sextet, 1H).

General polymerization of propene in chlorobenzene:

A solution of the precatalyst (0.025 mmol) in 0.5 mL chlorobenzene at -10 °C was added to the [$PhNMe_2$][$B(C_6F_5)_4$] (0.026 mmol) and agitated until dissolved. The resulting mixture was added to 29.5 mL chlorobenzene at -10 °C in a 250 mL Schlenk flask. The flask was charged to 5 psi with propene gas while stirring. Polymerization temperature was maintained at -10 ± 2 ºC. The pressure and stirring was maintained for the duration of the reaction where upon it was quenched with 1.0 mL of methanol and precipitated into 600 mL acidic methanol to isolate the polymer product. The polymer was collected and dried under vacuum. The resulting polymers were characterized by DSC, GPC, and ^{1}H/^{13}C NMR.

General polymerization of ethene in toluene:

A solution of the precatalyst (0.025 mmol) in cold 0.5 mL chlorobenzene was added to the [$PhNMe_2$][$B(C_6F_5)_4$] (0.021 mmol) and agitated until dissolved. The

resulting mixture was added to 29.5 mL toluene at 20 °C in a 250 mL Schlenk flask. The flask was charged with ethene gas while stirring. The pressure and stirring was maintained for the duration of the reaction where upon it was quenched with 1.0 mL of methanol and precipitated into 600 mL acidic methanol to isolate the polymer product. The polymer was collected and dried under vacuum. The resulting polymers were characterized by DSC, GPC, and $^{1}H/^{13}C$ NMR.

General polymerization of 1-hexene:

A solution of the precatalyst (0.025 mmol) in 0.5 mL chlorobenzene at -10 °C was added to the $[PhNMe_2][B(C_6F_5)_4]$ (0.026 mmol) and agitated until dissolved. The resulting mixture was added to 9.5 mL chlorobenzene and 200eq 1-hexene at -10 °C in a scintillation vial. The stirring and temperature was maintained for the duration of the reaction where upon it was quenched with 1.0 mL of methanol and precipitated into 600 mL acidic methanol to isolate the polymer. The final poly(1-hexene) was extracted with pentane before being dried under vacuum. The polymer was collected and dried under vacuum. The resulting polymers were characterized by DSC, GPC, and $^{1}H/^{13}C$ NMR.

3.8 References

(1) Jayaratne, K. C.; Sita, L. R. *J. Am. Chem. Soc.* **2000**, *122*, 958-959.

(2) Keaton, R. J.; Jayaratne, K. C.; Fettinger, J. C.; Sita, L. R. *J. Am. Chem. Soc.* **2000**, *122*, 12909-12910.

(3) Kissounko, D. A.; Fettinger, J. C.; Sita, L. R. *Inorg. Chim. Acta* **2003**, *345*, 121-129.

(4) Alfano, F.; Boone, H. W.; Busico, V.; Cipullo, R.; Stevens, J. C. *Macromolecules (Washington, DC, U. S.)* **2007**, *40*, 7736-7738.

(5) Duncan, A. P.; Mullins, S. M.; Arnold, J.; Bergman, R. G. *Organometallics* **2001**, *20*, 1808-1819.

(6) Coles, M. P.; Hitchcock, P. B. *Organometallics* **2003**, *22*, 5201-5211.

(7) Zhou, M.; Tong, H.; Wei, X.; Liu, D. *J. Organomet. Chem.* **2007**, *692*, 5195-5202.

(8) Zhou, M.; Zhang, S.; Tong, H.; Sun, W.-H.; Liu, D. *Inorg. Chem. Commun.* **2007**, *10*, 1262-1264.

(9) Haas, I.; Huebner, C.; Kretschmer, W. P.; Kempe, R. *Chem. - Eur. J.* **2013**, *19*, 9132-9136.

(10) Zhang, W.; Sita, L. R. *J. Am. Chem. Soc.* **2008**, *130*, 442-443.

(11) Zhang, Y.; Sita, L. R. *J. Am. Chem. Soc.* **2004**, *126*, 7776-7777.

(12) Vollmerhaus, R.; Rahim, M.; Tomaszewski, R.; Xin, S.; Taylor, N. J.; Collins, S. *Organometallics* **2000**, *19*, 2161-2169.

(13) Zhang, Y.; Reeder, E. K.; Keaton, R. J.; Sita, L. R. *Organometallics* **2004**, *23*, 3512-3520.

(14) Wei, J.; Zhang, W.; Wickham, R.; Sita, L. R. *Angew. Chem., Int. Ed.* **2010**, *49*, 9140-9144.

Chapter 4

Application of Hydrozirconation to Achieve Stereocontrol During LCCTP

4.1 Background

As mentioned in Chapter 1, living coordinative chain transfer polymerization (LCCTP) involves the addition of main group metal alkyl species, typically diethyl zinc, that act as surrogate chain growth sites during the polymerization. This exchange process has been instrumental in overcoming the 'one chain per metal site' limitation that has reduced the effectiveness of large-scale polymer production with living Ziegler-Natta polymerizations. One hurdle that has yet to be overcome in regard to this exchange process is that there is a loss of stereoselectivity during the LCCTP process which can be attributed to the transfer of the polymer group between two enantiomers of the active cationic species when the rate of chain transfer (v_{CT}) is much greater than the rate of propagation (v_P).

The answer to combat this loss of stereoselectivity is fairly simple to realize yet more challenging to bring forward. The most obvious way to preserve the stereoselectivity of the initiator is to create an enantiomerically pure initiator so that there is only one conformation for the exchanging polymer group to transfer onto as it returns from the surrogate growth site. The proposed synthetic pathway involves creating enantiomerically pure, configurationally stable, alkyl halides via hydrozirconation of terpenes so that they can be converted to the subsequent methyl-alkyl species available for use in living polymerizations. A large substituent, such as a terpene, coordinated

directly to the metal center should enhance the stereoselectivity under both non-LCCTP and LCCTP conditions.

Scheme 22. Synthetic route to **65.**

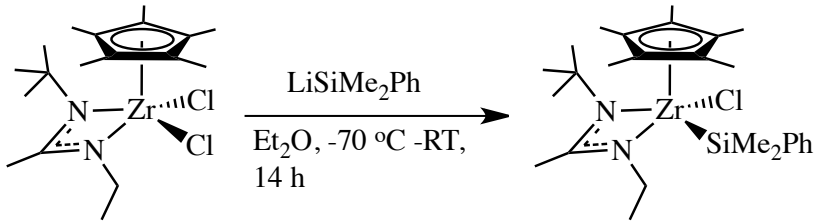

64 **65**

4.2 Synthesis

65 was synthesized via silylation of the metal using $LiSiMe_2Ph$ and **64** with concomitant production of LiCl in diethyl ether at -70 ^oC while warming to room temperature over 14 h per previously reported procedures (Scheme 22).[1] As seen with previous research within the group, it is imperative to perform this transformation in diethyl ether instead of tetrahydrofuran to discourage the deprotonation of the amidinate frame instead of the substitution of the metal center. Complex **65** can then be transformed into the hydrido, chloride species through hydrogenolysis (Scheme 23) of the Zr-Si bond under an atmosphere of H_2. This species is remarkably similar, in terms of reactivity, to Schwartz's reagent.[2-7] The addition of **66** to an external or internal olefin will result in its insertion into the Zr-H bond to create the corresponding alkyl-chloride complex.

Scheme 21. Hydrogenolysis of Zr-Si bond

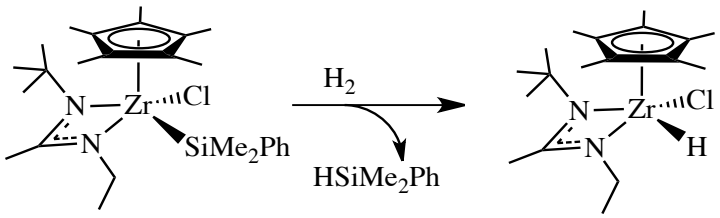

66

4.2.1 Hydrozirconation of Norbornene

Scheme 22. Synthesis of Cp*Zr(NB)Cl[tBuNC(Me)NEt] (**67**)

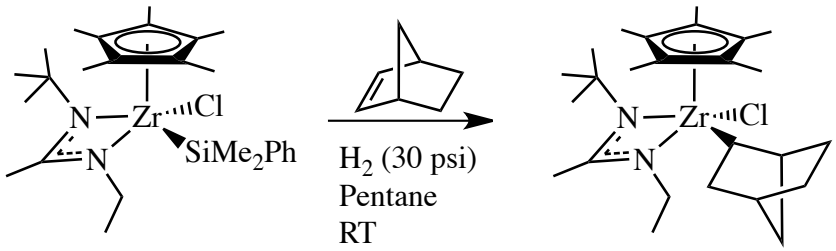

67

It is possible to obtain the norbornane-substituted zirconium **67** (Scheme 24) by reacting the silylated species **65** with 30 psi of H_2 gas, to generate the hydridochloride species in situ, in the presence of purified norbornene under ambient light. It is interesting to note that this reaction does not occur in the dark and will decompose upon targeted UV photolysis. A crystal structure of the exo conformation of the norbornane-chloride complex is shown in Figure 37. Several attempts to methylate the species with several different methylating agents were unsuccessful as a result of the steric bulk from the alkyl substituent. Analysis of the solid-state structure of **67** reveals subtle structural

differences of the neutral precatalyst species **51.** As shown in Table 9, the lengths of the Zr-N bonds of 2.2430(19) Å for Zr1-N1 is shorter than the same bond in **51** while Zr1-N2 bond is slightly more elongated at 2.2769(19) Å for **67**. This is likely a result of the complex accommodating for increased steric bulk on the ethyl side of the species by pushing the *t*-butyl substituent out more, thus elongating the bonds. The C-C bond at the back of the amidinate is comparable to that of **51** with a bond length of 1.509(3) Å. Looking at bond angles in the complex, it is worth pointing out that the angle between C3-N1-C2 is smaller at 121.3(2) º while the C3-N2-C4 angle is slightly larger at 125.7(2) º. The N1-C3-N2 angle is comparable between the two species, but the dihedral angle between the planes from Zr1-N2-C3 and Zr1-N1-C3 is larger at 21.09(19) º as the frame 'torques' to relieve steric strain with the norbornane group attached to the metal center.

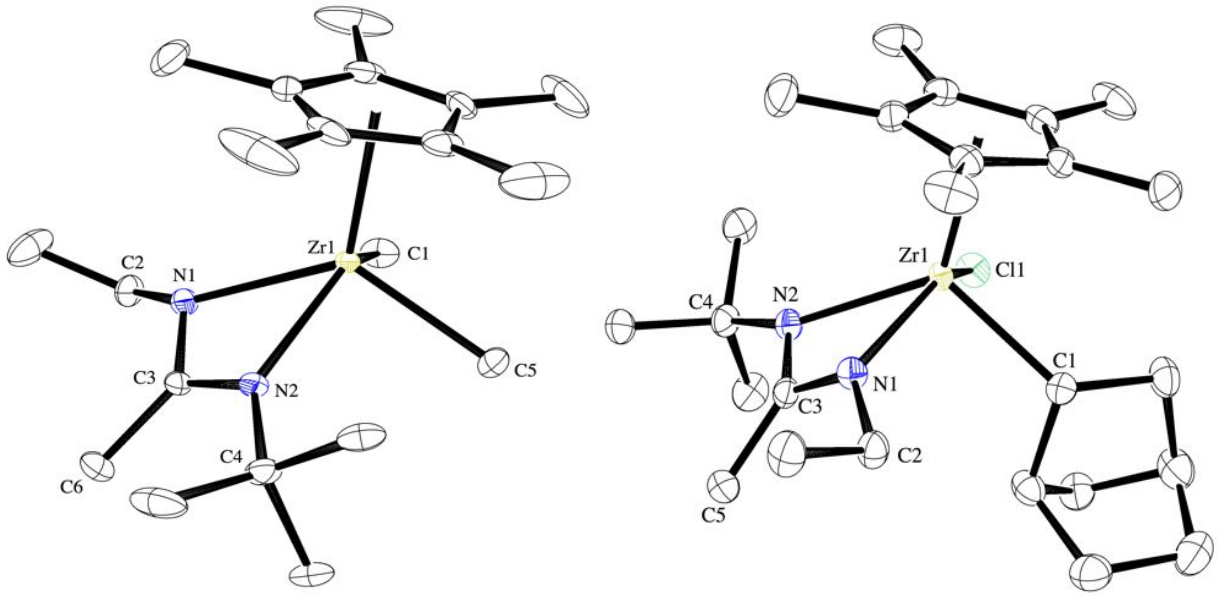

Figure 37. Crystal structure of (left) **51** and **67** (right) with hydrogen atoms omitted for clarity, ellipsoids for the non-hydrogen atoms are shown at the 30% probability level.

Table 9. Selected Bond Lengths and Bond Angles for the Molecular Structures of **51** and **67**.

	51	**67**
	Bond Lengths (Å)	
Zr1-N1	2.251(3)	2.2430(19)
Zr1-N2	2.265(2)	2.2769(19)
Zr1-C1	2.273(3)	2.257(2)
Zr1-X	C5	Cl1
	2.272(3)	2.4529(6)
N2-C3	1.332(4)	1.340(3)
N1-C3	1.323(4)	1.339(3)
C3-C6	1.515(4)	1.509(3)
	Bond Angles (deg)	
N1-Zr1-N2	58.40(9)	58.82(7)
Zr1-N1-C2	136.4(17)	136.62(15)
Zr1-N2-C4	142.5(16)	140.27(16)
C3-N1-C2	123.5(16)	121.3(2)
C3-N2-C4	122(2)	125.7(2)
N2-C3-N1	112.2(3)	111.9(2)
ϕ[a]	18.3	21.09(19)

[a] Angle between the mean planes defined by the following: Zr1-N2-C3 and Zr1-N1-C3.

4.2.3 Other Terpenes

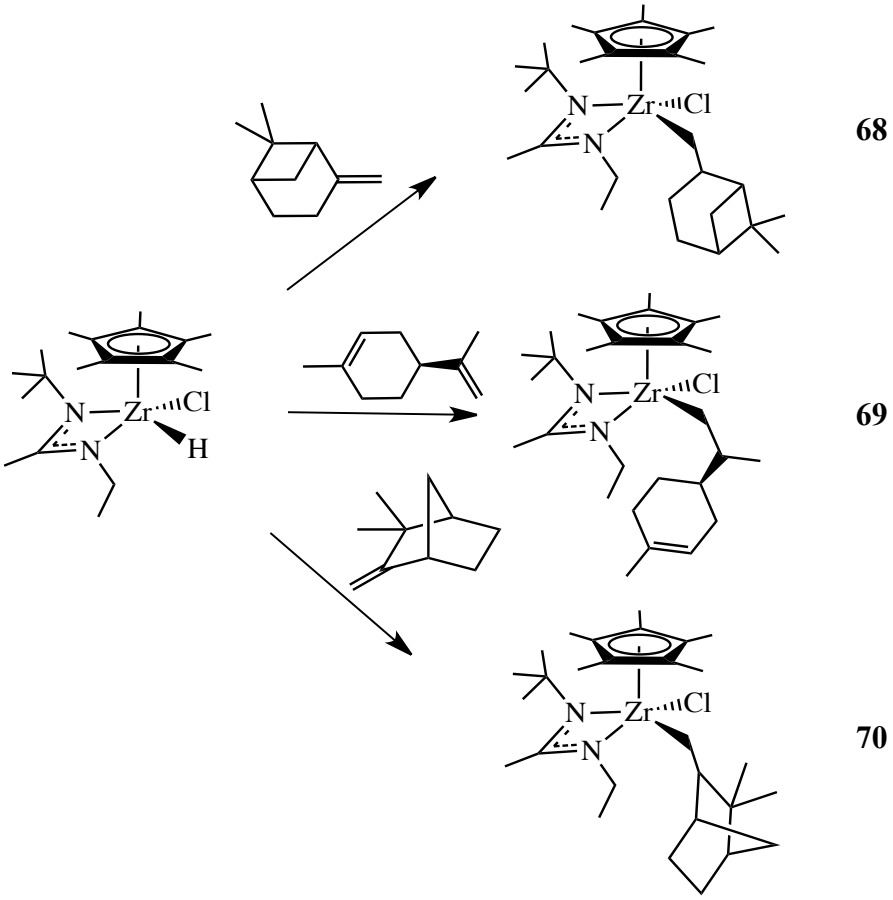

Figure 38. Reaction of **66** with β-pinene (top) (**68**), (-)-limonene (middle) (**69**), and camphene (bottom) (**70**).

In an effort to expand the range of the synthetic utility of this process, other terpenes such as camphene, β-pinene, and the enantiomerically pure (-)-limonene were screened as olefin sources to provide a pathway to enantiomerically pure zirconium complexes that could be used as initiators (Figure 38). The same procedure as in Scheme 24 was employed to successfully synthesize the proposed complexes. Although **68**, **69**, and **70** were unable to be structurally characterized due to issues with crystallinity, the general structures were confirmed by cleaving the Zr-C bond to release iodo-substituted organic products.[8] ^{1}H NMR and EI-GC/MS were used to conclusively show the

successful production of iodo-terpenes (Figure 39). The parent ion peaks agreed with the expected molecular mass of *m/z* 264, with the next major fragment occurring at *m/z* 137 to correspond with the loss of the iodide from the organic structure.

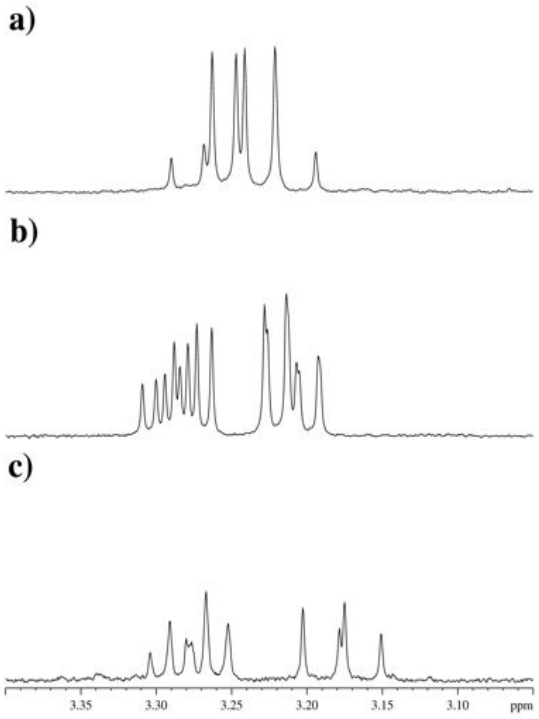

Figure 19. Partial ^{1}H NMR: 400 MHz, $CDCl_3$, 25 ^{o}C spectra of α-protons from idonolysis with (a) b-pinene, (b) (-)-limonene, and (c) camphene.

4.3 Chloride Degenerative Transfer Polymerization

Scheme 23. Proposed mechanism of chloride degenerative transfer polymerization.

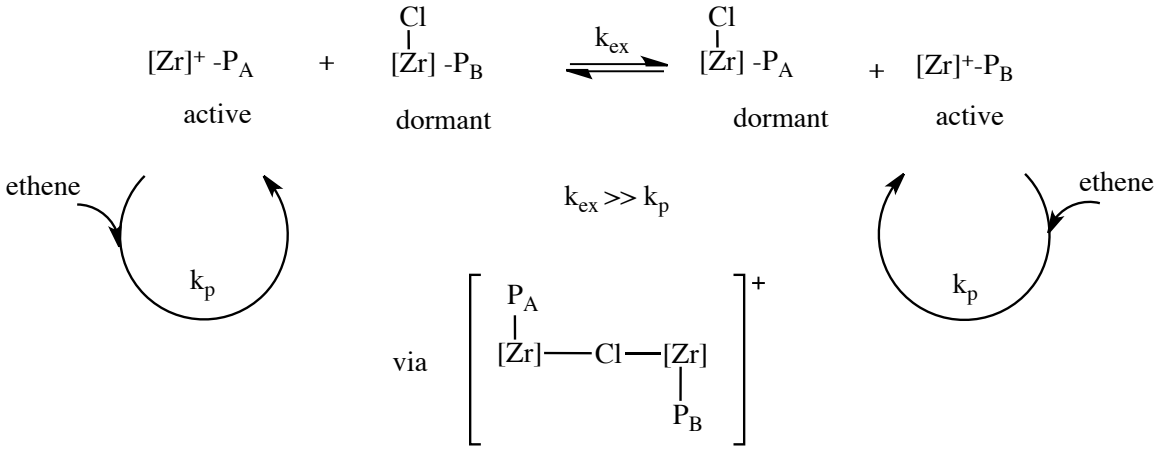

As mentioned previously, in Chapter 1, methyl degenerative transfer (MeDeT) process is used to program stereoerrors into the resulting polymer by exploiting the metal-centered epimerization about the dormant dimethyl species. Alkyl chlorides are configurationally stable due to the shortened bond distance between the amidinate and metal center blocking the amidinate's ability to epimerize. The lack of epimerization of the dormant species allows for the initiator to engage in a stereoselective degenerative transfer process (Scheme 25).[9] With the inability to dialkylate complex **67**, adapting this alkyl chloride for use in chloride degenerative transfer (ChloDeT) appeared to be a feasible option for this compound.

Scheme 24. ChloDeT polymerization of ethene using **67**.

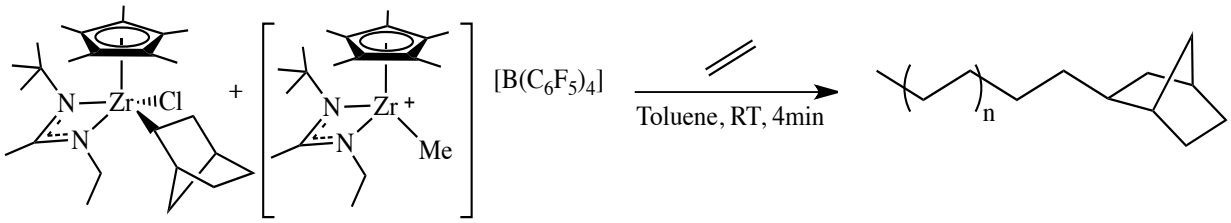

To test the ability of **67** to engage in ChloDeT, a polymerization using **51** as the precatalyst was used. **51** was activated with **49**, in a 1:1:1 ratio of **67**:**51**: **49** at 25 ^{o}C in toluene to generate the active zirconium cation and neutral alkyl chloride (Scheme 26). After four minutes under 5 psi of ethylene gas, the reaction turned turbid and 45 milligrams of polyethylene was obtained after quenching the reacting with acidified methanol. Although the isolated product was too insoluble for GPC analysis, the material was able to be characterized by high temperature ^{13}C (^{1}H) NMR to reveal the presence of a norbornane unit at the end of the polyethylene chain.[10,11] Attempts to use **67** in ChloDeT with propene were unsuccessful, likely due to the steric bulk of the norbornane substituent. Using ethylene resulted in a poor yield of material despite the normally rapid polymerization rate seen with the zirconium amidinate system.

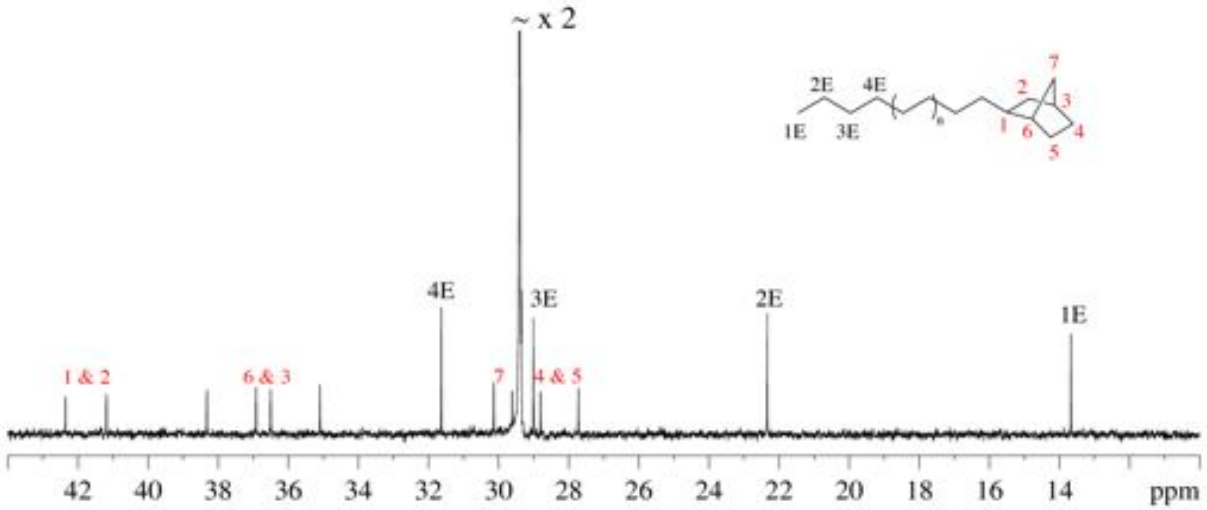

Figure 20. ^{13}C NMR: 150 MHz, 1,1,2,2-$C_2D_2Cl_4$, 110 ºC spectrum and resonance assignments of norbornane terminated polyethylene.

4.4 Cp*Zr(SiMe$_2$Ph)(Me)[*t*BuNC(Me)NEt]

4.4.1 Synthesis

Scheme 25. Synthetic route to **73**.

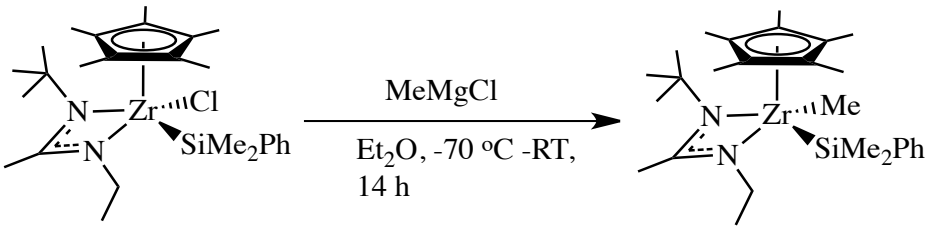

71

In an effort to bypass the alkyl chloride species, **65** was directly methylated using MeMgCl in diethyl ether from -70 ^{o}C to room temperature overnight to produce **71** (Scheme 27). As expected with the asymmetry of the amidinate frame, the ethyl side N-C bond is 2.241(2) Å compared to a bond length of 2.251(2) Å for the *t*-butyl side N-C bond. The N-C(CH$_3$) bonds in the amidinate frame are 1.334(3) Å and 1.337(3) Å which are in between 1.38 Å for a *sp*^{2} C-N bond and 1.28 Å C=N bond indicating that there is delocalization about the N-C-N fragment of the amidinate. It is also worth noting that the angle of the N-C-N fragment is 111.8(2) ^{o} and the dihedral angle between the N-C-N segment and the N-Zr-N is 24.2 ^{o}.

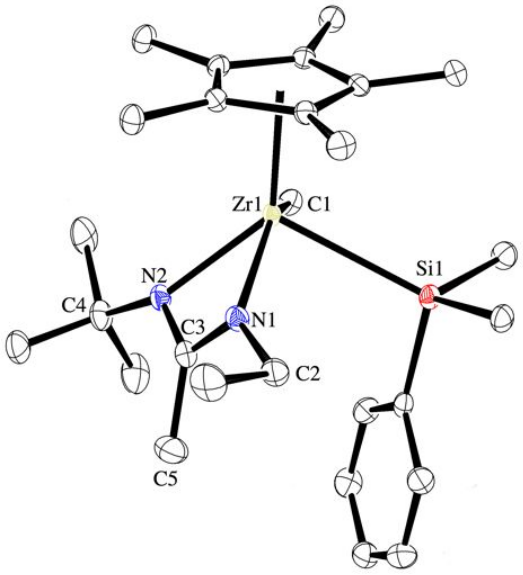

Figure 41. Crystal structure of **71** with hydrogen atoms omitted for clarity, ellipsoids for the non-hydrogen atoms are shown at the 30% probability level.

Table 10. Selected bond lengths and bond angles for the molecular structure of **71**.

Bond Angles (Å)	
Zr1-N1	2.241(2)
Zr1-N2	2.251(2)
Zr1-C1	2.291(3)
Zr1-Si1	2.8260(8)
N1-C3	1.467(3)
N2-C3	1.487(3)
C3-C5	1.510(4)
Bond Angles (deg)	
N1-Zr1-N2	58.99(8)
Zr1-N1-C2	120.9(2)
Zr1-N2-C4	140.86(18)
C3-N1-C2	120.9(2)
C3-N2-C4	124.4(2)
N1-C3-N2	111.(2)
ϕ[a]	24.2

[a] Angle between the mean planes defined by the following: Zr1-N1-C3 and Zr1-N2-C3.

4.4.2 Hydrozirconation using 71

Scheme 26. Hydrogenolysis of **71**.

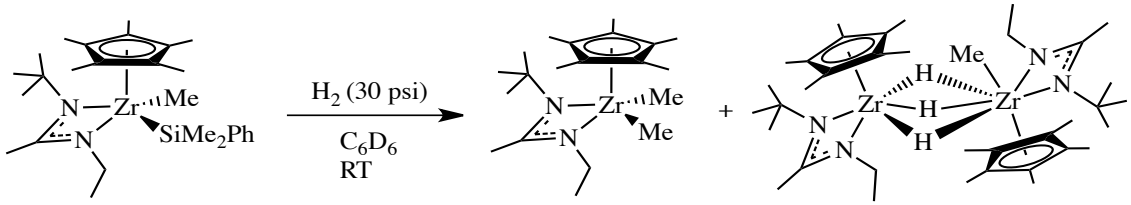

51 **72**

The silyl-methyl compound, **71**, was hydrogenated with 30 psi at room temperature to yield complex **51** and what is thought to be a trihydrido-dinuclear complex by ^{1}H NMR analysis. The inset in Figure 42 reveals a species containing two Cp* ligands in addition to **51** that is produced. The proposed hydride product appears to be unstable at room temperature for more than a few hours based on stability studies of the species. Attempts to isolate the trihydrido species resulted in its decomposition. Similar attempts to hydrozirconate with isobutylene were also met with failure due the instability of the products.

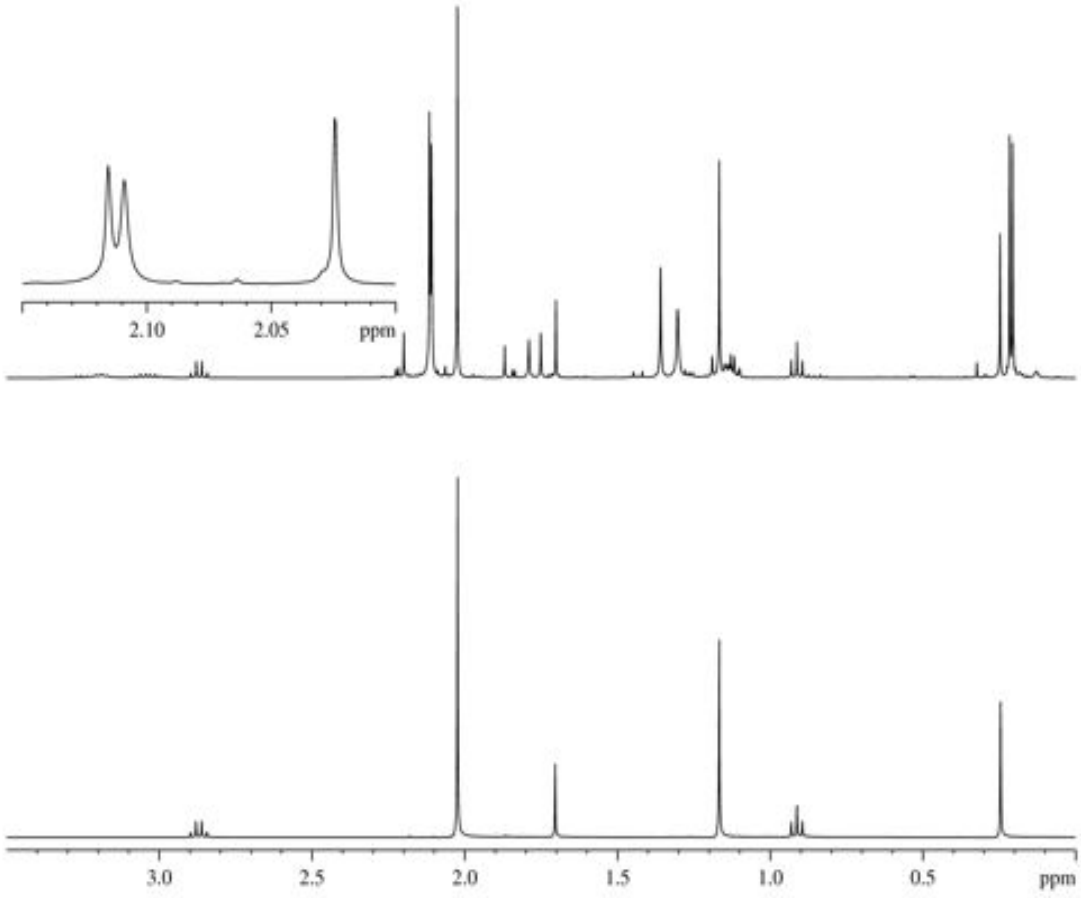

Figure 42. Partial ^{1}H NMR: 400 MHz, C_6D_6, 25 ^{o}C of the hydrogenolyis of **71** (top) and **51** (bottom).

4.5 Conclusions

Novel terpene substituted Cp* zirconium complexes were synthesized by taking advantage of hydrozirconation, a process that involves insertion of an olefin into a Zr-H bond, to add desired alkyl groups directly to the metal center in order influence the stereoselectivity during LCCTP. With the dialkyl species unable to be synthesized, the norbornane-substituted species was screened for activity under ChloDeT conditions only to find that it diminished the activity of the initiator making it unsuitable to use. Efforts to bypass the halogenated species and directly create the dialkyl species through

hydrozirconation of the isolated and characterized methyl-silyl complex were also fruitless due to the instability of the hydrido intermediate produced from hydrogenolysis.

4.6 Experimentals

Materials:

All manipulations were performed under an inert atmosphere of N_2 using standard Schlenk-line or glove-box techniques. All solvents were dried (Na/benzophenone for pentane and diethyl ether, and Na for toluene) and distilled under N_2 prior to use. Benzene-d_6 was dried over Na/K alloy and was vacuum transferred prior to being used for NMR spectroscopy. Celite was oven dried at 150 °C for several days before use. (η^5-C_5Me_5)$ZrCl_3$, $LiNMe_2$, and $[PhNMe_2][B(C_6F_5)_4]$ were purchased from Strem Chemicals, and used as received. 1-*tert*-butyl-3-ethylcarbodiimide was purchased from Sigma Aldrich and used as received. Camphene, norbornene, (-)-limonene, and β–pinene were purchased from Sigma Aldrich and distilled over sodium before use. 1-hexene was purchased from Sigma Aldrich and dried over Na/K alloy and was vacuum transferred prior to use. Polymer grade propene and ethene were purchased from Matheson Trigas, and passed over activated Q5 and molecular sieves.

Instrumental:

GPC analyses were performed using a Viscotek GPC system equipped with a column oven and a differential refractometer both maintained at 45 °C and four columns also maintained at 45 °C. THF was used as the eluent at a flow rate of 1.0 mL/min. M_n, M_w, and M_w/M_n values were obtained using a Viscotek GPC with OmniSEC software and ten polystyrene standards (M_n=580 Da to 3150 kDa) (Polymer Laboratories).

^{1}H NMR spectra were recorded at 400MHz with benzene-d_6. For polymer samples ^{13}C (^{1}H) NMR spectra were recorded at 600 MHz and 150 MHz, respectively, using 1,1,2,2-tetrachlorethane-d_2 at 110 °C with a Bruker AVIII-600MHz spectrometer equipped with a Bruker 5 mm C13/H1 dual probe with Z gradient. Spectra were recorded under the following conditions: 45° pulse; without NOE; acquisition time, 1.2 s; relaxation delay, 2.0 s; >10K transients.

Differential Scanning Calorimetry (DSC) thermograms were collected on a TA DSC Q1000 system with a heating and cooling rate of 5 or 10 ^{o}C/min. All samples were prepared in hermetically sealed pans (8 – 10 mg/sample) and were run using an empty pan as a reference and empty cells as a subtracted baseline. The samples were scanned for multiple cycles to remove recrystallization differences between the samples and the results reported are of the second and third scans in the cycles.

GC/MS were collected via a JEOL JMS-700 MS Station instrument with an EI ion source using a temperature program with a 10 ^{o}C/min ramp from 70 ^{o}C to 300 ^{o}C. All samples were prepared at 10 pmol/μL in diethyl ether.

Elemental analyses (C, H, and N) were performed by Midwest Microlabs,LLC.

Synthesis of Cp*ZrCl(SiMe$_2$Ph)[tBuNC(Me)NEt] (65):

To a solution of Cp*ZrCl$_2$[tBuNC(Me)NEt] (2.40 g, 5.5 mmol) in 80 mL Et$_2$O, 18.2 mL (5.5 mmol) of a 0.33 M solution of LiSiMe$_2$Ph in THF was added drop-wise via syringe at -78 ^{o}C. The mixture was stirred at -78 ^{o}C for 1 hour before warming up to 25 ^{o}C overnight, whereupon the volatiles were removed. The oily red residue was extracted with minimal pentane and passed through a short pad of celite on a glass frit. The filtrate was concentrated to ~ 3 mL and allowed to crystallize at -25 ^{o}C in the internal freezer of

the glovebox. Red crystals were washed with cold pentane and dried (2.15 g, 73% yield). ^{1}H NMR: δ 7.96 (d, 2H), 7.27 (m, 3H), 2.83 (m, 2H), 2.05 (s, 15 H), 1.21 (s, 9H), 1.21 (s, 3H), 0.71 (t, *J*=7.2 Hz, 3H), 0.66 (s, 3H), 0.51 (s, 3 H). Elemental Analysis and single x-ray diffraction analysis reported in previous literature.[1]

General Hydrozirconation Procedure using (65):

In a 50 mL Schlenk tube, fitted with a gas tight valve, Cp*ZrCl(SiMe$_2$Ph)[tBuNC(Me)NEt] (200 mg, 0.37 mmol) was dissolved in 5 mL of pentane. A three-fold excess of the terpene was added and the tube sealed. The resulting solution was degased before being charged to 30 psi of H_2 gas. The solution was stirred overnight whereupon the volatiles were removed. Minimal pentane was used to extract the residue and allowed to cyrstallize at -25 ^{o}C in the internal freezer of the glovebox. Yield for **67**: 446 mg (96%); ^{1}H NMR: δ 2.89 (m, 1H), 2.76 (m, 1H), 2.58 (d, 1H), 2.15 (s-broad, 1H), 2.07 (s, 3H), 2.05 (s, 15H), 1.76 (s, 3H), 1.33 (s, 9H), 0.86 (t, 3H), -0.33 (t, 1H).

General idonolysis procedure:

The same hydrozirconation procedure using **65** was employed. Once the volatiles were removed, approximately 1 mL of toluene was added to the crude mixture and subsequently added to a scintillation vial containing several I_2 crystals. After stirring for ten minutes at room temperature, the solution was removed from the glove box and filtered through a plug of silica. The volatiles were removed; ^{1}H NMR and GC/MS were used to confirm the synthesis of the iodo substituted products.

(**68**) camphene – GC/MS (EI) *m/z* : 264 [$C_{10}H_{17}I$], 137 [$C_{10}H_{17}]^+$; α ^{1}H NMR: δ 3.23 (m, 2H).

(**69**) β−pinene - GC/MS (EI) *m/z* : 264 [$C_{10}H_{17}I$], 137 [$C_{10}H_{17}]^+$; α ^{1}H NMR: δ 3.26 (m, 2H).

(**70**) (-) limonene - GC/MS (EI) *m/z* : 264 [$C_{10}H_{17}I$], 137 [$C_{10}H_{17}]^+$; α ^{1}H NMR: δ 3.29 (d, 2H).

Synthesis of Cp*ZrMe(SiMe$_2$Ph)[tBuNC(Me)NEt] (71):

To a solution of Cp*ZrCl(SiMe$_2$Ph)[tBuNC(Me)NEt] (1.08 g, 2.0 mmol), 0.85 mL of 2.47 M MeMgCl was added drop-wise via syringe at -78 ^{o}C. The mixture was stirred at -78 ^{o}C for 1 hour before warming up to 25 ^{o}C overnight, whereupon the volatiles were removed. The orange residue was extracted with minimal pentane and passed through a short pad of celite on a glass frit. The filtrate was concentrated to ~ 3 mL and allowed to crystallize at -25 ^{o}C in the internal freezer of the glovebox. Orange crystals were washed with cold pentane and dried (632 mg, 61% yield). ^{1}H NMR: δ 7.83 (d, 2H), 7.29 (t, 2H), 7.22 (m, 1H), 2.94 (m, 1H), 2.76 (m, 1H), 2.02 (s, 15H), 1.42 (s, 3H), 1.06 (s, 9H), 0.60 (t, 3H), 0.46 (s, 3H), 0.45 (d, 6H).

General Hydrozirconation Procedure using (71):

In a 50 mL Schlenk tube, fitted with a gas tight valve, Cp*ZrMe(SiMe$_2$Ph)[tBuNC(Me)NEt] (130 mg, 0.25 mmol) was dissolved in 5 mL of pentane. A three-fold excess of isobutylene (42 mg, 0.75mmol), precooled to -25 ^{o}C, was added quickly and the tube sealed. The resulting solution was degased before being charged to 30 psi of H_2 gas. The solution was stirred overnight whereupon the volatiles were removed. Minimal pentane was used to extract the residue and allowed to cyrstallize at -25 ^{o}C in the internal freezer of the glovebox.

General polymerization of propene in chlorobenzene:

A solution of the precatalyst (0.025 mmol) in 0.5 mL chlorobenzene at -10 °C was added to the $[PhNMe_2][B(C_6F_5)_4]$ (0.026 mmol) and agitated until dissolved. The resulting mixture was added to 29.5 mL chlorobenzene at -10 °C in a 250 mL Schlenk flask. The flask was charged to 5 psi with propene gas while stirring. Polymerization temperature was maintained at -10 ± 2 ºC. The pressure and stirring was maintained for the duration of the reaction where upon it was quenched with 1.0 mL of methanol and precipitated into 600 mL acidic methanol to isolate the polymer product. The polymer was collected and dried under vacuum. The resulting polymers were characterized by DSC, GPC, and $^{1}H/^{13}C$ NMR.

General polymerization of ethene in toluene:

A solution of the precatalyst (0.025 mmol) in cold 0.5 mL chlorobenzene was added to the $[PhNMe_2][B(C_6F_5)_4]$ (0.021 mmol) and agitated until dissolved. The resulting mixture was added to 29.5 mL toluene at 20 °C in a 250 mL Schlenk flask. The flask was charged with ethene gas while stirring. The pressure and stirring was maintained for the duration of the reaction where upon it was quenched with 1.0 mL of methanol and precipitated into 600 mL acidic methanol to isolate the polymer product. The polymer was collected and dried under vacuum. The resulting polymers were characterized by DSC, GPC, and $^{1}H/^{13}C$ NMR.

General polymerization of 1-hexene:

A solution of the precatalyst (0.025 mmol) in 0.5 mL chlorobenzene at -10 °C was added to the $[PhNMe_2][B(C_6F_5)_4]$ (0.026 mmol) and agitated until dissolved. The resulting mixture was added to 9.5 mL chlorobenzene and 200eq 1-hexene at -10 °C in a scintillation vial. The stirring and temperature was maintained for the duration of the

reaction where upon it was quenched with 1.0 mL of methanol and precipitated into 600 mL acidic methanol to isolate the polymer. The final poly(1-hexene) was extracted with pentane before being dried under vacuum. The polymer was collected and dried under vacuum. The resulting polymers were characterized by DSC, GPC, and $^{1}H/^{13}C$ NMR.

4.7 References

(1) Zhang, Y.; Keaton, R. J.; Sita, L. R. *J. Am. Chem. Soc.* **2003**, *125*, 8746-8747.

(2) Buchwald, S. L.; LaMaire, S. J.; Nielsen, R. B.; Watson, B. T.; King, S. M. *Org. Synth.* **1993**, *71*, 77-82.

(3) Kalesse, M. *Acros Org. Acta* **1995**, *1*, 29-31.

(4) Fernandez-Megia, E. *Synlett* **1999**, 1179.

(5) Erker, G.; Zwettler, R.; Krueger, C.; Schlund, R.; Hyla-Kryspin, I.; Gleiter, R. *J. Organomet. Chem.* **1988**, *346*, C15-C18.

(6) Erker, G.; Zwettler, R.; Krueger, C.; Hyla-Kryspin, I.; Gleiter, R. *Organometallics* **1990**, *9*, 524-530.

(7) Chirik, P. J.; Day, M. W.; Labinger, J. A.; Bercaw, J. E. *J. Am. Chem. Soc.* **1999**, *121*, 10308-10317.

(8) Labinger, J. A.; Hart, D. W.; Seibert, W. E., III; Schwartz, J. *J. Am. Chem. Soc.* **1975**, *97*, 3851-3852.

(9) Zhang, Y.; Sita, L. R. *J. Am. Chem. Soc.* **2004**, *126*, 7776-7777.

(10) Randall, J. C. *J. Macromol. Sci., Rev. Macromol. Chem. Phys.* **1989**, *C29*, 201-317.

(11) Wendt, R. A.; Mynott, R.; Hauschild, K.; Ruchatz, D.; Fink, G. *Macromol. Chem. Phys.* **1999**, *200*, 1340-1350.

Chapter 5

'Chiral' Amidinates

5.1 Background

Returning the methyl substituent to the distal position with the results from Chapters 3 and 4, the N-substituents on the amidinate frame became the next avenue to potentially increase stereoselectivity during LCCTP. The use of a larger substituent in addition to an ethyl group is expected to provide the same asymmetry as seen in **51**, while providing more steric bulk at the metal center. Utilization of a chiral substituent will allow the ligand to retain its chirality even with racemization about the metal center. The retention of this chirality should create the same enantiofacial selective insertion of the incoming prochiral olefin allowing for stereoselectivity under LCCTP conditions.[1] Previous success with producing stereoregular polypropylene under LCCTP conditions with the C_6-tethered dinuclear analogue of **51**, due to local and regional steric influences, has also warranted the placement of the chiral ligand within the dinuclear framework.[2,3]

Another advantage to using a chiral substituent on the amidinate is the expected production of optically active polymers from prochrial monomers (stereo*e*lectivity). The optical activity is a result of the helices, formed when highly isotactic polymers crystallize, adopting a preferred screw-sense, and the goal is to use a 'chiral' precatalyst to favor only one helical conformation. Since there is a racemic mixture of **51**, it is understood that the isotactic material it produces will contain equal distribution of left and right-handed helices and be non-optically active. The discrimination of the

enantiofacial insertion from the chiral group should exhibit the same helical preference despite racemization, creating an optically active polyolefin.

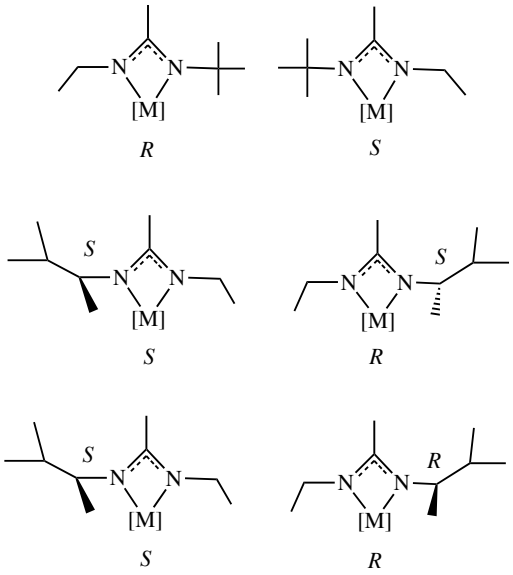

Figure 43. Different conformations of the '*t*-butyl' (top), chiral (middle), racemic (bottom) amidinates with respect to the metal. Note: Conformations of the metal center are arbitrarily assigned.

There has been recent success using chiral initiators to create enantio-enriched oligostyrenes.[1,4-6] This has only been successful with polyolefins using styrene because the larger the substituent is, the more readily it can prevent the helix from changing conformations.[7] It is widely accepted that the smaller the substituent on the polymer is, the easier it is for the helix to change conformations. Another challenge is that high molecular weight poly(α-olefins) possess pseudo-C_s symmetry (coined 'cryptochirality') so the net optical rotation is zero.[5] Synthesis of optically active polymers is worth investigating due to novel optics applications that these materials might have from their unique properties.

5.2 Synthesis

The desired substituted ethyl isocyanate was reacted with both the desired chiral and racemic amines to undergo nucelophilic attack from the amine to produce the urea. In regards to the synthesis of the bisureas; hexamethylene diisocyanate and 2 equivalents of amine were used. The resulting products were precipitated into pentane and then filtered, isolating a white solid. After synthesis, the ureas were converted to the carbodiimides via a previously reported procedure via dehydration by bromotriphenylphosphonium bromide and triethylamine to be isolated as reported.[8] The resulting liquids were dried overnight under vacuum before use.

Scheme 29. 'One-pot' synthetic route to mononuclear amidinate precatalysts.

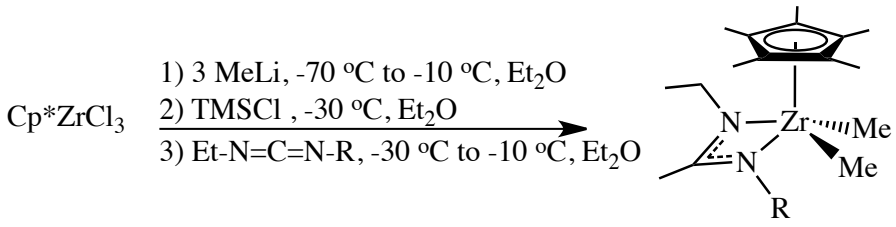

51 R = *t*Bu
73 R = (+/-)-3-methyl-2-butyl
74 R = (+)-3-methyl-2-butyl

The mononuclear and the C_6-linked bimetallic complexes, **51** and **73-74**, were synthesized by the one-pot, direct synthesis previously reported.[2,9] The mononuclear complexes were isolated as oils, despite multiple attempts to yield crystalline materials with the solvents available. The resulting oils were washed with toluene and dried several times to remove any impurities before use in polymerizations. Unlike the mononuclear species, the C_6-dinuclear complexes were easily recrystallized with a 1:2

mixture of toluene to pentane at -25 °C in the internal freezer of the glove box. Despite their crystalline nature, multiple attempts to slow down the crystallization process did not provide single crystals for use in x-ray diffraction. Specific rotations were determined via polarimetry to be (+) 98.89 ± 1.58° for **76**, (-) 84.05 ± 1.21° for **77**, and (+) 0.48 ± 0.40° for the racemic dinuclear precatalyst (**75**) in toluene at ambient temperatures.

Scheme 30. 'One-pot' synthetic route to dinuclear amidinate precatalysts.

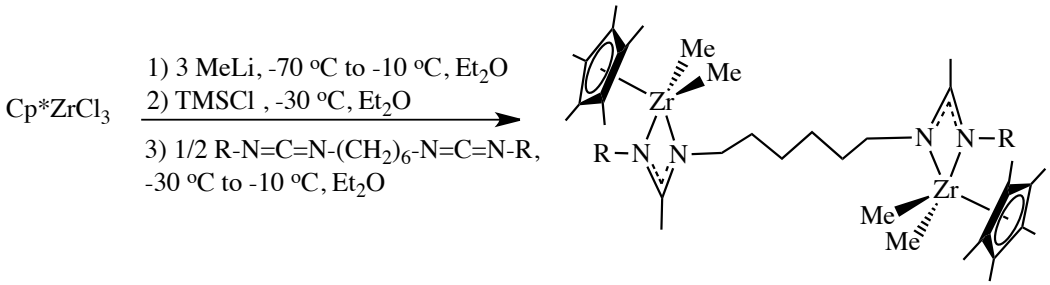

52 R = *t*Bu
75 R = (+/-)-3-methyl-2-butyl
76 R = (+)-3-methyl-2-butyl
77 R = (-)-3-methyl-2-butyl

5.3 Propene Polymerizations

5.3.1 Dinuclear

Scheme 31. General activation procedure for dinuclear amidinate precatalysts.

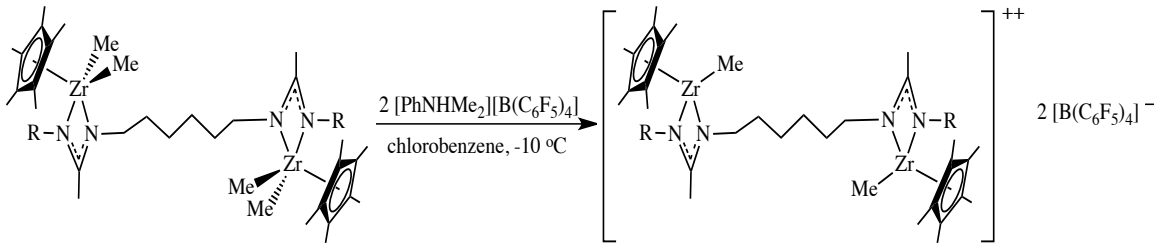

It is interesting to note that the chiral (entry 3) and racemic (entry 2) dinuclear catalysts behave in similar fashion under non-LCCTP conditions. The polymers produced appear to have the same physical properties such as T_g, T_m, T_c, and %*mmmm* values (Table 11). It is also interesting that **75** (entry 2) is more active than **76** (entry 3) in that the yield produced from **75** is nearly double of that produced from **76**. Also the racemic precatalyst **75** produces a higher molecular weight (M_w) polymer than the chiral catalyst **76**. The PDIs for these polymers also appear broader than what is typically expected for living polymerizations (<1.10) but can be attributed to low solubility given such high molecular weights. ^{1}H NMR analysis of these materials confirms that these are living polymerizations from the lack of vinylic resonances that would indicate termination via β hydride elimination.

Table 11. Polymerizations of propene with dinuclear precatalysts.

Run	Precat.	DEZ	Time[a] (h)	M_n[b] (kDa)	PDI[d]	T_g[e] (°C)	T_m[e] (°C)	T_c[f] (°C)	Yield (g)	% *mmmm*[g]
1	**52**	0	3	23.5	1.32	-7.1	112.8	84.4	0.30	0.70
2	**75**	0	3	74.1	1.14	-9.6	111.9	78.0	0.92	0.64
3	**76**	0	3	66.5	1.19	-9.6	112.8	77.7	0.42	0.63
4	**52**	10	20	3.57	2.51	-19.4	106.9	78.9	1.48	0.65
5	**75**	10	20	5.97	1.28	-17.4	88.3	54.7	2.75	0.51
6	**76**	10	20	4.02	1.86	-25.5	98.9	71.0	0.98	0.54

[a] Polymerizations were terminated by precipitation into acidic MeOH. [b,c,d] Determined by gel permeation chromatography (GPC) analysis. [e,f,g]Determined by differential scanning calorimetry (DSC) analysis. [g]Determined by ^{1}H (600 MHz) and ^{13}C (150 MHz) NMR at 110 °C in 1,1,2,2-tetrachloroethane-d_2

As seen in Figure 44, there is no discernable difference between the polymers from **76** and **75** by ^{13}C NMR analysis. The two catalysts show some differences from each other under LCCTP conditions. The % *mmmm* value for **76** is lower than expected, giving rise to the notion that the chirality of the substituent is not influencing the

stereoselectivity as much as was anticipated. Had the chiral substituents controlled the stereoselectivity by decreasing the $m_x(r)m_y$ type stereoerror, the % *mmmm* value would have been closer to the % *mmmm* value of the precatalyst under non-LCCTP conditions. A reduction in the $m_x(r)m_y$ pentad was expected as the chirality should be providing more enantiomorphic site control. Preliminary specific rotation values indicate that polymers produced from **76** are not optically active at the 589 nm wavelength of the polarimeter. This can arise from several issues including decrease in isotacticity, size of the propene unit, and lack of influence from the catalyst. It was discovered by Natta and coworkers that completely isotactic polypropylene will coil into a helix upon crystallization.

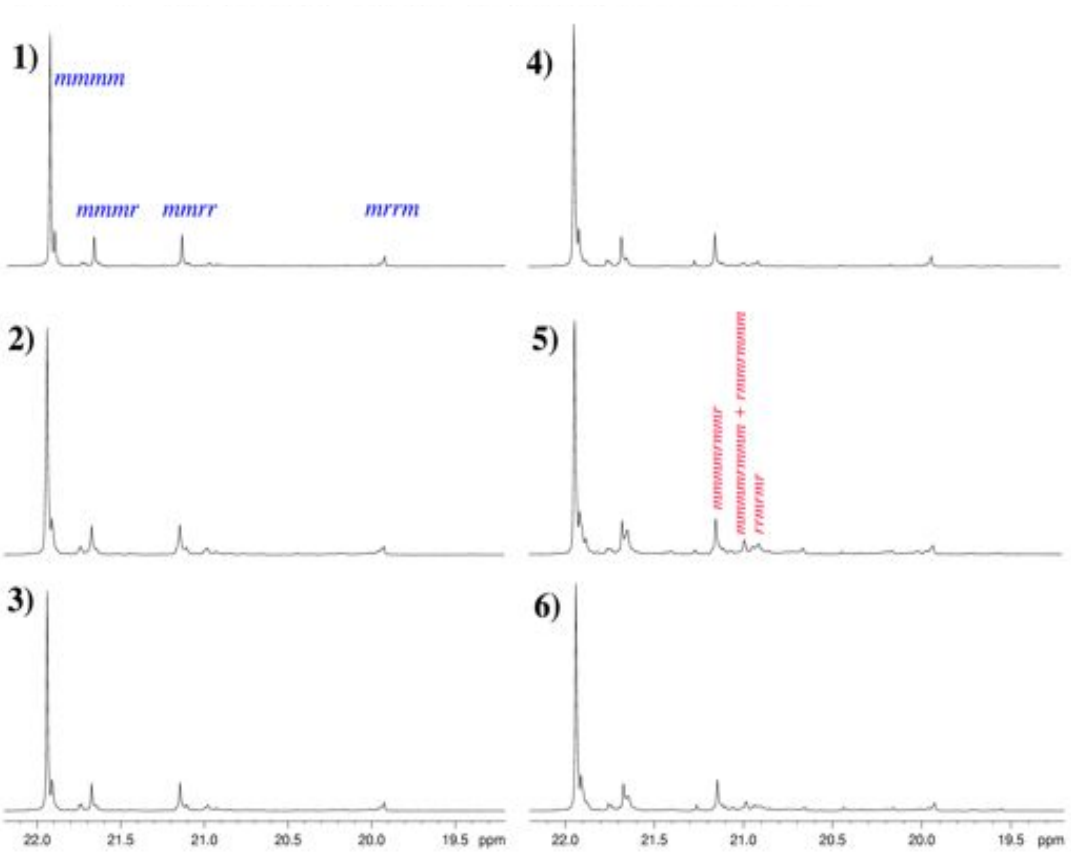

Figure 44. Partial ^{13}C NMR: 150 MHz, 1,1,2,2-tetrachloroethane-d_2, 110°C of polypropylene materials from (entries 1-6, Table 11).

As seen in Figure 44 there are stereoerrors at δ 20.98 ppm, δ 20.90 ppm, and δ 20.68 ppm corresponding to the *mmmmrmmr*, *mmmmrmmm* + *rmmrmmm* , *rrmrmr* stereoerrors respectively, that occur with both **76** and **75**, but not **52**.[11] These stereoerrors arise from the $m_x rm_y$ pentad, a result from rapid chain transfer, so it is understandable that the more rapid chain transfer reactions seen with **76** and **75** would have more errors of this type. Unfortunately, based on the %*mmmm* values, neither the chiral nor racemic catalysts show more stereocontrol under chain transfer conditions than **52** (Table 11). It is also interesting to note that the same 2,1-insertions appear in both designs (Figure 45) and there is not a clear distinction between the two in regards to those insertions.[12]

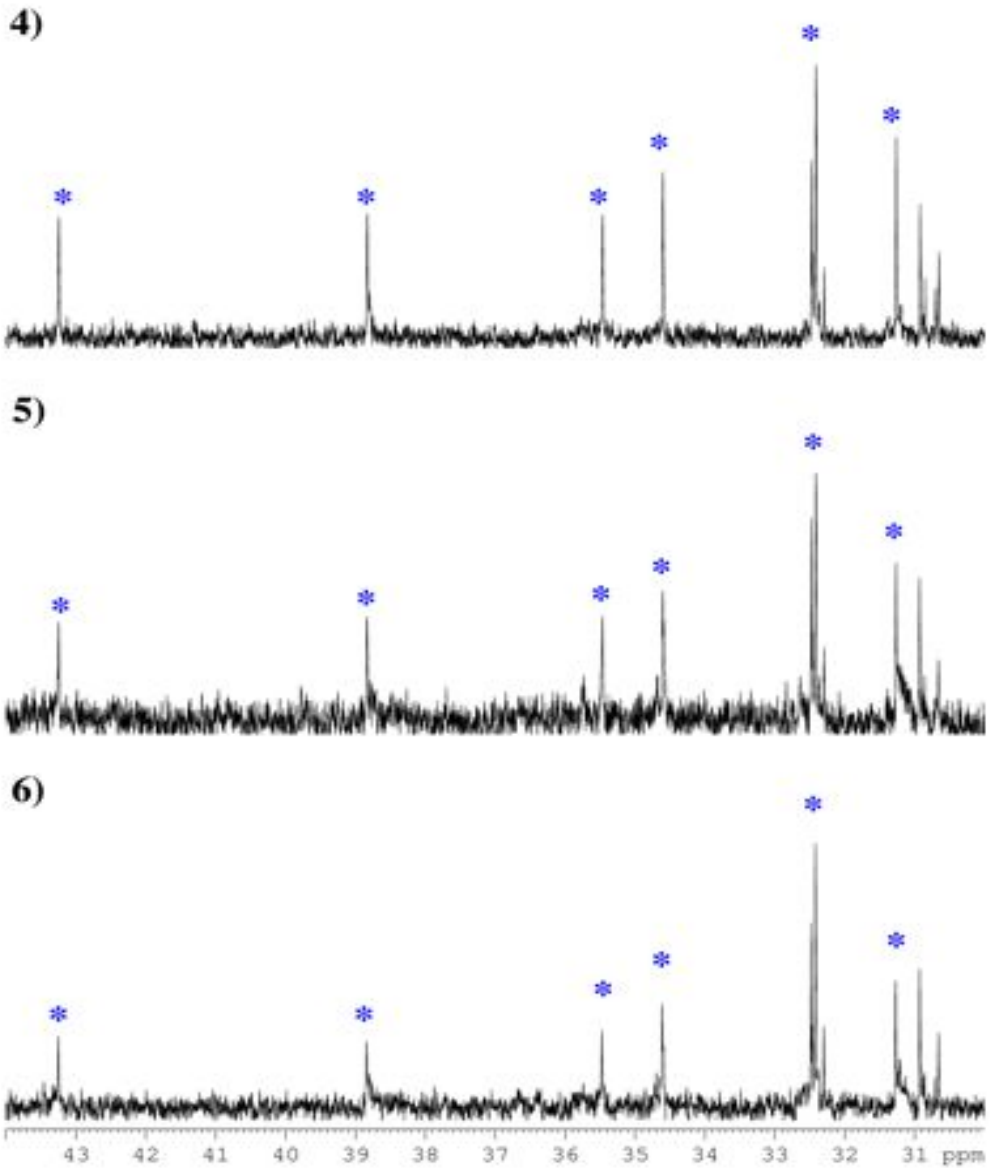

Figure 45. Partial ^{13}C: 150 MHz, 1,1,2,2-$C_2D_2Cl_4$, 110 ^{o}C of LCCTP polypropylene from Table 11 entries 4-6, showing 2,1-insertions (stars).

5.3.2 Mononuclear

Scheme 32. General activation procedure for mononuclear amidinates.

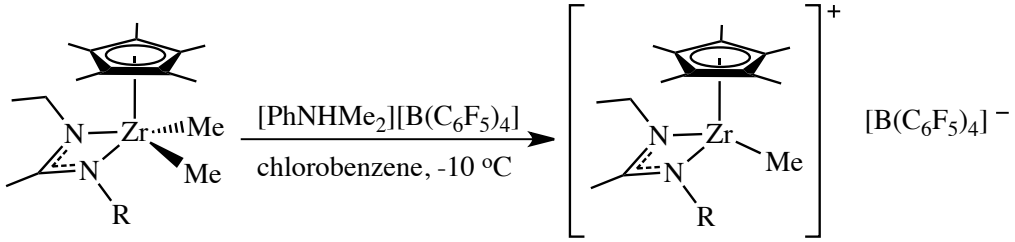

Polymerizations were carried out based on the following general reaction Scheme 43 at -10 °C in chlorobenzene to form the active cationic species by reacting the dimethyl initiator with 2 equivalents of the cocatalyst, $[PhNHMe_2][B(C_6F_5)_4]$ (**49**). After the designated reaction time, the polymerizations were quenched and precipitated with acidic methanol and isolated by filtration. The resulting polymers were dried and characterized through the use of ^1H and ^{13}C NMR to determine their microstructures. They were also characterized via differential scanning calorimetry (DSC) and gel permeation chromatography (GPC) to obtain information about their material characteristics including the T_m, T_c, T_g, molecular weight, and polydispersity.

Table 12. Polymerization of propene with mononuclear precatalysts.

Run	Precat.	DEZ	Time[a] (h)	M_n[b] (kDa)	PDI[d]	T_g[e] (°C)	T_m[e] (°C)	T_c[f] (°C)	Yield (g)	% *mmmm*[g]
1	**51**	0	3	23.4	1.28	-9.4	110.4	78.5	0.40	0.69
2	**74**	0	3	80.6	1.08	-10.0	95.8	50.8	0.48	0.50
3	**51**	10	20	4.92	1.18	-17.7	73.2	28.4	1.80	0.49
4	**74**	10	20	3.00	1.36	-23.1	--	--	0.58	0.19

[a] Polymerizations were terminated at precipitation into acidic MeOH. [b,c,d] Determined by gel permeation chromatography (GPC) analysis. [e,f,g]Determined by differential scanning calorimetry (DSC) analysis. [g]Determined by ^1H (600 MHz) and ^{13}C (150 MHz) NMR at 110 °C in 1,1,2,2-tetrachloroethane-d_2

Precatalyst **74** (Run 2) is more active than the '*t*-butyl' (Run 1) version as it was with the dinuclear precatalysts, but there is a loss of stereocontrol based on the %*mmmm* values for the two precatalysts (Table 12). This trend was also seen for the dinuclear precatalysts **76** and **75**, which can be attributed to the decreased sterics at the α-carbon on the N-C bond of the amidinate. As evident from the table and Figure 46, there is a loss

of isotacticity under chain transfer conditions for **74**, indicating that the chirality is not providing enantiomorphic site control as it did with the dinuclear analogues. **76** also produced a higher molecular weight polymer, which can explain the differences between the polymers' physical characteristics T_g, T_m, and T_c..

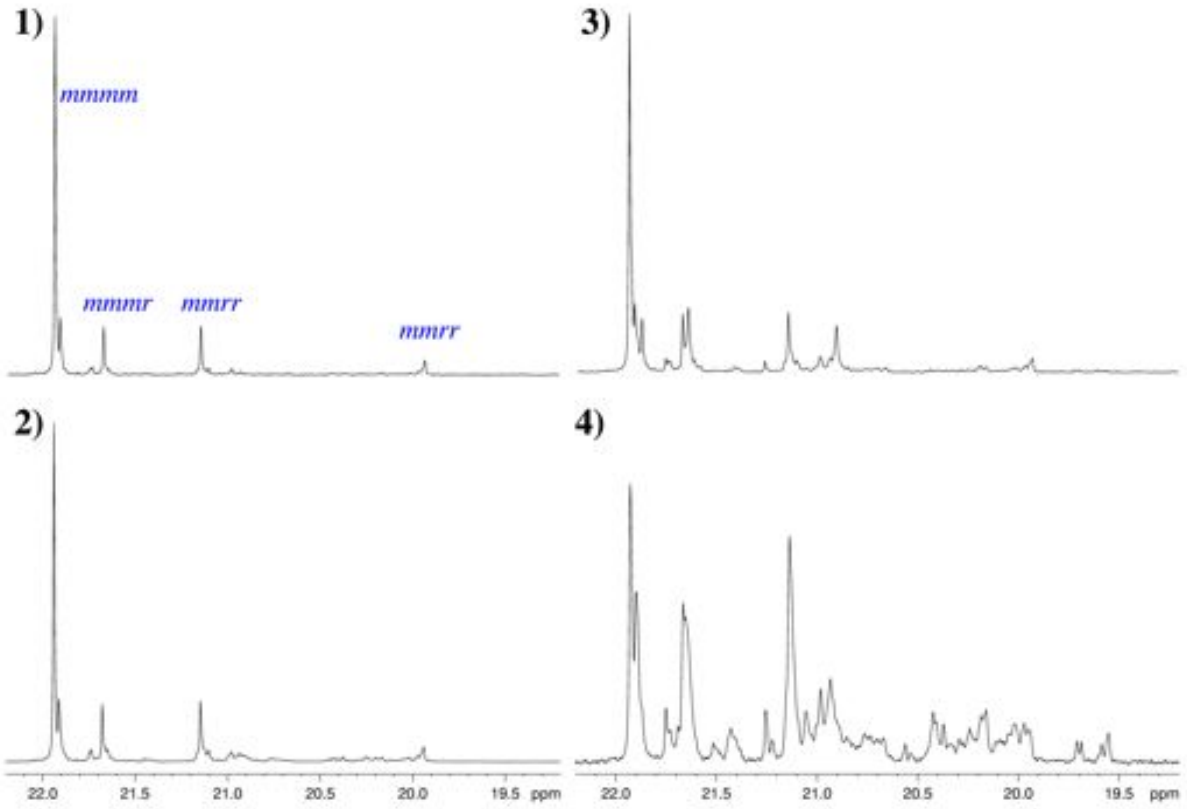

Figure 46. Partial ^{13}C NMR: 150 MHz, 1,1,2,2-tetrachloroethane-d_2, 110°C of polypropylene materials from (entries 1-4, Table 12).

5.3.3 'Chiral' vs. *t*Bu Amidinate Frame

When comparing the results obtained from the newly designed catalysts (3-methyl-2-butyl /Et frame), it is worth comparing the resulting polymers' microstructures to those produced from **51,** which has also been developed by our group.[2] Firstly, **73**-**74** and **75**-**76** are more active than the previously reported **51** (Table 11 and Table 12). This can be attributed to larger sterics at the α-carbon on the amidinate substituent of the '*t*-

butyl' group versus the less crowded α-carbon on the amidinate substituent of the 'isopropyl' group. This can allow for the substituent to rotate around the axial N-C bond so that the smaller hydrogen replaces the methyl group in the active center. Overall this reduces the bulkiness in the active center and as a result some enantiomorphic site control is lost. This issue does not arise when using the *t*-butyl substituent since there are two methyl groups on the α-carbon on the amidinate substituent (Figure 47).

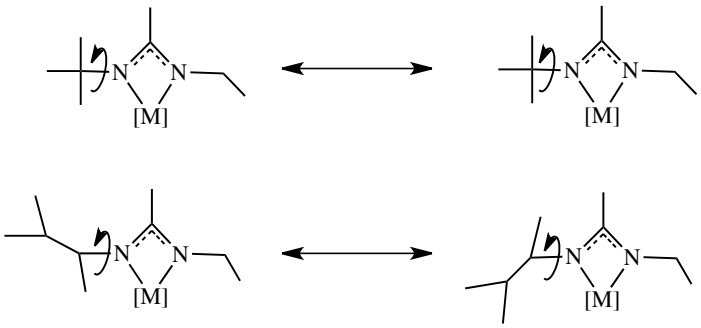

Figure 47. Sterics at a-carbon with chiral amidinate design.

From these results it is reasonable to conclude that the decrease in stereocontrol under LCCTP is not a result from misinsertions, but rather a lack of enantiomorphic site control. This stems from the precatalysts' ability to reduce the sterics in the active center by rotating so that the smaller hydrogen is in the active center instead of the methyl group. As stated earlier, should the precatalysts have shown to provide stereocontrol under the LCCTP conditions, the %*mmmm* value for **76** would not have varied much from the value under non-chain transfer conditions showing that the chirality of the catalyst was contributing to stereocontrol of the microstructure.

5.3.4 Mononuclear vs. Dinuclear Precatalysts

When comparing the dinuclear catalysts to their mononuclear analogues (Table 13) there is a definite advantage of the dinuclear species over the mononuclear species. Overall, **76** produced a more isotactic polymer than **74** under the same non-LCCTP conditions. It is also apparent that under LCCTP conditions **76** was able to retain more stereoselectivity than **74**. This trend agrees with some recent results that have been found by our group when comparing catalysts **51** and **52** under LCCTP conditions (Tables 11 and 12). It is also interesting that under LCCTP conditions **76** is substantially more active than **74** when comparing the yield/time for both of the precatalysts.

Table 12. Polymerizations of propene using **74** and **76**.

Entry	Precat.	DEZ	Time[a] (h)	M_n[b] (kDa)	PDI[d]	T_g[e] (°C)	T_m[e] (°C)	T_c[f] (°C)	Yield (g)	% *mmmm*[g]
1	**76**	0	3	66.5	1.19	-9.6	112.8	77.7	0.42	0.63
2	**76**	10	2	4.02	1.86	-25.5	98.9	71.0	0.98	0.54
3	**74**	0	3	80.6	1.08	-10.0	95.8	50.8	0.48	0.50
4	**74**	10	20	3.00	1.36	-23.1	--	--	0.58	0.19

[a] Polymerizations were terminated at precipitation into acidic MeOH. [b,c,d] Determined by gel permeation chromatography (GPC) analysis. [e,f,g]Determined by differential scanning calorimetry (DSC) analysis. [g]Determined by ^{1}H (600 MHz) and ^{13}C (150 MHz) NMR at 110 °C in 1,1,2,2-tetrachloroethane-d_2

5.4 1-Butene & Rotations

5.4.1 1-Butene Polymerizations

Scheme 33. General polymerization procedure for poly(1-butene) with **75-77**.

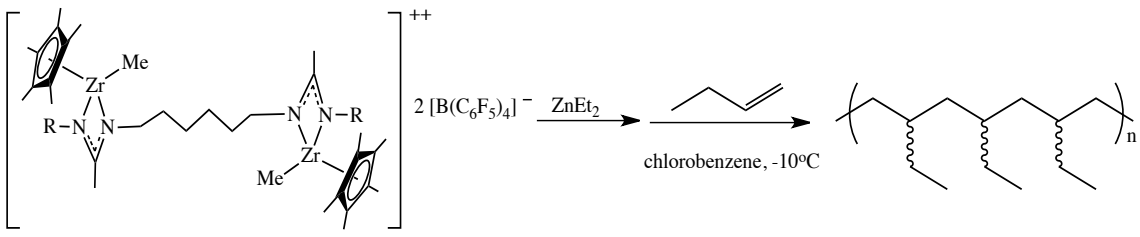

The polymerizations were conducted with 1-butene, a larger monomer well known to create highly isotactic and crystalline materials, as shown in Scheme 33 using diethyl zinc as the chain transfer agent in chlorobenzene at -10 ^{o}C for entries 4-6. As expected, **75-77**, proved to be adept at polymerizing 1-butene in a living process under both non-LCCTP and LCCTP conditions (Table 14). GPC analysis of the resulting polymers confirmed that the molecular weight distributions were monomodal. The polydispersities obtained from the analysis do not agree with values <1.10 that are typically expected from living polymerizations but ^{1}H NMR analysis (600 MHz in1,1,2,2-tetrachlorethane-d_2 at 110 °C) did not reveal any vinylic resonances that would result from β-hydride elimination confirming that the polymerization proceeded via a living process. It is no surprise that the initiators have similar activities given their nearly identical structures.

Table 13. Polymerizations of 1-butene using **75-77**.

Run	Precat.	DEZ	Time[a] (h)	M_n[b] (kDa)	PDI[d]	T_g[e] (°C)	T_m[e] (°C)	T_c[f] (°C)	Yield (g)	% *mmmm*[g]
1	**75**	0	3	11.3	1.78	-38.8	93.9	58.2	0.11	0.88
2	**76**	0	3	16.2	1.36	-36.6	94.0	52.5	0.05	0.88
3	**77**	0	3	16.7	1.61	-31.2	97.5	62.7	0.04	0.93
4	**75**	10	20	1.73	1.28	--	52.1; 64.1; 74.2	37.9	0.09	0.71
5	**76**	10	20	1.22	1.36	--	54.5; 63.2; 75.5	37.6	0.04	0.69
6	**77**	10	20	4.33	2.64	--	56.6; 66.5; 76.6	39.2	0.06	0.71

[a] Polymerizations were terminated at precipitation into acidic MeOH. [b,c,d] Determined by gel permeation chromatography (GPC) analysis. [e,f,g]Determined by differential scanning calorimetry (DSC) analysis. [g]Determined by ^{1}H (600 MHz) and ^{13}C (150 MHz) NMR at 110 °C in 1,1,2,2-tetrachloroethane-d_2

Thermal analysis of the second heating and cooling cycles by DSC, Figure 48, reveals that the materials are remarkably similar in terms of their material properties. The polymer samples produced under non-LCCTP conditions (Table 14, 1-3) have comparable T_c's, T_m's, and T_g's. This is expected given that the sterics of the initiators, which will affect the bulk properties, are completely the same with the only difference the chirality on the N-substituent of the amidinate frame. Similarities in the T_c's, T_m's, and T_g's are seen for the materials produced under LCCTP conditions (Table 14, 4-6). It is interesting to note the three different melting temperatures from the three crystalline forms were detected with a 10 ^{o}C/min temperature program during the analysis.[13]

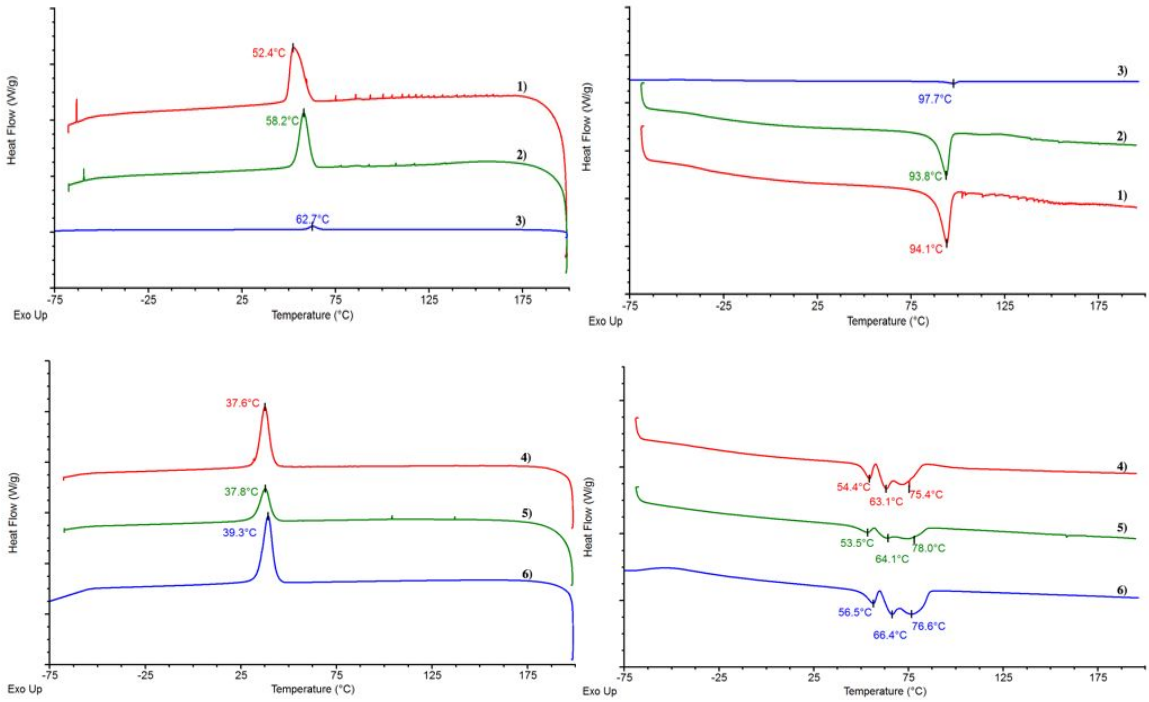

Figure 48. DSC thermograms of poly(1-butene) materials from Table 14.

As seen in Figure 49, there is not a discernable difference between the polymers from the initiators by ^{13}C NMR analysis. Pentad analysis reveals that the initiators are adept at producing highly stereoselective poly(1-butene) that is comparable to **52** which was studied earlier in Chapter 1 under non-LCCTP conditions (Table 14, 1-3). As expected, there is a decrease in the isotacticity under LCCTP conditions with the presence of DEZ in solution. Several stereoerrors of the m_xrm_y type are easily identifiable in the ^{13}C NMR as a result from rapid chain transfer process during LCCTP.

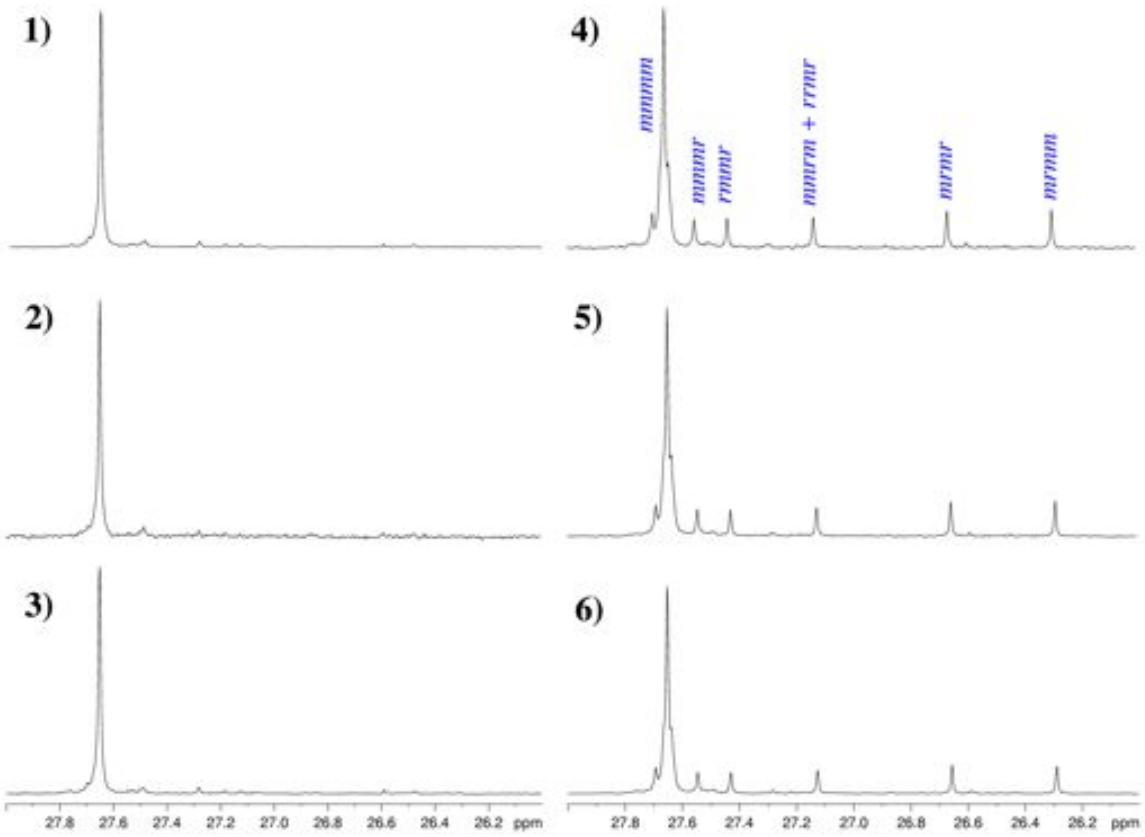

Figure 49. Partial ^{13}C NMR: 150 MHz, 1,1,2,2-tetrachloroethane-d_2, 110°C of poly(1-butene) materials from (entries 1-6, Table 14).

5.4.2 Optical Rotations

Specific rotations were measured of each precatalyst and their highly isotactic poly(1-butene) materials from non-LCCTP conditions, in triplicate, using a JASCO P-1010 Polarimeter at 23 ^{o}C in a 10 cm cell. As expected, the precatalyst with the racemic mixture on the amidinate frame shows a negligible specific rotation whereas the other two complexes show large rotations with their respective signs (Table 15). The material produced from **76** has an observed specific rotation of (-) 126.94 ± 9.45° and the poly(1-butene) produced from **77** has a specific rotation of (+) 41.19 ± 1.12°. It is unclear as to why the magnitude of the rotation for X is considerably less than X given that the

materials are nearly identical in terms of physical properties and microstructure. It is worth noting that the precatalyst appear to have produced polymeric materials with the opposite sense of handedness, **76** produced a negatively handed material and **77** produced a positively handed material. As of yet, this is the first known instance of an optically active polymer that is not comprised of oligostyrenes.

Table 14. Specific rotations of dinuclear precatalysts **75-77** and their poly(1-butene) materials.

Entry	Precatalyst	Precatalyst Rotation	Std. Dev	Poly(1-butene) Rotation	Std. Dev
1	**75**	+ 0.48	0.40	- 4.65	2.54
2	**76**	+ 98.88	1.57	- 126.94	9.45
3	**77**	- 84.05	1.21	+ 41.19	1.12

Preliminary specific rotations of the polypropylenes produced from the precatalysts indicated that the polymers were not optically active. If a chiral precatalyst is able to produce highly isotactic polymers, then it is expected that there will be a preferred helix conformation, creating an optically active polymer. It is likely that the larger size of the monomer played a role in the ability for the optical activity to be detected. The larger 1-butene unit does allow for a more isotactic polymer to be produced, as seen with the amidinate system and it's ability to polymerize larger α-olefins.[9] As a result of the increased isotacticity, the polymers were inherently more crystalline which allows for the helix of the chain to 'freeze' and optical activity to be detected.

5.5 Conclusions

The precatalyst designs were successfully polymerized in a living fashion with a high degree of stereoselectivity. They were also proven to be competent initiators under LCCTP conditions. Both the dinuclear and mononuclear analogues are more active than the '*t*-butyl' designs (**51** and **52**) that were previously reported by this group due to the decreased steric discrimination at the α-carbon on the N-substituent. This decreased steric discrimination resulted in materials with higher molecular weights and a decrease in isotacticity. Secondly, the dinuclear design produced a more stereoregular polymer under non-LCCTP conditions and LCCTP conditions than the mononuclear design.

Specific rotations of the polypropylenes produced from the 'chiral' precatalysts indicated that the polymers were not optically active. This can arise from several issues including lack of crystallinity due to the loss of isotacticity from the decreased steric influence. This loss in stereoselectivity can be attributed to a combination of the small monomer size and less steric influence exerted by the ligand frame. Additionally, with a racemic mixture of the precatalyst, it is expected to produce an equal amount of left and right handed helices creating a net specific rotation of zero.[10] Success in creating optically active polymers was found by switching from propene to 1-butene under non-LCCTP conditions. The larger monomer unit allows for a higher degree of stereoselectivity to be achieved, thus creating highly crystalline material. Results indicate that the optically active initiators produce optically active materials while the non-optically active initiators produced materials with negligible specific rotations. Further mechanistic studies are needed to explain the exact nature of the system in explaining why materials of the opposite handedness are produced.

5.7 Experimentals

Materials:

All manipulations were performed under an inert atmosphere of N_2 using standard Schlenk-line or glove-box techniques. All solvents were dried (Na/benzophenone for pentane and diethyl ether, and Na for toluene) and distilled under N_2 prior to use. Benzene-d_6 was dried over Na/K alloy and was vacuum transferred prior to being used for NMR spectroscopy. Celite was oven dried at 150 °C for several days before use. Cooling for the reactions was performed in the internal freezer (-25 °C) of the glove box used. $(\eta^5\text{-}C_5Me_5)MCl_3$, where M=Zr,Hf, and $[PhNMe_2][B(C_6F_5)_4]$ were purchased from Strem Chemicals, and used as received. (*S*)-(+)-2-amino-3-methylbutane, (+/-)-2-amino-3-methylbutane, and hexamethylene diisocyanate were purchased from Sigma Aldrich and used as received. 1-butene was purchased from Sigma Aldrich and used as received. Polymer grade propene was purchased from Matheson Trigas and passed through activated Q5 and molecular sieves (4 Å) before use. $ZnEt_2$ was purchased from Sigma Aldrich and added to the reaction as a 1.1M (15% wt) solution in toluene. $[(\eta^5\text{-}C_5Me_5)ZrMe_2]_2$[tBuNC(Me)NEt] **(51)** was prepared as previously reported in the literature.

Instrumental:

GPC analyses were performed using a Viscotek GPC system equipped with a column oven and a differential refractometer both maintained at 45 °C and four columns also maintained at 45 °C. THF was used as the eluent at a flow rate of 1.0 mL/min. M_n, M_w, and M_w/M_n values were obtained using a Viscotek GPC with OmniSEC software and ten polystyrene standards (M_n=580 Da to 3150 kDa) (Polymer Laboratories).

^{1}H NMR spectra were recorded at 400MHz with benzene-d_6. For polymer samples ^{13}C ^{14} NMR spectra were recorded at 600 MHz and 150 MHz, respectively, using 1,1,2,2-tetrachlorethane-d_2 at 110 °C with a Bruker AVIII-600MHz spectrometer equipped with a Bruker 5 mm C13/H1 dual probe with Z gradient. Spectra were recorded under the following conditions: 45° pulse; without NOE; acquisition time, 1.2 s; relaxation delay, 2.0 s; >10K transients.

Differential Scanning Calorimetry (DSC) thermograms were collected on a TA DSC Q1000 system with a heating and cooling rate of 5 or 10 ^{o}C/min. All samples were prepared in hermetically sealed pans (8 – 10 mg/sample) and were run using an empty pan as a reference and empty cells as a subtracted baseline. The samples were scanned for multiple cycles to remove recrystallization differences between the samples and the results reported are of the second and third scans in the cycles.

Specific rotation was measured, in triplicates, using a JASCO P-1010 Polarimeter. Solutions of 50.0 mg prepared in 10.0 mL of toluene as indicated below were used for measuring the specific rotations (path length 10 cm, volume 10 mL, 589 nm at 23 °C).

Elemental analyses (C, H, and N) were performed by Midwest Microlabs,LLC.

Preparation of [(+)-3-methyl-2-butyl-NH-CO-NH-$(CH_2)_6$-NH-CO-NH-[(+)-3-methyl-2-butyl] :

To a solution of 3.49 g (40.0 mmol) (*S*)-(+)-2-amino-3-methylbutane in 125 mL $CHCl_3$ at 0 °C was added a solution of 3.42 g (20.0 mmol) 1,6-diisocyanatohexane in 125 mL $CHCl_3$ over 30 min. The resulting solution was stirred for 30 min before being concentrated under vacuum and then precipitated into 500 mL pentane. The product was isolated as a white powder *via* filtration and washed with several portions of pentane before being dried under vacuum (6.65g, 97.1%); ^{1}H NMR (400 MHz, DMF, 25 °C): δ

0.85 (m, 6H), 0.98 (d, 3H), 1.29 (m, 2H), 1.41 (m, 2H), 1.64 (sextet, 1H), 3.08 (q, 2H), 3.50 (s, 5H), 3.59 (sextet, 1H), 5.66 (d, 1H), 5.78 (t, 1H).

Preparation of [(+)-3-methyl-2-butyl]-N=C=N-$(CH_2)_6$-N=C=N-[(+)-3-methyl-2-butyl] :

To a solution of 16.4 g (62.5 mmol) triphenylphosphine in 225 mL CH_2Cl_2 under a nitrogen atmosphere and at 0 °C was added dropwise, a solution of 9.99 g (62.5 mmol) bromine in 20 mL CH_2Cl_2 *via* pressure-equalizing addition funnel over a period of 30 min. After stirring for an additional 15 min, 12.8 g (126 mmol) triethylamine was added dropwise in a similar fashion into the reaction mixture over 15 min. During the next hour, 8.6 g (25 mmol) [(+)-*i*Pr]-NH-CO-NH-$(CH_2)_6$-NH-CO-NH-[(+)- *i*Pr] were added in four equal portions. The solution was stirred overnight, washed with 125 mL of distilled water, and the organic layer separated and dried with anhydrous sodium sulfate. After being concentrated under vacuum, the solution was slowly added into 700 mL cold pentane, filtered, and the volatiles were removed under vacuum to provide the crude product as a yellow liquid, which was then filtered through celite and dried under vacuum; (2.53g, 33.0%); ^{1}H NMR (400 MHz, C_6D_6, 25 °C): δ 0.88 (m, 12H), 1.08 (d, 6H), 1.17 (m, 4H), 1.39 (m, 4H), 1.51 (sextet, 2H), 3.01 (t, 4H), 3.13 (p, 2H).

Preparation of [(η^5-C_5Me_5)$ZrMe_2$]$_2$[N((+)-3-methyl-2-butyl)C(Me)N$(CH_2)_6$NC(Me)N((+)-3-methyl-2-butyl)] (76) :

To a solution of 0.99 g (3.0 mmol) (η^5-C_5Me_5)$ZrCl_3$ in 80 mL Et_2O at -65°C was added a solution of 6.2 mL of MeLi (1.60 M in Et_2O) *via* gas tight syringe over 10 min. The mixture was stirred for 3 h at -30 °C and then quenched with the addition of 0.3 mL Me_3SiCl *via* syringe. A solution of 0.24 g (1.5 mmol) [(+)-*i*Pr]-N=C=N-$(CH_2)_6$-N=C=N-[(+)- *i*Pr] in 15 mL of Et_2O was then added *via* cannula at -30 °C over 45 min. The

mixture was stirred for 1 h at -30 °C and then allowed to warm up to room temperature overnight, after which, the volatiles were removed under vacuum. The white residue was extracted with minimal toluene and filtered through a pad of Celite in a glass frit. The solution was concentrated to 1 mL where 2 mL of pentane was added and allowed to crystallize at -25 °C in the freezer. The resulting white powder was collected and dried under vacuum; (0.581g, 47.0%); ^{1}H NMR (400 MHz, C_6D_6, 25 °C): δ 0.29 (d, 12H), 0.86 (d, 6H), 1.00 (d, 6H), 1.10 (d, 6H), 1.59 (s, 6H), 2.01 (s, 30H), 2.93 (m, 6H).

Preparation of [(+)-3-methyl-2-butyl]-NH-CO-NH-Et :

To a solution of 4.36 g (50.0mmol) (*S*)-(+)-2-amino-3-methylbutane in 125 mL $CHCl_3$ at 0 °C was added a solution of 3.55 g (50.0 mmol) ethyl isocyanate in 125 mL $CHCl_3$ over 30 min. The resulting solution was stirred for 30 min before being concentrated under vacuum and then precipitated into 500 mL pentane. The product was isolated as a white powder *via* filtration and washed with several portions of pentane before being dried under vacuum; (7.40g, 94.0%); ^{1}H NMR (400 MHz, $CDCl_3$, 25 °C): δ 0.90 (m, 6H), 1.07 (d, 3H), 1.14 (t, 3H), 1.60 (s, 1H), 1.68 (m, 1H), 3.20 (m, 2H), 3.63 (m, 1H), 4.10 (m, 2H).

Preparation of [(+)-3-methyl-2-butyl]-N=C=N-Et :

To a solution of 13.1 g (50.0 mmol) triphenylphosphine in 225 mL CH_2Cl_2 under a nitrogen atmosphere and at 0 °C was added dropwise, a solution of 7.99 g (50.0 mmol) bromine in 20 mL CH_2Cl_2 *via* pressure-equalizing addition funnel over a period of 30 min. After stirring for an additional 15 min, 10.2 g (101.0 mmol) triethylamine was added dropwise in a similar fashion into the reaction mixture over 15 min. During the next hour, 6.3 g (40.0 mmol) [(+)-*i*Pr]-NH-CO-NH-Et was added in four equal portions.

The solution was stirred overnight, washed with 125 mL of distilled water, and the organic layer separated and dried with anhydrous sodium sulfate. After being concentrated under vacuum, the solution was slowly added into 700 mL cold pentane, filtered, and the volatiles were removed under vacuum to provide the crude product as a yellow liquid, which was then filtered through celite and dried under vacuum; (1.40g, 25.0%); ^{1}H NMR (400 MHz, $CDCl_3$, 25 °C): δ 0.87 (d, 6H), 1.16 (m, 6H), 1.60 (sextet, 1H), 3.25 (m, 3H).

Preparation of [(η^5-C_5Me_5)$ZrMe_2$]$_2$[N((+)-3-methyl-2-butyl)C(Me)NEt] (74) :

To a solution of 0.67 g (2.0 mmol) (η^5-C_5Me_5)$ZrCl_3$ in 80 mL Et_2O at -65 °C was added a solution of 4.1 mL of MeLi (1.60 M in Et_2O) *via* syringe over 10 min. The mixture was stirred for 3 h at -30 °C and then quenched with the addition of 0.2 mL Me_3SiCl *via* syringe. A solution of 0.28 g (2.0 mmol) [(+)-*i*Pr]-N=C=N-Et in 15 mL of Et_2O was then added *via* cannula at -30 °C over 45 min. The mixture was stirred for 1 h at -30 °C and then allowed to warm up to -10 °C, after which, the volatiles were removed under vacuum. The white residue was extracted with minimal pentane and filtered through a pad of Celite in a glass frit. The solution was concentrated to 1 mL allowed to crystallize at -25 °C in the freezer. Crystals did not form after several attempts to crystallize so the product was dried under vacuum for several hours and used as the resulting oil; (0.696g, 84.4%); ^{1}H NMR (400 MHz, C_6D_6, 25 °C): δ 0.24 (d, 6H), 0.84 (d, 4H), 0.96 (d, 6H), 1.09 (d, 6H), 1.50 (s, 3H), 1.98 (s, 15H), 2.88 (m, 3H), 3.25 (q, 2H).

Preparation of [(+/-)-3-methyl-2-butyl]-NH-CO-NH-$(CH_2)_6$-NH-CO-NH-[(+/-)- 3-methyl-2-butyl] :

To a solution of 3.66 g (50.0mmol) (*S*)-(+/-)-2-amino-3-methylbutane in 125 mL $CHCl_3$ at 0 °C was added a solution of 4.20 g (25.0 mmol) 1,6-diisocyanatohexane in 125

mL $CHCl_3$ over 30 min. The resulting solution was stirred for 30 min before being concentrated under vacuum and then precipitated into 500 mL pentane. The product was isolated as a white powder *via* filtration and washed with several portions of pentane before being dried under vacuum;(6.98g, 88.7%); ^{1}H NMR (400 MHz, DMF, 25 °C): δ 0.86 (m, 6H), 0.99 (d, 3H), 1.30 (m, 2H), 1.42 (m, 2H), 1.64 (sextet, 1H), 3.09 (q, 2H), 3.50 (s, 10H), 5.67 (d, 1H), 5.79 (t, 1H).

Preparation of [(+/-)-3-methyl-2-butyl]-N=C=N-$(CH_2)_6$-N=C=N-[(+/-)-3-methyl-2-butyl] :

To a solution of 9.84 g (37.5 mmol) triphenylphosphine in 225 mL CH_2Cl_2 under a nitrogen atmosphere and at 0 °C was added dropwise, a solution of 6.0 g (37.5 mmol) bromine in 20 mL CH_2Cl_2 *via* pressure-equalizing addition funnel over a period of 30 min. After stirring for an additional 15 min, 7.65 g (75.0 mmol) triethylamine was added dropwise in a similar fashion into the reaction mixture over 15 min. During the next hour, 5.1 g (15.0 mmol) [(+/-)-*iPr*]-NH-CO-NH-$(CH_2)_6$-NH-CO-NH-[(+/-)-*i*Pr] were added in four equal portions. The solution was stirred overnight, washed with 125 mL of distilled water, and the organic layer separated and dried with anhydrous sodium sulfate. After being concentrated under vacuum, the solution was slowly added into 700 mL cold pentane, filtered, and the volatiles were removed under vacuum to provide the crude product as a yellow liquid, which was then filtered through celite and dried under vacuum; (1.70g, 18.5%); ^{1}H NMR (400 MHz, C_6D_6, 25 °C): δ 0.87 (m, 12H), 1.08 (m, 6H), 1.17 (m, 4H), 1.39 (m, 4H), 1.50 (m, 2H), 3.01 (t, 4H), 3.12 (p, 2H).

Preparation of [(η^5-C_5Me_5)$ZrMe_2$]$_2$[N((+/-)-3-methyl-2-butyl)C(Me)N$(CH_2)_6$NC(Me)N((+/-)-3-methyl-2-butyl)] (75) :

To a solution of 0.50 g (1.5 mmol) (η^5-C_5Me_5)$ZrCl_3$ in 80 mL Et_2O at -65 °C was added a solution of 3.1 mL of MeLi (1.60 M in Et_2O) *via* gas tight syringe over 10 min. The mixture was stirred for 3 h at -30 °C and then quenched with the addition of 0.3 mL Me_3SiCl *via* syringe. A solution of 0.23 g (1.5 mmol) [(+/-)-*i*Pr]-N=C=N-$(CH_2)_6$-N=C=N-[(+/-)- *i*Pr] in 15 mL of Et_2O was then added *via* cannula at -30 °C over 45 min. The mixture was stirred for 1 h at -30 °C and then allowed to warm up to room temperature overnight, after which, the volatiles were removed under vacuum. The white residue was extracted with minimal toluene and filtered through a pad of Celite in a glass frit. The solution was concentrated to 1 mL where 2 mL of pentane was added and allowed to crystallize at -25 °C in the freezer. The resulting white powder was collected and dried under vacuum; (0.821g, 67.0%); ^{1}H NMR (400 MHz, C_6D_6, 25 °C): δ 0.29 (d, 12H), 0.86 (d, 6H), 1.01 (d, 6H), 1.10 (d, 6H), 1.60 (s, 6H), 2.01 (s, 30H), 2.93 (m, 6H).

Preparation of [(+/-)-3-methyl-2-butyl]-NH-CO-NH-Et :

To a solution of 4.36 g (50.0mmol) (*S*)-(+/-)-2-amino-3-methylbutane in 125 mL $CHCl_3$ at 0 °C was added a solution of 3.55 g (50.0 mmol) ethyl isocyanate in 125 mL $CHCl_3$ over 30 min. The resulting solution was stirred for 30 min before being concentrated under vacuum and then precipitated into 500 mL pentane. The product was isolated as a white powder *via* filtration and washed with several portions of pentane before being dried under vacuum; (7.59g, 96.0%); ^{1}H NMR (400 MHz, $CDCl_3$, 25 °C): δ 0.90 (m, 6H), 1.07 (d, 3H), 1.14 (t, 3H), 1.64 (m, 1H), 3.21 (m, 2H), 3.63 (m, 1H), 4.08 (m, 2H).

Preparation of [(+/-)-3-methyl-2-butyl]-N=C=N-Et :

To a solution of 13.1 g (50.0 mmol) triphenylphosphine in 225 mL CH_2Cl_2 under a nitrogen atmosphere and at 0 °C was added dropwise, a solution of 7.99 g (50.0 mmol) bromine in 20 mL CH_2Cl_2 *via* pressure-equalizing addition funnel over a period of 30 min. After stirring for an additional 15 min, 10.2 g (101.0 mmol) triethylamine was added dropwise in a similar fashion into the reaction mixture over 15 min. During the next hour, 6.3 g (40.0 mmol) [(+/-)-*i*Pr]-NH-CO-NH-Et was added in four equal portions. The solution was stirred overnight, washed with 125 mL of distilled water, and the organic layer separated and dried with anhydrous sodium sulfate. After being concentrated under vacuum, the solution was slowly added into 700 mL cold pentane, filtered, and the volatiles were removed under vacuum to provide the crude product as a yellow liquid, which was then filtered through celite and dried under vacuum; (0.34g (6.0%); ^{1}H NMR (400 MHz, $CDCl_3$, 25 °C): δ 0.87 (d, 6H), 1.16 (m, 6H), 1.60 (sextet, 1H), 3.25 (m, 3H).

Preparation of [(η^5-C_5Me_5)$ZrMe_2$]$_2$[N((+/-)-3-methyl-2-butyl)C(Me)NEt] (73) :

To a solution of 0.67 g (2.0 mmol) (η^5-C_5Me_5)$ZrCl_3$ in 80 mL Et_2O at -65 °C was added a solution of 4.1 mL of MeLi (1.60 M in Et_2O) *via* syringe over 10 min. The mixture was stirred for 3 h at -30 °C and then quenched with the addition of 0.2 mL Me_3SiCl *via* syringe. A solution of 0.28 g (2.0 mmol) [(+/-)-*i*Pr]-N=C=N-Et in 15 mL of Et_2O was then added *via* cannula at -30 °C over 45 min. The mixture was stirred for 1 h at -30 °C and then allowed to warm up to -10 °C, after which, the volatiles were removed under vacuum. The white residue was extracted with minimal pentane and filtered through a pad of Celite in a glass frit. The solution was concentrated to 1 mL allowed to crystallize at -25 °C in the freezer. Crystals did not form after several attempts to

crystallize so the product was dried under vacuum for several hours. ^{1}H NMR (400 MHz, C_6D_6, 25 °C) revealed more than one product was formed. Attempts to resynthesize cleanly are underway.

General polymerization of propene in chlorobenzene:

A solution of the precatalyst (0.025 mmol) in 0.5 mL chlorobenzene at -10 °C was added to the $[PhNMe_2][B(C_6F_5)_4]$ (0.026 mmol) and agitated until dissolved. The resulting mixture was added to 29.5 mL chlorobenzene at -10 °C in a 250 mL Schlenk flask. The flask was charged to 5 psi with propene gas while stirring. Polymerization temperature was maintained at -10 ± 2 ºC. The pressure and stirring was maintained for the duration of the reaction where upon it was quenched with 1.0 mL of methanol and precipitated into 600 mL acidic methanol to isolate the polymer product. The polymer was collected and dried under vacuum. The resulting polymers were characterized by DSC, GPC, and $^{1}H/^{13}C$ NMR.

General LCCTP of propene in toluene:

A solution of the catalyst (0.020 mmol) in 0.5 mL chlorobenzene at -10 °C was added to the $[PhNMe_2][B(C_6F_5)_4]$ (0.021 mmol) and agitated until dissolved. 10 equivalents of 15% w/w solution of diethyl zinc was added to the activated solution and agitated. The resulting mixture was added to 29.5 mL toluene at -10 °C in a 250 mL Schlenk flask. The flask was charged to 5 psi with propene gas while stirring. The pressure and stirring was maintained for the duration of the reaction where upon it was quenched with 0.5 mL of methanol and precipitated into 650 mL acidic methanol to isolate the polymer product. The polymer was collected and dried under vacuum. The resulting polymers were characterized by DSC, GPC, and $^{1}H/^{13}C$ NMR.

General polymerization of 1-butene in chlorobenzene:

A solution of the catalyst (0.020 mmol) in 0.5 mL chlorobenzene at -10 °C was added to the $[PhNMe_2][B(C_6F_5)_4]$ (0.021 mmol) and agitated until dissolved. The resulting mixture was added to 9.5 mL chlorobenzene and 400eq 1-butene at -10 °C in a scintillation vial. The stirring was maintained for the duration of the reaction where upon it was quenched with 0.5 mL of methanol and precipitated into 650 mL acidic methanol to isolate the polymer product. The polymer was collected and dried under vacuum. The resulting polymers were characterized by DSC, GPC, and $^{1}H/^{13}C$ NMR.

General LCCTP of 1-butene in toluene:

A solution of the catalyst (0.020 mmol) in 0.5 mL chlorobenzene at -10 °C was added to the $[PhNMe_2][B(C_6F_5)_4]$ (0.021 mmol) and agitated until dissolved. 10eq of 15% w/w solution of diethyl zinc was added to the activated solution and agitated. The resulting mixture was added to 9.5 mL toluene and 400eq of 1-butene at -10°C in a scintillation vial. The stirring was maintained for the duration of the reaction where upon it was quenched with 0.5 mL of methanol and precipitated into 650 mL acidic methanol to isolate the polymer product. The polymer was collected and dried under vacuum. The resulting polymers were characterized by DSC, GPC, and $^{1}H/^{13}C$ NMR.

5.8 References

(1) Beckerle, K.; Manivannan, R.; Lian, B.; Meppelder, G.-J. M.; Raabe, G.; Spaniol, T. P.; Ebeling, H.; Pelascini, F.; Muelhaupt, R.; Okuda, J. *Angew. Chem., Int. Ed.* **2007**, *46*, 4790-4793.

(2) Zhang, W.; Sita, L. R. *Adv. Synth. Catal.* **2008**, *350*, 439-447.

(3) Wei, J.; Hwang, W.; Zhang, W.; Sita, L. R. *J. Am. Chem. Soc.* **2013**, *135*, 2132-2135.

(4) Hopkins, T. E.; Wagener, K. B. *Adv. Mater. (Weinheim, Ger.)* **2002**, *14*, 1703-1715.

(5) Meppelder, G.-J. M.; Beckerle, K.; Manivannan, R.; Lian, B.; Raabe, G.; Spaniol, T. P.; Okuda, J. *Chem.--Asian J.* **2008**, *3*, 1312-1323.

(6) Kawasaki, T.; Hohberger, C.; Araki, Y.; Hatase, K.; Beckerle, K.; Okuda, J.; Soai, K. *Chem. Commun. (Cambridge, U. K.)* **2009**, 5621-5623.

(7) Baugh, L. S.; Canich, J. A. M.; Editors *Stereoselective Polymerization with Single-Site Catalysts*; CRC Press LLC, 2008.

(8) Palomo, C.; Mestres, R. *Synthesis* **1981**, 373-347.

(9) Jayaratne, K. C.; Sita, L. R. *J. Am. Chem. Soc.* **2000**, *122*, 958-959.

(10) Pasquini, N.; Editor *Polypropylene Handbook, 2nd Edition*; Carl Hanser Verlag, 2005.

(11) Busico, V.; Cipullo, R.; Monaco, G.; Vacatello, M.; Segre, A. L. *Macromolecules* **1997**, *30*, 6251-6263.

(12) Busico, V.; Cipullo, R. *Prog. Polym. Sci.* **2001**, *26*, 443-533.

(13) Belfiore, L. A.; Editor *Physical properties of macromolecules*; Wiley, 2010.

(14) Koterwas, L. A.; Fettinger, J. C.; Sita, L. R. *Organometallics* **1999**, *18*, 4183-4190.

Chapter 6

Conclusions

The living Ziegler-Natta polymerization system based on the pentamethyl cyclopentadienyl amidinate zirconium **51** was shown to create a wide variety of poly(1-butene) materials through stereoengineering with reversible group transfer polymerizations. With substoichiometric amounts of **49**, methyl degenerative transfer polymerization (MeDeT) occurs to program stereoerrors into the polymer microstructure. Also comonomer incorporation can be tuned through the use of two propagating species present in solution with activation of **53** with **49** and **63**. A careful study of the resulting polymers reveal a 'blocky' structure as one ion pair has a higher affinity for the propagation of 1-butene than the other ion pair. Scalable quantities of atactic poly(1-butene) were achieved with the addition of a surrogate chain growth site in living coordinative chain transfer polymerization (LCCTP).

With the fast and reversible polymer chain group transfer between different conformations of the initiator via the chain transfer agent (CTA) it is impossible to obtain isospecific polymers with **51**. Guanidinate based initiators were developed to attempt to impart stereocontrol under LCCTP conditions by creating enanitiomerically pure initiators through tuning of the distal position on the amidinate frame. Guanidinate complexes were readily synthesized and characterized. The combination of the extra steric bulk and electron donation from the distal nitrogen on the guanidinate frame compromised both the activity and stereoselectivity of the initiators. The increased electron donation to the metal center allowed for the polymer chains to terminate via β-

hydride elimination, thus losing their living nature and therefore unsuitable for use in LCCTP.

The N-side arms on the amidinate frame were the next viable location for tuning on the amidinate frame and the same enantiofacial insertion should occur through the addition of an enanitiomerically pure side group despite the relative conformation at the metal center. Compounds bearing resolved amidinate side groups were successfully synthesized and used for living polymerizations, both under non-LCCTP and LCCTP conditions. The newly designed amidinate initiators displayed less stereoselectivity than the traditional design for both the mononuclear and dinuclear analogues. Interestingly, polymerizations with 1-butene yielded optically active polymers as a result of the increased crystallinity and isotacticity of the material produced.

The last viable location to attempt to impart stereoselectivity during LCCTP was the metal center itself. The metal centers were alkylated with large terpene groups via the insertion of the olefin into a Zr-H bond produced by hydrogenation of **65**. With the dialkyl species unable to be synthesized, the norbornane-substituted species was screened for activity under ChloDeT conditions only to find that it diminished the activity of the initiator making it unsuitable to use. Efforts to bypass the halogenated species and directly create the dialkyl species through hydrozirconation of the isolated and characterized methyl-silyl complex were also fruitless due to the instability of the hydrido intermediate produced from hydrogenolysis.

Comprehensive List of References

Chapter 1: Introduction

(1) Natta, G.; Corradini, P. *Makromol. Chem.* **1955**, *16*, 77-80.

(2) Ziegler, K.; Holzkamp, E.; Breil, H.; Martin, H. *Angew. Chem.* **1955**, *67*, 426.

(3) Nexant, I. 2007; Vol. 2012.

(4) Natta, G.; Pino, P.; Corradini, P.; Danusso, F.; Mantica, E.; Mazzanti, G.; Moraglio, G. *J. Am. Chem. Soc.* **1955**, *77*, 1708-1710.

(5) Natta, G. *Angew. Chem.* **1956**, *68*, 393-403.

(6) Natta, G.; Mazzanti, G.; Crespi, G.; Moraglio, G. *Chim. Ind. (Milan, Italy)* **1957**, *39*, 275-283.

(7) Natta, G.; Pino, P.; Mazzanti, G.; Giannini, U. *J. Am. Chem. Soc.* **1957**, *79*, 2975-2976.

(8) Cossee, P. *Tetrahedron Lett.* **1960**, 12-16.

(9) Cossee, P. *Tetrahedron Lett.* **1960**, 17-21.

(10) Arlman, E. J. *J. Catal.* **1964**, *3*, 89-98.

(11) Arlman, E. J.; Cossee, P. *J. Catal.* **1964**, *3*, 99-104.

(12) Cossee, P. *J. Catal.* **1964**, *3*, 80-88.

(13) Maier, C.; Calafut, T. *Polypropylene: A Definitive User's Guide and Handbook* Norwich, NY, 1998.

(14) Hillman, M.; Weiss, A. J.; Hahne, R. M. A. *Radiochim. Acta* **1969**, *12*, 200-202.

(15) Chen, E. Y.-X.; Marks, T. J. *Chem. Rev. (Washington, D. C.)* **2000**, *100*, 1391-1434.

(16) Pedeutour, J.-N.; Radhakrishnan, K.; Cramail, H.; Deffieux, A. *Macromol. Rapid Commun.* **2001**, *22*, 1095-1123.

(17) Baugh, L. S.; Canich, J. A. M.; Editors *Stereoselective Polymerization with Single-Site Catalysts*; CRC Press LLC, 2008.

(18) Herwig, J.; Kaminsky, W. *Polym. Bull. (Berlin)* **1983**, *9*, 464-469.

(19) Kaminsky, W.; Miri, M.; Sinn, H.; Woldt, R. *Makromol. Chem., Rapid Commun.* **1983**, *4*, 417-421.

(20) Schneider, M. J.; Suhm, J.; Muelhaupt, R.; Prosenc, M.-H.; Brintzinger, H.-H. *Macromolecules* **1997**, *30*, 3164-3168.

(21) Grassi, A.; Zambelli, A.; Resconi, L.; Albizzati, E.; Mazzocchi, R. *Macromolecules* **1988**, *21*, 617-622.

(22) Cheng, H. N.; Ewen, J. A. *Makromol. Chem.* **1989**, *190*, 1931-1943.

(23) Mizuno, A.; Tsutsui, T.; Kashiwa, N. *Polymer* **1992**, *33*, 254-258.

(24) Resconi, L.; Cavallo, L.; Fait, A.; Piemontesi, F. *Chem. Rev. (Washington, D. C.)* **2000**, *100*, 1253-1345.

(25) Ewen, J. A. *J. Am. Chem. Soc.* **1984**, *106*, 6355-6364.

(26) Kaminsky, W.; Kuelper, K.; Brintzinger, H. H.; Wild, F. R. W. P. *Angew. Chem.* **1985**, *97*, 507-508.

(27) Resconi, L.; Piemontesi, F.; Nifant ev, I. E.; Ivchenko, P. V.; Montell Technology Company B.V., Neth. . 1996, p 39.

(28) Herrmann, W. A.; Rohrmann, J.; Herdtweck, E.; Spaleck, W.; Winter, A. *Angew. Chem.* **1989**, *101*, 1536-1538.

(29) Winter, A.; Antberg, M.; Spaleck, W.; Rohrmann, J.; Dolle, V.; Hoechst A.-G., Germany . 1992, p 19.

(30) Han, T. K.; Woo, B. W.; Park, J. T.; Do, Y.; Ko, Y. S.; Woo, S. I. *Macromolecules* **1995**, *28*, 4801-4805.

(31) Spaleck, W.; Kueber, F.; Winter, A.; Rohrmann, J.; Bachmann, B.; Antberg, M.; Dolle, V.; Paulus, E. F. *Organometallics* **1994**, *13*, 954-963.

(32) Stehling, U.; Diebold, J.; Kirsten, R.; Roell, W.; Brintzinger, H. H.; Juengling, S.; Muelhaupt, R.; Langhauser, F. *Organometallics* **1994**, *13*, 964-970.

(33) Coates, G. W.; Waymouth, R. M. *Science (Washington, D. C.)* **1995**, *267*, 217-219.

(34) Hauptman, E.; Waymouth, R. M.; Ziller, J. W. *J. Am. Chem. Soc.* **1995**, *117*, 11586-11587.

(35) Bruce, M. D.; Coates, G. W.; Hauptman, E.; Waymouth, R. M.; Ziller, J. W. *J. Am. Chem. Soc.* **1997**, *119*, 11174-11182.

(36) Kravchenko, R.; Masood, A.; Waymouth, R. M. *Organometallics* **1997**, *16*, 3635-3639.

(37) Petoff, J. L. M.; Bruce, M. D.; Waymouth, R. M.; Masood, A.; Lal, T. K.; Quan, R. W.; Behrend, S. J. *Organometallics* **1997**, *16*, 5909-5916.

(38) Bruce, M. D.; Waymouth, R. M. *Macromolecules* **1998**, *31*, 2707-2715.

(39) Kravchenko, R.; Masood, A.; Waymouth, R. M.; Myers, C. L. *J. Am. Chem. Soc.* **1998**, *120*, 2039-2046.

(40) Petoff, J. L. M.; Agoston, T.; Lal, T. K.; Waymouth, R. M. *J. Am. Chem. Soc.* **1998**, *120*, 11316-11322.

(41) Lin, S.; Waymouth, R. M. *Macromolecules* **1999**, *32*, 8283-8290.

(42) Tagge, C. D.; Kravchenko, R. L.; Lal, T. K.; Waymouth, R. M. *Organometallics* **1999**, *18*, 380-388.

(43) Ewen, J. A.; Jones, R. L.; Razavi, A.; Ferrara, J. D. *J. Am. Chem. Soc.* **1988**, *110*, 6255-6256.

(44) Razavi, A.; Atwood, J. L. *J. Organomet. Chem.* **1993**, *459*, 117-123.

(45) Shiomura, T.; Kohno, M.; Inoue, N.; Asanuma, T.; Sugimoto, R.; Iwatani, T.; Uchida, O.; Kimura, S.; Harima, S.; et, a. *Macromol. Symp.* **1996**, *101*, 289-299.

(46) Yamaguchi, M.; Ohba, K.; Tomonaga, H.; Yamagishi, T. *J. Mol. Catal. A: Chem.* **1999**, *140*, 255-258.

(47) Farina, M.; Di Silvestro, G.; Sozzani, P. *Macromolecules* **1993**, *26*, 946-950.

(48) Herfert, N.; Fink, G. *Makromol. Chem., Macromol. Symp.* **1993**, *66*, 157-178.

(49) Antberg, M.; Dolle, V.; Klein, R.; Rohrmann, J.; Spaleck, W.; Winter, A. *Catalytic Olefin Polymerization, Studies in Surface Science and Catalysis* Tokyo, 1990.

(50) Dolle, V.; Rohrmann, J.; Winter, A.; Antberg, M.; Klein, R.; Hoechst A.-G., Germany . 1990, p 15.

(51) Ewen, J. A.; Elder, M. J.; Harlan, C. J.; Jones, R. L.; Atwood, J. L.; Bott, S. G.; Robinson, K. *Polym. Prepr. (Am. Chem. Soc., Div. Polym. Chem.)* **1991**, *32*, 469-470.

(52) Ewen, J. A.; Elder, M. J.; Jones, R. L.; Haspeslagh, L.; Atwood, J. L.; Bott, S. G.; Robinson, K. *Makromol. Chem., Macromol. Symp.* **1991**, *48-49*, 253-295.

(53) Spaleck, W.; Antberg, M.; Aulbach, M.; Dolle, V.; Rohrmann, J.; Winter, A.; Kuber, F.; Haftka, S. *Ziegler Catalysts*, 1995.

(54) Spaleck, W.; Kuber, F.; Bachmann, B.; Fritze, C.; Winter, A. *J. Mol. Catal. A: Chem.* **1998**, *128*, 279-287.

(55) Coates, G. W.; Hustad, P. D.; Reinartz, S. *Angew. Chem., Int. Ed.* **2002**, *41*, 2236-2257.

(56) Doi, Y.; Ueki, S.; Keii, T. *Macromolecules* **1979**, *12*, 814-815.

(57) Foster, P.; Rausch, M. D.; Chien, J. C. W. *J. Organomet. Chem.* **1997**, *527*, 71-74.

(58) Van Der Zeijden, A. A. H.; Mattheis, C. *J. Organomet. Chem.* **1999**, *584*, 274-285.

(59) Chien, J. C.; Yu, Z.; Marques, M. M.; Flores, J. C.; Rausch, M. D. *J. Polym. Sci., Part A: Polym. Chem.* **1998**, *36*, 319-328.

(60) Blais, M. S.; Chien, J. C. W.; Rausch, M. D. *Organometallics* **1998**, *17*, 3775-3783.

(61) Flores, J. C.; Chien, J. C. W.; Rausch, M. D. *Organometallics* **1994**, *13*, 4140-4142.

(62) Skoog, S. J.; Mateo, C.; Lavoie, G. G.; Hollander, F. J.; Bergman, R. G. *Organometallics* **2000**, *19*, 1406-1421.

(63) Bochmann, M.; Lancaster, S. J. *Organometallics* **1993**, *12*, 633-640.

(64) Marques, M. M.; Correia, S. G.; Ascenso, J. R.; Ribeiro, A. F. G.; Gomes, P. T.; Dias, A. R.; Foster, P.; Rausch, M. D.; Chien, J. C. W. *J. Polym. Sci., Part A: Polym. Chem.* **1999**, *37*, 2457-2469.

(65) Ioku, A.; Hasan, T.; Shiono, T.; Ikeda, T. *Macromol. Chem. Phys.* **2002**, *203*, 748-755.

(66) Santos, J. M.; Ribeiro, M. R.; Portela, M. F.; Cramail, H.; Deffieux, A.; Antinolo, A.; Otero, A.; Prashar, S. *Macromol. Chem. Phys.* **2002**, *203*, 139-145.

(67) Klosin, J.; Kruper, W. J., Jr.; Nickias, P. N.; Roof, G. R.; De Waele, P.; Abboud, K. A. *Organometallics* **2001**, *20*, 2663-2665.

(68) Kotov, V. V.; Avtomonov, E. V.; Sundermeyer, J.; Harms, K.; Lemenovskii, D. A. *Eur. J. Inorg. Chem.* **2002**, 678-691.

(69) Scollard, J. D.; McConville, D. H. *J. Am. Chem. Soc.* **1996**, *118*, 10008-10009.

(70) Scollard, J. D.; McConville, D. H.; Payne, N. C.; Vittal, J. J. *Macromolecules* **1996**, *29*, 5241-5243.

(71) Tsubaki, S.; Jin, J.; Ahn, C.-H.; Sano, T.; Uozumi, T.; Soga, K. *Macromol. Chem. Phys.* **2001**, *202*, 482-487.

(72) Uozumi, T.; Tsubaki, S.; Jin, J.; Sano, T.; Soga, K. *Macromol. Chem. Phys.* **2001**, *202*, 3279-3282.

(73) Ziniuk, Z.; Goldberg, I.; Kol, M. *Inorg. Chem. Commun.* **1999**, *2*, 549-551.

(74) Nomura, K.; Naga, N.; Takaoki, K.; Imai, A. *J. Mol. Catal. A: Chem.* **1998**, *130*, L209-L213.

(75) Nomura, K.; Oya, K.; Imanishi, Y. *Polymer* **2000**, *41*, 2755-2746.

(76) Baumann, R.; Davis, W. M.; Schrock, R. R. *J. Am. Chem. Soc.* **1997**, *119*, 3830-3831.

(77) Baumann, R.; Stumpf, R.; Davis, W. M.; Liang, L.-C.; Schrock, R. R. *J. Am. Chem. Soc.* **1999**, *121*, 7822-7836.

(78) Schrock, R. R.; Liang, L. C.; Baumann, R.; Davis, W. M. *J. Organomet. Chem.* **1999**, *591*, 163-173.

(79) Baumann, R.; Schrock, R. R. *J. Organomet. Chem.* **1998**, *557*, 69-75.

(80) Goodman, J. T.; Schrock, R. R. *Organometallics* **2001**, *20*, 5205-5211.

(81) Schrock, R. R.; Baumann, R.; Reid, S. M.; Goodman, J. T.; Stumpf, R.; Davis, W. M. *Organometallics* **1999**, *18*, 3649-3670.

(82) Aizenberg, M.; Turculet, L.; Davis, W. M.; Schattenmann, F.; Schrock, R. R. *Organometallics* **1998**, *17*, 4795-4812.

(83) Schrock, R. R.; Bonitatebus, P. J., Jr.; Schrodi, Y. *Organometallics* **2001**, *20*, 1056-1058.

(84) Schrock, R. R.; Casado, A. L.; Goodman, J. T.; Liang, L.-C.; Bonitatebus, P. J., Jr.; Davis, W. M. *Organometallics* **2000**, *19*, 5325-5341.

(85) Averbuj, C.; Tish, E.; Eisen, M. S. *J. Am. Chem. Soc.* **1998**, *120*, 8640-8646.

(86) Volkis, V.; Shmulinson, M.; Averbuj, C.; Lisovskii, A.; Edelmann, F. T.; Eisen, M. S. *Organometallics* **1998**, *17*, 3155-3157.

(87) Vollmerhaus, R.; Shao, P.; Taylor, N. J.; Collins, S. *Organometallics* **1999**, *18*, 2731-2733.

(88) Duncan, A. P.; Mullins, S. M.; Arnold, J.; Bergman, R. G. *Organometallics* **2001**, *20*, 1808-1819.

(89) Chen, C.-T.; Rees, L. H.; Cowley, A. R.; Green, M. L. H. *J. Chem. Soc., Dalton Trans.* **2001**, 1761-1767.

(90) Makio, H.; Fujita, T. *Bull. Chem. Soc. Jpn.* **2005**, *78*, 52-66.

(91) Ishii, S.-I.; Mitani, M.; Saito, J.; Matsuura, S.; Kojoh, S.-I.; Kashiwa, N.; Fujita, T. *Chem. Lett.* **2002**, 740-741.

(92) Saito, J.; Mitani, M.; Mohri, J.-I.; Ishii, S.-I.; Yoshida, Y.; Matsugi, T.; Kojoh, S.-I.; Kashiwa, N.; Fujita, T. *Chem. Lett.* **2001**, 576-577.

(93) Ishii, S.; Saito, J.; Matsuura, S.; Suzuki, Y.; Furuyama, R.; Mitani, M.; Nakano, T.; Kashiwa, N.; Fujita, T. *Macromol. Rapid Commun.* **2002**, *23*, 693-697.

(94) Milano, G.; Cavallo, L.; Guerra, G. *J. Am. Chem. Soc.* **2002**, *124*, 13368-13369.

(95) Tshuva, E. Y.; Versano, M.; Goldberg, I.; Kol, M.; Weitman, H.; Goldschmidt, Z. *Inorg. Chem. Commun.* **1999**, *2*, 371-373.

(96) Tshuva, E. Y.; Goldberg, I.; Kol, M.; Weitman, H.; Goldschmidt, Z. *Chem. Commun. (Cambridge)* **2000**, 379-380.

(97) Tshuva, E. Y.; Goldberg, I.; Kol, M.; Goldschmidt, Z. *Inorg. Chem. Commun.* **2000**, *3*, 611-614.

(98) Tshuva, E. Y.; Groysman, S.; Goldberg, I.; Kol, M.; Goldschmidt, Z. *Organometallics* **2002**, *21*, 662-670.

(99) Olonde, X.; Mortreux, A.; Petit, F.; Bujadoux, K. *J. Mol. Catal.* **1993**, *82*, 75-82.

(100) Pelletier, J.-F.; Mortreux, A.; Olonde, X.; Bujadoux, K. *Angew. Chem., Int. Ed. Engl.* **1996**, *35*, 1854-1856.

(101) Britovsek, G. J. P.; Cohen, S. A.; Gibson, V. C.; van Meurs, M. *J. Am. Chem. Soc.* **2004**, *126*, 10701-10712.

(102) Chenal, T.; Olonde, X.; Pelletier, J.-F.; Bujadoux, K.; Mortreux, A. *Polymer* **2007**, *48*, 1844-1856.

(103) Kempe, R. *Chem. - Eur. J.* **2007**, *13*, 2764-2773.

(104) Zinck, P.; Valente, A.; Mortreux, A.; Visseaux, M. *Polymer* **2007**, *48*, 4609-4614.

(105) Amin, S. B.; Marks, T. J. *Angew. Chem., Int. Ed.* **2008**, *47*, 2006-2025.

(106) Arriola, D. J.; Carnahan, E. M.; Hustad, P. D.; Kuhlman, R. L.; Wenzel, T. T. *Science (Washington, DC, U. S.)* **2006**, *312*, 714-719.

(107) Sita, L. R. *Angew. Chem., Int. Ed.* **2009**, *48*, 2464-2472.

(108) Valente, A.; Mortreux, A.; Visseaux, M.; Zinck, P. *Chem. Rev. (Washington, DC, U. S.)* **2013**, *113*, 3836-3857.

(109) Barsties, E.; Schaible, S.; Prosenc, M.-H.; Rief, U.; Roell, W.; Weyand, O.; Dorer, B.; Brintzinger, H.-H. *J. Organomet. Chem.* **1996**, *520*, 63-68.

(110) Leino, R.; Luttikhedde, H. J. G.; Lehmus, P.; Wilen, C.-E.; Sjoeholm, R.; Lehtonen, A.; Seppaelae, J. V.; Naesman, J. H. *Macromolecules* **1997**, *30*, 3477-3483.

(111) Naga, N.; Mizunuma, K. *Polymer* **1998**, *39*, 5059-5067.

(112) Lieber, S.; Brintzinger, H.-H. *Macromolecules* **2000**, *33*, 9192-9199.

(113) Fan, G.; Dong, J.-Y. *J. Mol. Catal. A: Chem.* **2005**, *236*, 246-252.

(114) Hild, S.; Cobzaru, C.; Troll, C.; Rieger, B. *Macromol. Chem. Phys.* **2006**, *207*, 665-683.

(115) Tynys, A.; Eilertsen, J. L.; Rytter, E. *Macromol. Chem. Phys.* **2006**, *207*, 295-303.

(116) Byun, D.-J.; Shin, D.-K.; Kim, S. Y. *Macromol. Rapid Commun.* **1999**, *20*, 419-422.

(117) Bhriain, N. N.; Brintzinger, H.-H.; Ruchatz, D.; Fink, G. *Macromolecules* **2005**, *38*, 2056-2063.

(118) Hoffmann, E. G. *Trans. Faraday Soc.* **1962**, *58*, 642-649.

(119) Yamamoto, O.; Hayamizu, K. *J. Phys. Chem.* **1968**, *72*, 822-828.

(120) Valente, A.; Zinck, P.; Mortreux, A.; Visseaux, M. *Macromol. Rapid Commun.* **2009**, *30*, 528-531.

(121) Valente, A.; Zinck, P.; Mortreux, A.; Bria, M.; Visseaux, M. *J. Polym. Sci., Part A: Polym. Chem.* **2011**, *49*, 3778-3782.

(122) Valente, A.; Zinck, P.; Mortreux, A.; Visseaux, M. *J. Polym. Sci., Part A: Polym. Chem.* **2011**, *49*, 1615-1620.

(123) Khariwala, D. U.; Taha, A.; Chum, S. P.; Hiltner, A.; Baer, E. *Polymer* **2008**, *49*, 1365-1375.

(124) Wang, H. P.; Khariwala, D. U.; Cheung, W.; Chum, S. P.; Hiltner, A.; Baer, E. *Macromolecules (Washington, DC, U. S.)* **2007**, *40*, 2852-2862.

(125) Jayaratne, K. C.; Sita, L. R. *J. Am. Chem. Soc.* **2000**, *122*, 958-959.

(126) Koterwas, L. A.; Fettinger, J. C.; Sita, L. R. *Organometallics* **1999**, *18*, 4183-4190.

(127) Harney, M. B.; Keaton, R. J.; Sita, L. R. *J. Am. Chem. Soc.* **2004**, *126*, 4536-4537.

(128) Zhang, Y.; Keaton, R. J.; Sita, L. R. *J. Am. Chem. Soc.* **2003**, *125*, 9062-9069.

(129) Zhang, Y.; Sita, L. R. *J. Am. Chem. Soc.* **2004**, *126*, 7776-7777.

(130) Zhang, W.; Sita, L. R. *J. Am. Chem. Soc.* **2008**, *130*, 442-443.

Chapter 2: Stereoengineering of Poly(1-butene)

(1) Zhang, W.; Sita, L. R. *Adv. Synth. Catal.* **2008**, *350*, 439-447.

(2) Zhang, W.; Sita, L. R. *J. Am. Chem. Soc.* **2008**, *130*, 442-443.

(3) Sita, L. R. *Angew. Chem., Int. Ed.* **2009**, *48*, 2464-2472.

(4) Jayaratne, K. C.; Sita, L. R. *J. Am. Chem. Soc.* **2000**, *122*, 958-959.

(5) Jayaratne, K. C.; Sita, L. R. *J. Am. Chem. Soc.* **2001**, *123*, 10754-10755.

(6) De Rosa, C.; Auriemma, F.; Ruiz de Ballesteros, O.; Esposito, F.; Laguzza, D.; Di Girolamo, R.; Resconi, L. *Macromolecules (Washington, DC, U. S.)* **2009**, *42*, 8286-8297.

(7) Wei, J.; Hwang, W.; Zhang, W.; Sita, L. R. *J. Am. Chem. Soc.* **2013**, *135*, 2132-2135.

(8) Zhang, W.; Wei, J.; Sita, L. R. *Macromolecules (Washington, DC, U. S.)* **2008**, *41*, 7829-7833.

(9) Wei, J.; Zhang, W.; Wickham, R.; Sita, L. R. *Angew. Chem., Int. Ed.* **2010**, *49*, 9140-9144.

(10) Arriola, D. J.; Carnahan, E. M.; Hustad, P. D.; Kuhlman, R. L.; Wenzel, T. T. *Science (Washington, DC, U. S.)* **2006**, *312*, 714-719.

(11) Sahoo, S. K.; Zhang, T.; Reddy, D. V.; Rinaldi, P. L.; McIntosh, L. H.; Quirk, R. P. *Macromolecules* **2003**, *36*, 4017-4028.

(12) Wunderlich, B.; Academic: **1981**, p 91.

(13) McFaddin, D. C.; Russell, K. E.; Wu, G.; Heyding, R. D. *J. Polym. Sci., Part B: Polym. Phys.* **1993**, *31*, 175-183.

(14) Kossuth, M. B.; Morse, D. C.; Bates, F. S. *J. Rheol. (N. Y.)* **1999**, *43*, 167-196.

(15) Leclere, P.; Lazzaroni, R.; Bredas, J. L.; Yu, J. M.; Dubois, P.; Jerome, R. *Langmuir* **1996**, *12*, 4317-4320.

(16) Hobbs, J. K.; Register, R. A. *Macromolecules* **2006**, *39*, 703-710.

(17) Stocker, W.; Beckmann, J.; Stadler, R.; Rabe, J. P. *Macromolecules* **1996**, *29*, 7502-7507.

(18) van Dijk, M. A.; van den Berg, R. *Macromolecules* **1995**, *28*, 6773-6778.

Chapter 3: Guanidinate Based Initiators for Stereocontrol During LCCTP

(1) Jayaratne, K. C.; Sita, L. R. *J. Am. Chem. Soc.* **2000**, *122*, 958-959.

(2) Keaton, R. J.; Jayaratne, K. C.; Fettinger, J. C.; Sita, L. R. *J. Am. Chem. Soc.* **2000**, *122*, 12909-12910.

(3) Kissounko, D. A.; Fettinger, J. C.; Sita, L. R. *Inorg. Chim. Acta* **2003**, *345*, 121-129.

(4) Alfano, F.; Boone, H. W.; Busico, V.; Cipullo, R.; Stevens, J. C. *Macromolecules (Washington, DC, U. S.)* **2007**, *40*, 7736-7738.

(5) Duncan, A. P.; Mullins, S. M.; Arnold, J.; Bergman, R. G. *Organometallics* **2001**, *20*, 1808-1819.

(6) Coles, M. P.; Hitchcock, P. B. *Organometallics* **2003**, *22*, 5201-5211.

(7) Zhou, M.; Tong, H.; Wei, X.; Liu, D. *J. Organomet. Chem.* **2007**, *692*, 5195-5202.

(8) Zhou, M.; Zhang, S.; Tong, H.; Sun, W.-H.; Liu, D. *Inorg. Chem. Commun.* **2007**, *10*, 1262-1264.

(9) Haas, I.; Huebner, C.; Kretschmer, W. P.; Kempe, R. *Chem. - Eur. J.* **2013**, *19*, 9132-9136.

(10) Zhang, W.; Sita, L. R. *J. Am. Chem. Soc.* **2008**, *130*, 442-443.

(11) Zhang, Y.; Sita, L. R. *J. Am. Chem. Soc.* **2004**, *126*, 7776-7777.

(12) Vollmerhaus, R.; Rahim, M.; Tomaszewski, R.; Xin, S.; Taylor, N. J.; Collins, S. *Organometallics* **2000**, *19*, 2161-2169.

(13) Zhang, Y.; Reeder, E. K.; Keaton, R. J.; Sita, L. R. *Organometallics* **2004**, *23*, 3512-3520.

(14) Wei, J.; Zhang, W.; Wickham, R.; Sita, L. R. *Angew. Chem., Int. Ed.* **2010**, *49*, 9140-9144.

Chapter 4: Application of Hydrozirconation to Achieve Stereocontrol During LCCTP

(1) Zhang, Y.; Keaton, R. J.; Sita, L. R. *J. Am. Chem. Soc.* **2003**, *125*, 8746-8747.

(2) Buchwald, S. L.; LaMaire, S. J.; Nielsen, R. B.; Watson, B. T.; King, S. M. *Org. Synth.* **1993**, *71*, 77-82.

(3) Kalesse, M. *Acros Org. Acta* **1995**, *1*, 29-31.

(4) Fernandez-Megia, E. *Synlett* **1999**, 1179.

(5) Erker, G.; Zwettler, R.; Krueger, C.; Schlund, R.; Hyla-Kryspin, I.; Gleiter, R. *J. Organomet. Chem.* **1988**, *346*, C15-C18.

(6) Erker, G.; Zwettler, R.; Krueger, C.; Hyla-Kryspin, I.; Gleiter, R. *Organometallics* **1990**, *9*, 524-530.

(7) Chirik, P. J.; Day, M. W.; Labinger, J. A.; Bercaw, J. E. *J. Am. Chem. Soc.* **1999**, *121*, 10308-10317.

(8) Labinger, J. A.; Hart, D. W.; Seibert, W. E., III; Schwartz, J. *J. Am. Chem. Soc.* **1975**, *97*, 3851-3852.

(9) Zhang, Y.; Sita, L. R. *J. Am. Chem. Soc.* **2004**, *126*, 7776-7777.

(10) Randall, J. C. *J. Macromol. Sci., Rev. Macromol. Chem. Phys.* **1989**, *C29*, 201-317.

(11) Wendt, R. A.; Mynott, R.; Hauschild, K.; Ruchatz, D.; Fink, G. *Macromol. Chem. Phys.* **1999**, *200*, 1340-1350.

Chapter 5: 'Chiral' Amidinates

(1) Beckerle, K.; Manivannan, R.; Lian, B.; Meppelder, G.-J. M.; Raabe, G.; Spaniol, T. P.; Ebeling, H.; Pelascini, F.; Muelhaupt, R.; Okuda, J. *Angew. Chem., Int. Ed.* **2007**, *46*, 4790-4793.

(2) Zhang, W.; Sita, L. R. *Adv. Synth. Catal.* **2008**, *350*, 439-447.

(3) Wei, J.; Hwang, W.; Zhang, W.; Sita, L. R. *J. Am. Chem. Soc.* **2013**, *135*, 2132-2135.

(4) Hopkins, T. E.; Wagener, K. B. *Adv. Mater. (Weinheim, Ger.)* **2002**, *14*, 1703-1715.

(5) Meppelder, G.-J. M.; Beckerle, K.; Manivannan, R.; Lian, B.; Raabe, G.; Spaniol, T. P.; Okuda, J. *Chem.--Asian J.* **2008**, *3*, 1312-1323.

(6) Kawasaki, T.; Hohberger, C.; Araki, Y.; Hatase, K.; Beckerle, K.; Okuda, J.; Soai, K. *Chem. Commun. (Cambridge, U. K.)* **2009**, 5621-5623.

(7) Baugh, L. S.; Canich, J. A. M.; Editors *Stereoselective Polymerization with Single-Site Catalysts*; CRC Press LLC, 2008.

(8) Palomo, C.; Mestres, R. *Synthesis* **1981**, 373-347.

(9) Jayaratne, K. C.; Sita, L. R. *J. Am. Chem. Soc.* **2000**, *122*, 958-959.

(10) Pasquini, N.; Editor *Polypropylene Handbook, 2nd Edition*; Carl Hanser Verlag, 2005.

(11) Busico, V.; Cipullo, R.; Monaco, G.; Vacatello, M.; Segre, A. L. *Macromolecules* **1997**, *30*, 6251-6263.

(12) Busico, V.; Cipullo, R. *Prog. Polym. Sci.* **2001**, *26*, 443-533.

(13) Belfiore, L. A.; Editor *Physical properties of macromolecules*; Wiley, 2010.

(14) Koterwas, L. A.; Fettinger, J. C.; Sita, L. R. *Organometallics* **1999**, *18*, 4183-4190.